FINAL REPORT

Project Title: "Evaluation of Composite Post-Tensioning Systems on SCI-23-0096, Scioto County"

Authors:	Dr. Henry R. Busby Dr. William E. Wolfe Dr. Tarunjit S. Butalia
Research Agency:	The Ohio State University Research Foundation
Date:	March, 2003
Sponsoring Agencies:	Ohio Department of Transportation Federal Highway Administration

"Prepared in cooperation with the Ohio Department of Transportation and the U.S. Department of Transportation, Federal Highway Administration"

1. Report No.	2. Government Accession No.	3. Recipient's Catalog No.
FHWA/OH-2003/005		

4. Title and subtitle	5. Report Date
Evaluation of Composite Post-Tensioning System on Bridge SCI-23-0096, Scioto County	**March 2003**
	6. Performing Organization Code
	8. Performing Organization Report No.
7. Author(s)	
Dr. Henry R. Busby **Dr. William E. Wolfe** **Dr. Tarunjit S. Butalia**	10. Work Unit No. (TRAIS)
9. Performing Organization Name and Address	11. Contract or Grant No.
Ohio State University **Civil and Environmental Engineering & Geodetic Science** **College of Engineering** **2070 Neil Avenue** **Columbus, OH 43212-1275**	**State Job No. 14723(0)**
	13. Type of Report and Period Covered
	Final Report
12. Sponsoring Agency Name and Address	14. Sponsoring Agency Code
Ohio Department of Transportation 1980 W Broad Street Columbus, OH 43223	

15. Supplementary Notes

16. Abstract

Aging highway infrastructure, increasing traffic loads and the high cost of rehabilitation have combined to make novel repair methodologies increasingly attractive. Several new products now receiving attention in bridge rehabilitation are made from high strength, durable composite materials. In the current project, carbon fiber rods were affixed to a four span steel girder, concrete deck bridge. The project was divided into three phases. The first phase consisted of the installation of strain and displacement sensors on the existing structure and the measurement of deflections during controlled traffic loads. Carbon fiber rods were attached in the second phase. During the third phase the response of the newly reinforced bridge to vehicular and environmental loads was monitored. No actual improvement in bridge performance was detected after the carbon fiber rods were installed. The slight difference between the before and after deflections and strains was less than the variability that should be expected in the readings.

17. Key Words	18. Distribution Statement
Composites, bridge rehabilitation, retrofit	No Restrictions. This document is available to the public through the National Technical Information Service, Springfield, Virginia 22161

19. Security Classif. (of this report)	20. Security Classif. (of this page)	21. No. of Page	22. Price
Unclassified	Unclassified		

Form DOT F 1700.7 (8-72) Reproduction of competed page authorized

ACKNOWLEDGEMENTS

This report was prepared as part of a research project "Evaluation of Composite Post-Tensioning Systems on Bridge SCI-23-0096, Scioto County," and was performed at The Ohio State University. The principal sponsor of the research was the Ohio Department of Transportation. Substantial additional support was provided by The Ohio State University, College of Engineering. The cooperation of the staff at ODOT and the Federal Highway Administration is appreciated. The efforts of a number of students and staff of the Department of Civil and Environmental Engineering and Geodetic Science were required to bring this monitoring program to a successful conclusion. In particular, the authors would like to thank the following individuals: H. Jason Hughes, Ross Baldwin, Stephen Taliaferro, Richard D. Fortner, David R. Davis, A. Ray Hunter, Todd G. Guttman and Floyd Rister.

TABLE OF CONTENTS

LIST OF FIGURES

LIST OF TABLES

INTRODUCTION

According to the Federal Highway Administration's 1999 annual report titled "Status of the Nation's Highways, Bridges, and Transit" an estimated 29% of the nation's bridges need to be either rehabilitated or replaced. Aging highway infrastructure, increasing traffic loads and the high cost of rehabilitation have combined to make novel repair methodologies increasingly attractive to transportation officials. Several new products now receiving attention in bridge rehabilitation are comprised of composite components, which, because of their high strength and stiffness to weight ratios and durability, are logical substitutes for conventional highway materials. The rehabilitation method being studied in the current project consists of attaching composite rods to an existing concrete bridge. After the rods are affixed to the bridge, each rod is loaded to a design tension. The design tension is intended to improve the capacity of the bridge by changing the mean stress in its principal structural members. There are several advantages to this rehabilitation technique; the stiffening members can be applied with little or no traffic interruption, scaffolding and site preparation may be minimized, and tendons and anchors can be prefabricated to reduce work in the field.

The Ohio Department of Transportation (ODOT) contracted with The Ohio State University (OSU) to observe the installation of external post-tensioned fiber reinforced polymer rods on the Bridge SCI-23-0096 in Scioto County and perform any testing and analysis sufficient to evaluate the effectiveness of the reinforcement. Fiber Reinforced Systems, Ltd. of Columbus, Ohio (FRS) was selected by ODOT to design and install the reinforcing rods. Typical instrumentation installed by OSU consisted of strain gauges placed in locations where high stresses were anticipated, displacement devices at the center of spans, and load cells on selected rods.

The study bridge, ODOT designation SCI-23-0.96 in Scioto County, is located just north of Portsmouth on US Route 23 in Scioto County (See Figure 1). This bridge has four spans (50.5', 63', 56', and 43') with ten continuous steel girders and reinforced concrete deck and superstructure. Four lanes of traffic are supported by the bridge as it crosses over railroad tracks and a two-lane street. The bridge is skewed at an angle of 30˚32'04". The purpose of post-tensioning this bridge was to increase load capacity by reducing the maximum negative

moment. Figure 2 is photograph of the bridge looking east. Table 1 is a summary of the characteristics of the Portsmouth bridge.

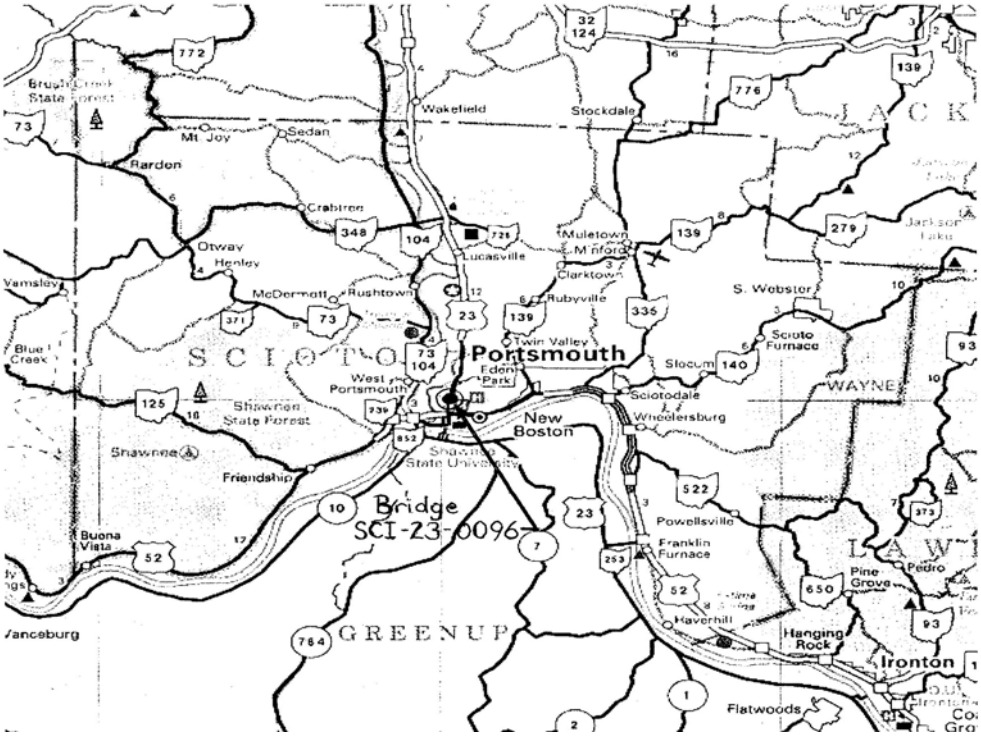

Figure 1 Map of Scioto County (Ohio Department of Transportation, 2001)

Figure 2 Bridge SCI-23-0096. (looking East)

The project was divided into three phases. The first phase consisted of the installation of strain sensors on the existing structure and the measurement of deflections prior to the

installation of the structural composite rods. In the second phase FRS attached the composite rods, brackets and, on select rods, load cells supplied by OSU to the bridge. The design of the rods, their attachments and locations was performed by FRS in direct consultation with ODOT bridge engineers before OSU was approached to monitor the performance of the bridge. During the third phase of the project the response of the reinforced bridge to vehicular and environmental loads was monitored. The loads in the instrumented rods were monitored for the remainder of the project duration. Although the proposal considered only a short term project, some extended monitoring of the installed instrumentation was carried out to adequately evaluate the performance of the composite post-tensioning system.

RESEARCH OBJECTIVES

This study was designed to focus on measuring the effects of the attachment of carbon fiber tension rods to an existing reinforced concrete bridge subjected to various types of static and dynamic traffic loads and environmental conditions. In the proposal, the following research objectives were identified:

1. Evaluate the material and structural properties of the carbon fiber reinforcing rods in laboratory tests by performing tests on representative small-scale specimens;
2. Instrument the bridge with monitoring devices to evaluate structural response to traffic loads and environmental conditions;

Bridge	SCI-23-0096
Location (County)	Scioto
Spans	4
Span Lengths (ft)	50.5, 63, 56, 43
Deck	Reinforced Concrete
Beams	Continuous steel girders
Number Longitudinal Girders	10
Transverse Girders	0
Number of Lanes on bridge	4
Skewness	30º 32' 04"
Spanning	Railroad and Street
Structural Deficiency	Negative Moment
Post-Tensioning Rods	
Material	Carbon fiber
Length (ft)	20
Diameter (in)	3/8
Design Tension Force (lbs)	13000
Bracket Connection	Welded
Number of Transducers	
Load Cells	6
Strain Gauges	29
LVDTs	5

Table 1 Portsmouth bridge.

3. Begin taking measurements that should lead to an evaluation of the effects of environmental factors on the performance of the reinforcing rods;
4. Use the data collected to assist ODOT in the development of standard guidelines for the use of composites in bridge repair in Ohio.
5. Evaluate the material and structural properties of the carbon fiber reinforcing rods in laboratory tests by performing tests on representative small-scale specimens;

The contractor expressed concern that the proprietary nature of the rods and their attachments would not be protected if representative specimens were provided to OSU researchers. Since the laboratory test program proposed in research objective No. 5 above

required specimens to test, ODOT engineers were informed that, under the circumstances, no laboratory testing was possible.

GENERAL DESCRIPTION OF RESEARCH

In the last two decades, fiber reinforced composites have become important components of many engineered structures. Although the majority of these applications have been in the area of high performance structures, several demonstration and full-scale composite bridge structures to support pedestrian, bike, and vehicular traffic have been proposed.

This study focused on measuring the effects of the attachment of glass fiber tension rods to an existing reinforced concrete bridge subjected to various types of static and dynamic traffic loads and environmental conditions. The rods at Portsmouth were located at the top of the web, as shown in Figure 3, to reduce the negative moment over the piers. Two rods were placed on each side of the web of every beam above each pier (Figure 4) – a total of 120 rods. All rods at this site were made of CFRP and were 20-feet long with 3/8-inch diameter. The design tension of these rods was 58.2 kN. The brackets were welded to the girders.

The rods were attached to steel brackets. Figure 3 is a typical bracket assembly. The brackets were welded to the girders of the bridge and the rods tensioned by tightening the nut, shown in Figure 3 to the left of the bracket, with a torque wrench.

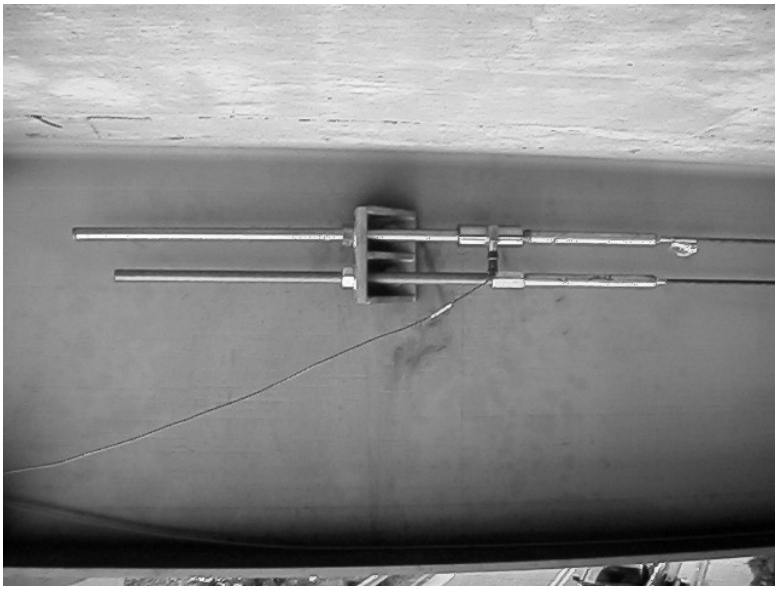

Figure 3 Rod placement

Figure 4 Rod layout.

FIELD TESTING

Static and dynamic load tests were performed on the bridge before and after tensioning the composite rods. The loading consisted of two ODOT trucks with assumed axle spacing and weight distributions. Both static tests (the trucks were placed a specific locations on the bridge) and dynamic tests (the trucks were driven across the bridge at a specified speed) were conducted. The location of the applied load was recorded for the static tests and the vehicle speed and truck locations (relative to each other) were monitored and recorded for each dynamic test. The loads applied at Portsmouth were a semi-tractor and trailer with axle weights of 44.5 kN, 115.6 kN, and 195.7 kN (from front to rear) and a tandem dump truck with axle weights of 74.7 and 178.8 kN (front and rear respectively. See Table 2 for the protocol details. As described in Table 2, the dynamic tests varied both speed and position of the trucks relative to one another. Speeds varied from 10 to 35 miles per hour with trucks positioned either side-by-side or front-to-back. Since the speed limit was 35 mph, this was used as the maximum test speed. The static tests positioned the trucks at various locations to produce either maximum mid-span deflection (produced by the side-by-side truck configuration) or maximum negative moment (produced by the front-to-back truck configuration) over the pier.

INSTRUMENTATION

The loads in selected rods, deflection at mid span, and strain at selected locations were measured. Load cells, linear variable differential transformers (LVDTs), and strain gauges were the transducers used to measure these quantities. Figure 5 gives the bridge instrumentation layout for SCI-23-0096. The data collection rate for each test was 100 samples per channel. The key for the Portsmouth layout is given in Table 3.

Load Cells

Figure 6 shows a typical load cells in place on the top rod inside each of the outer beams of the bridge. Notice the end of the composite rod is screwed directly into

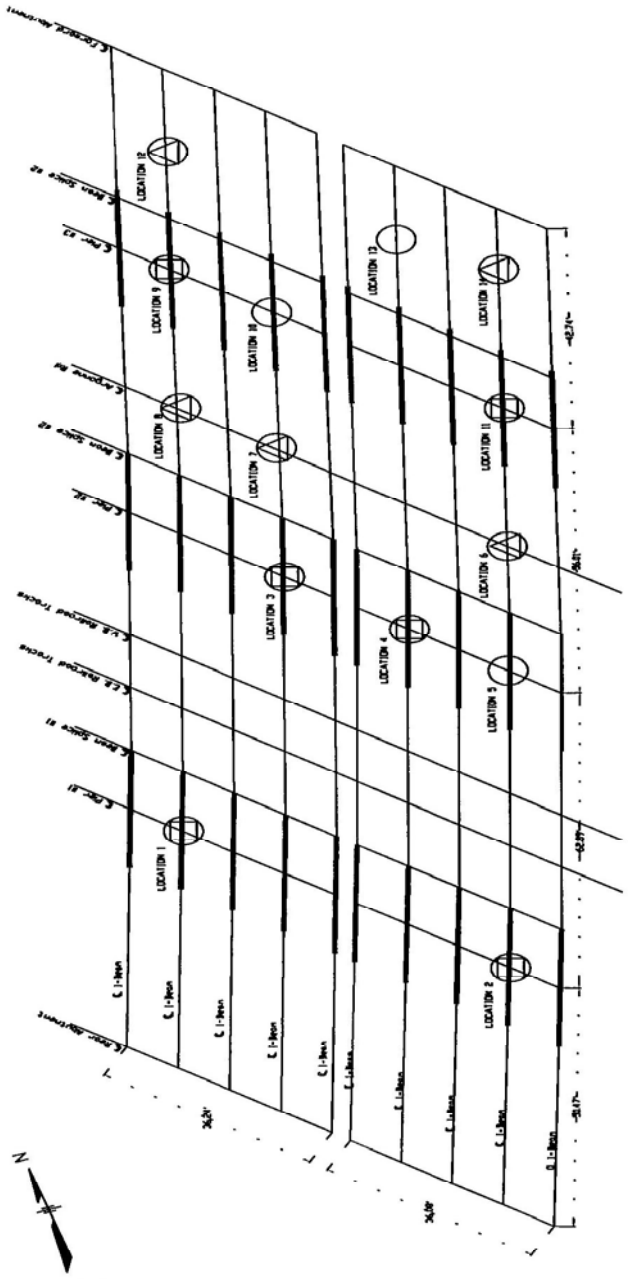

Figure 5 Instrumentation Layout of Portsmouth Bridge

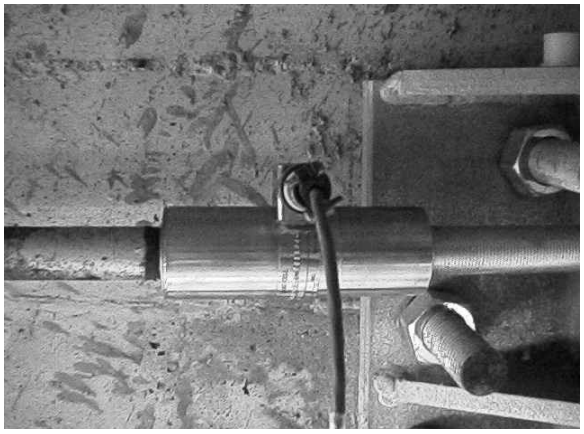

Figure 6. Typical Load Cell installation

the left end of load cell. Two load cells were installed at each set of piers (six total). Load was recorded over a period of months to determine whether the rods maintained the design tension.

Strain Gauges

Typical strain gauges were installed as shown in Figure 5. The typical location of the strain gages on the top flange and bottom of the deck is shown in Figure 7 and on the bottom of the flange in Figure 8.

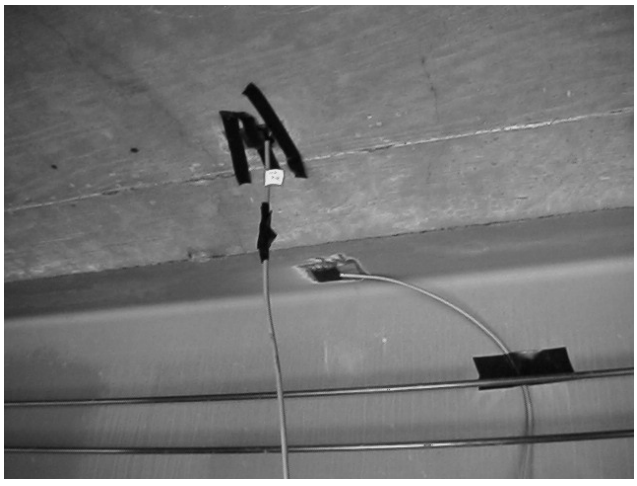

Figure 7. Strain gauges on top flange and bottom of deck

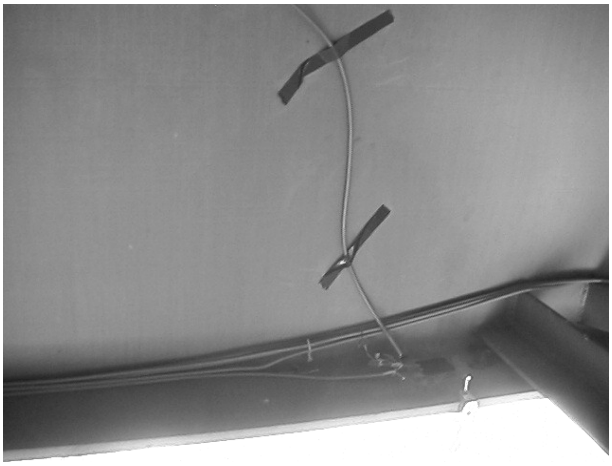

Figure 8. Strain gauge on bottom flange

Linear Variable Differential Transformers

The LVDTs were mounted to a steel frame beneath the two innermost beams at the midspan (adjacent to the strain gauges) to measure the deflection of the bridge deck. The steel frame served as the stationary or reference point for the LVDT. As shown in The spring-loaded tip of the LVDT was placed in contact with the bottom of the steel bridge beam. The bridge deck was the moveable point but the stationary point (the ground) was 23 feet below the deck. A permanent attachment would have interfered with local traffic under the bridge and invited vandalism; therefore, a removable setup was required. The distance from the deck to the ground created a challenge for installation and removal of the LVDTs for subsequent tests (once the man-lifts used to install the instrumentation were no longer on site). The solution employed a wire extending down from the steel beam with a weight attached to the end. The weight then moved with the motion of the bridge deck. The frame of the LVDT was attached to a weight on the ground to make it stationary and the movable rod was attached to the weight suspended from the bridge (Figure 9). In this way, relative displacements were accurately measured even though the LVDTs were physically located on the ground and not immediately under the deck.

Figure 9. Typical LVDT installation

Test	Lane Location		Direction	Speed	Span	
	Semi	Dump Truck			Semi	Dump Truck
0600-01	Inside	Outside	S	10		
0600-02	Inside	Outside	N	10		
0600-03	Inside	Outside	S	32		
0600-04	Inside	Outside	N	31		
0600-05	Inside	Inside	S	10		
0600-06	Inside	Inside	N	10		
0600-07	Inside	Inside	S	28		
0600-08	Inside	Inside	N	34		
0600-09	Outside	Outside	S	10		
0600-10	Outside	Outside	N	10		
0600-11	Outside	Outside	S	29		
0600-12	Outside	Outside	N	32		
0600-13	Inside	Inside	S	Static	2	1
0600-14	Inside	Inside	S	Static	3	2
0600-15	Inside	Inside	S	Static	4	3
0600-16	Inside	Inside	N	Static	3	4
0600-17	Outside	Inside	N	Static	2	3
0600-18	Outside	Inside	N	Static	1	2
0900-01	Outside	Inside	N	10		
0900-03	Outside	Inside	S	20		
0900-04	Outside	Inside	N	20		
0900-05	Outside	Inside	S	22-23		
0900-06	Outside	Inside	N	25-22		
0900-07	Outside	Inside	S	30		
0900-08	Outside	Inside	N	25-23		
0900-09	Outside	Inside	S		1	
0900-10	Outside	Inside	S		2	
0900-11	Outside	Inside	S		3	
0900-12	Outside	Inside	S		4	
0900-13	Outside	Inside	N		4	
0900-14	Outside	Inside	N		3	
0900-15	Outside	Inside	N		2	
0900-16	Outside	Inside	N		1	
0900-17	XXX	Outside	S	35		
0900-18	XXX	Outside	N	35		

Note: FB is front-to-back. SS is side-by-side. Spans are numbered from North to South.

Table 2. Testing Program

Location	Strain Gauges ◯	Load Cells □	LVDTs △
1	SG1.2 SG1.3	LC1.1	
2	SG2.2 SG2.3	LC2.1	
3	SG3.2 SG3.3 SGD3.4	LC3.1	
4	SG4.2 SG4.3	LC4.1	
5	SGD5.1		
6	SGD6.1 SG6.3 SG6.4		LVDT6.2
7	SG7.2 SG7.3		LVDT7.1
8	SG8.2 SG8.3		LVDT8.1
9	SG9.2 SG9.3	LC9.1	
10	SGD10.1		
11	SG11.2 SG11.3 SGD11.4	LC11.1	
12	SG12.2 SG12.3		LVDT12.1
13	SG13.2 SG13.3		
14	SG14.2 SG14.3		LVDT14.1

Table 3 Map for Portsmouth layout

TEST RESULTS

Plots of the measured response time histories for each test are compiled in the appendix. Summaries of those tests are presented in this section. Tables 4 and 5 are a listing of selected maximum deflections recorded during each load test. Where two values are given they represent the peak responses of each LVDT for tests where trucks crossed the bridge one after the other. The first value is the maximum deflection due to the first truck (less heavily loaded) and the second value corresponds to the second truck (greater load). Figure 10 is an example of one of these deflection time histories. The mean decrease in deflection for all speeds and LVDT locations was 0.04 mm or about 4%. The standard deviation for the deflections was 0.05 mm, which is greater than the decrease. Therefore, although there appears to be a slight decrease in the deflections after the composite rods were tensioned that decrease is less than the variability in the data.

		Microstrain (μcm/cm)						Deflection (cm)	
Test		SG7.3	SG8.2	SG8.3	SG11.3	SGD11.4	SG12.3	LVDT6.2	LVDT14.1
0600-01	Max	0	0	0	6	47	3	0.0000	0.0000
	Min	-1	0	0	-25	-10	-1	0.0000	0.0000
0600-02	Max	0	1	1	9	49	10	0.0234	0.1295
	Min	-2	0	0	-44	-17	-40	-1.7424	-0.1290
0600-03	Max	0	0	0	2	12	0	0.1803	0.1041
	Min	-1	0	0	-29	-9	-6	-0.0457	-0.0381
0600-04	Max	0	0	0	2	12	0	0.1803	0.1041
	Min	-1	0	0	-29	-9	-6	-0.0457	-0.0381
0600-05	Max	1	0	0	14	9	5	0.0000	0.0000
	Min	0	0	0	-21	-17	0	0.0000	0.0000
0600-06	Max	2	0	0	6	8	2	0.0279	0.0127
	Min	0	0	0	-22	-9	-2	-0.0178	-0.0178
0600-07	Max	0	1	1	6	3	1	0.0025	0.0000
	Min	0	0	0	-17	-14	-2	0.000	0.0000
0600-08	Max	0	0	0	0	4	1	0.0406	0.0152
	Min	-1	0	0	-27	-13	-1	-0.0645	-0.0177
0600-09	Max	0	0	0	5	76	2	0.0000	0.0000
	Min	-2	0	0	-22	-14	-1	0.0000	0.0000
0600-10	Max	0	0	0	7	13	2	0.1524	0.1041
	Min	-2	0	0	-24	-16	-2	-0.0330	-0.0203
0600-11	Max	0	0	0	9	71	2	0.0000	0.0000
	Min	-1	0	0	-23	-11	-1	0.0000	0.0000
0600-12	Max	1	0	0	4	7	1	0.1575	0.0965
	Min	-2	0	0	-20	-15	-2	-0.0330	-0.0254
0600-13	Max	4	0	0	0	12	0	0.0025	0.0000
	Min	0	0	0	-21	-11	-3	0.0000	-0.0025
0600-14	Max	3	1	1	5	11	1	0.0025	0.0000
	Min	0	0	0	-17	-13	-2	0.0000	-0.0025
0600-15	Max	4	1	1	3	0	0	0.0025	0.0000
	Min	0	0	0	-24	-16	-5	0.0000	-0.0025
0600-16	Max	0	0	0	0	51	0	0.0000	0.0000
	Min	-4	0	0	-31	0	-39	-0.0203	0.0000
0600-17	Max	0	0	0	7	26	1	0.0051	0.0000
	Min	-5	0	0	-10	0	-2	0.0000	-0.0178
0600-18	Max	0	0	0	8	22	0	0.0152	0.0000
	Min	-7	0	0	-18	0	-5	0.0000	-0.0102

Table 4 Maximum strain and deflection results from load tests before tensioning rods.

		Deflection (cm)				
Test		LVDT6.2	LVDT7.1	LVDT8.1	LVDT12.1	LVDT14.1
0900-01	Max	0.2387	0.3708	0.0000	0.0000	0.1498
	Min	-0.0838	0.0000	0.0000	0.0000	-0.0305
0900-03	Max	0.0000	0.3708	0.2209	0.1371	0.1676
	Min	0.0000	-0.0203	-0.0533	-0.0025	0.0000
0900-04	Max	0.2667	0.3708	0.0000	0.0000	0.1676
	Min	-0.0686	-0.0025	0.0000	0.0000	-0.0483
0900-05	Max	0.0000	0.3708	0.2515	0.1448	0.1702
	Min	0.0000	-0.0229	-0.0584	-0.0076	0.0000
0900-06	Max	0.2032	0.3683	0.0000	0.0000	0.1702
	Min	-0.0356	0.0000	0.0000	0.0000	-0.0305
0900-07	Max	0.0025	0.0609	0.2591	0.1488	0.0025
	Min	-0.0025	-0.0914	-0.0609	-0.0076	-0.0025
0900-08	Max	0.2032	0.3683	0.0000	0.0000	0.1727
	Min	-0.0356	0.0000	0.0000	0.0000	-0.0279
0900-09	Max	0.0000	0.0051	0.0000	0.1346	0.0000
	Min	0.0000	0.0000	-0.0381	0.0000	0.0000
0900-10	Max	0.0000	-0.0178	0.2540	-0.0076	0.0000
	Min	0.0000	-0.0178	0.2540	-0.0076	0.0000
0900-11	Max	0.0000	0.0102	-0.0609	0.0000	0.0000
	Min	0.0000	0.0102	-0.0609	0.0000	0.0000
0900-12	Max	0.0000	0.0025	-0.0025	0.0000	0.0000
	Min	0.0000	0.0025	-0.0025	0.0000	0.0000
0900-13	Max	0.0051	0.0025	-0.0025	0.0000	0.0000
	Min	0.0051	0.0025	-0.0025	0.0000	0.0000
0900-14	Max	0.0533	0.0025	-0.0025	0.0000	-0.0051
	Min	0.0533	0.0025	-0.0025	0.0000	-0.0051
0900-15	Max	0.0051	0.0000	0.0000	-0.0076	0.0813
	Min	0.0051	0.0000	0.0000	-0.0076	0.0813
0900-16	Max	0.0025	0.0508	0.0025	-0.0076	0.0838
	Min	-0.0025	-0.0635	-0.0051	-0.0106	0.0787
0900-17	Max	0.0000	0.0025	0.1397	0.0838	0.0000
	Min	0.0000	-0.0102	-0.0279	-0.0076	0.0000
0900-18	Max	0.1524	0.3683	0.0000	0.0000	0.1753
	Min	-0.0152	0.0025	0.0000	0.0000	-0.0229

Table 5 Deflection results from load tests after tensioning rods.

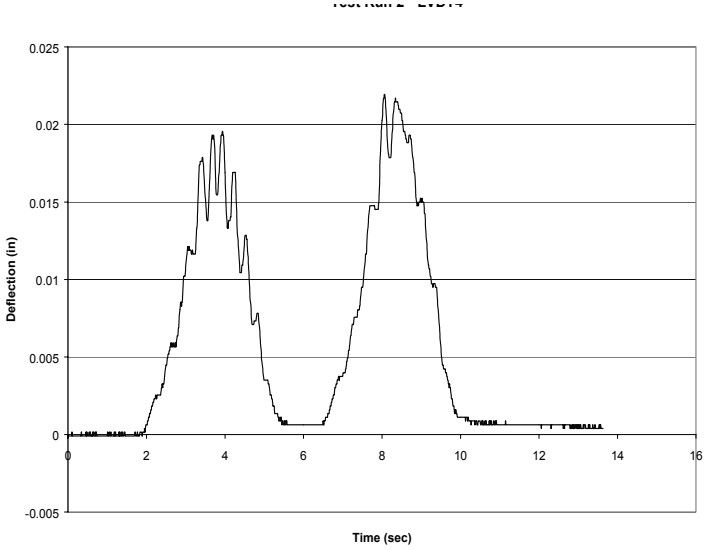

Figure 10 Typical field deflection data

Tables 6 and 7 lists selected maximum strains for each test. As in Tables 4 and 5, two values are given for each strain gauge for tests where trucks crossed the bridge one after the other. The strains varied widely but the recorded average peak strain appears to have increased after the rods were tensioned by 2%. However, the measured increases in strain the scatter in the results are likely due to the very small values recorded. It should be noted that, with small amplitudes such as those measured during the load tests, a change from one test to the next of the position one truck relative to the other, or the truck speed could account for the strain differences observed.

The load on the rods did not change as the trucks crossed the bridge. This can be seen in the plots of the load data (after tensioning) shown in Appendix B.

Figure 11 is a summary of the monthly readings to date of load on the rods for both bridges. As demonstrated in the table, the rods have maintained the load or shown a slight increase. The temperature was just above freezing when the rods where initially

		Microstrain (μcm/cm)						
Test		SG1.2	SG1.3	SG2.2	SG2.3	SG4.3	SGD5.1	SGD6.1
0600-01	Max	4	24	0	0	0	0	0
	Min	-1	-9	-1	-2	-1	-1	0
0600-02	Max	0	0	1	4	4	1	0
	Min	-1	0	-2	-20	-1	-2	-1
0600-03	Max	0	1	4	3	4	1	0
	Min	0	0	0	-16	0	-1	0
0600-04	Max	0	1	4	3	4	1	0
	Min	0	0	0	-16	0	-1	0
0600-05	Max	1	5	2	0	1	0	0
	Min	-1	-2	0	-1	0	0	0
0600-06	Max	2	2	2	2	4	1	0
	Min	0	0	0	-11	0	0	0
0600-07	Max	3	5	0	0	0	1	0
	Min	-1	-1	0	0	0	0	-1
0600-08	Max	1	1	1	1	2	0	0
	Min	0	0	0	-9	0	-1	0
0600-09	Max	4	14	0	0	0	0	0
	Min	-1	-14	-3	-3	-1	-1	0
0600-10	Max	1	1	1	1	2	2	0
	Min	-1	0	-1	-29	0	-2	0
0600-11	Max	4	9	0	0	0	0	0
	Min	-1	-13	-1	-1	-2	-1	0
0600-12	Max	0	0	2	2	1	1	0
	Min	0	0	-1	-24	0	-1	0
0600-13	Max	1	0	3	1	1	6	0
	Min	0	-1	0	0	0	0	0
0600-14	Max	0	6	3	1	1	6	0
	Min	-1	0	0	0	0	0	-1
0600-15	Max	2	7	4	2	2	6	0
	Min	0	0	0	0	0	0	-1
0600-16	Max	0	0	0	0	1	0	0
	Min	-9	-6	-4	-11	0	-4	0
0600-17	Max	0	0	0	0	0	0	0
	Min	-11	-9	-7	-8	-1	-7	0
0600-18	Max	0	0	0	0	0	0	0
	Min	-11	-8	-10	-6	-4	-7	0

Note: All values given in microstrain (μ).

Table 6 Maximum strain results from load tests before tensioning rods.

Test		SG1.2	SG1.3	SG2.2	SG2.3	SG3.2	SG3.3	SGD3.4
0900-01	Max	1	0	2	4	92	5	0
	Min	0	0	0	-33	-28	-5	-1
0900-03	Max	5	20	0	0	0	2	17
	Min	0	-10	0	0	0	-1	-3
0900-04	Max	1	1	2	5	92	7	0
	Min	0	0	0	-33	-25	-7	0
0900-05	Max	5	20	1	0	1	3	16
	Min	0	-11	0	0	0	0	-3
0900-06	Max	0	0	3	2	63	11	0
	Min	0	0	0	-27	-18	-7	0
0900-07	Max	10	23	3	4	3	3	17
	Min	-4	-14	-1	-5	-7	-7	-2
0900-08	Max	0	0	3	3	63	11	0
	Min	0	-2	0	-26	-18	-8	-1
0900-09	Max	0	0	0	0	0	0	0
	Min	-6	-7	-7	-9	-7	-7	-1
0900-10	Max	-7	-4	-5	-9	-5	-5	7
	Min	-7	-4	-5	-10	-6	-7	7
0900-11	Max	-4	-18	-7	-12	-7	-9	18
	Min	-5	-18	-8	-12	-8	-12	17
0900-12	Max	-2	-7	-8	-14	-10	-10	-1
	Min	-2	-8	-9	-15	-11	-12	-1
0900-13	Max	-10	-14	-6	-18	-12	-14	-1
	Min	-10	-14	-7	-18	-13	-14	-1
0900-14	Max	-11	-17	-7	-14	-14	-12	-1
	Min	-12	-17	-9	-16	-16	-14	-1
0900-15	Max	16	16	21	19	76	18	-7
	Min	15	15	20	19	76	15	-7
0900-16	Max	18	15	21	18	114	19	-5
	Min	9	10	12	13	104	10	-10
0900-17	Max	4	10	0	0	0	0	8
	Min	0	-6	0	0	0	0	-1
0900-18	Max	0	0	2	2	18	9	0
	Min	0	0	0	-17	-7	-7	0

Note: All values given in microstrain (μ).

Table 7 Strain results from load tests after tensioning rods.

tightened in November, therefore any deviations above or below freezing could result in different expansion or contraction of the rods relative to the concrete beams. These results suggest that relaxation of the fiberglass rods should not be a concern.

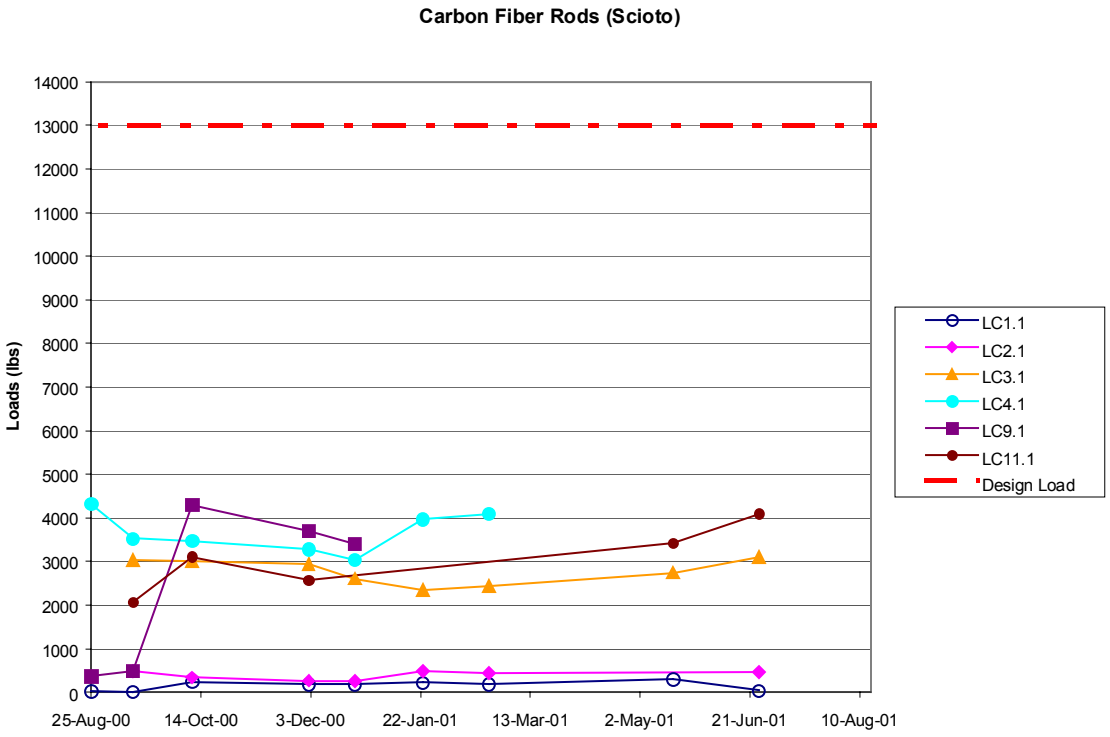

Figure 11 Summary of monthly readings

MODALL DESCRIPTION

In order to perform an independent check of the field measurements and to suggest an approach to predicting the effect of external reinforcements on similar bridges, a finite element model using the commercial software package, ANSYS, was developed. To compare the measurements recorded during the load tests with a computed dynamic deflection, the bridge was modeled as a twenty element, two-dimensional beam using standard elements included in the ANSYS library (see Figure 12). Each node had three degrees of freedom, translation along the length of the bridge, vertical translation, and rotation in the plane of the allowed translations. End conditions were modeled by allowing limited rotation of the bridge deck by adding vertical beam elements to the node at each end of the bridge to simulate the abutments. The two end elements were fixed at their bases resulting in bending being allowed at the node connected to the bridge deck but restricted by the beam stiffness. Figure 13 is a detail of one end of the bridge showing one of the vertical elements. The response of the structure to load was assumed to be linear and elastic.

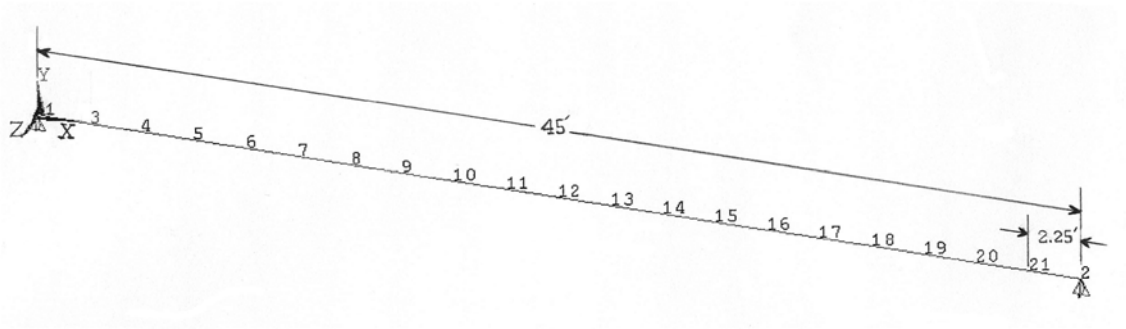

Figure 12. 20-element simply supported model.

For a linear elastic beam element, the stiffness (K) is a function of the elastic modulus (E), the moment of inertia (I), and the beam length (L). Since the length of the bridge was known, stiffness was evaluated in terms of the effective modulus and moment of inertia (I_e).

Modeling the bridge as one material required the use of one modulus for both concrete and the reinforcing steel. This should result in a slightly higher value than would be appropriate for concrete alone. Initially, the elastic modulus of the bridge was assumed

equivalent to a standard value for elastic modulus of normal strength concrete, 22,000 MPa (4.608×10^8 psf , Hibbeler, 1994).

The moment of inertia is a function of the height, width, reinforcement, cracking and distribution of area with respect to the neutral axis. The moment of inertia was 0.3 m^4 and the area 3.6 m^2 which were calculated from the plan for the bridge provided by ODOT. The Adding external stiffeners, such as the composite rods in this study, can increase both the moment of inertia (similar to the addition of reinforcing steel) and the elastic modulus for the bridge. The damping ratio was assigned a value of 0.10 and assumed equal for all modes as suggested by Weaver and Johnson (1987). However, as a check on this assumption, the effect on the calculated deflection of damping values ranging from 0.0 to 0.15 was evaluated. For truck speeds up to 50 km per hour the calculated deflections differed by no more than 10%.

Since no truck load data were available for the COS-79-0955 tests, the loads to simulate the test trucks as they moved across the bridge were taken from the axle weights obtained for the trucks used to load SCI-23 . The front axle weight was taken to be 75 kN and for the rear axle the load was 180 kN. Since the load tests before and after tensioning were conducted on the same day with the same trucks, any effects of small discrepancies between assumed and actual weights should be expected to be negligible. The loading time step (the increment of time required to reach the peak value) was taken to be equal to the time required for the truck to travel the distance of one element. Therefore different time steps were used for the load function in order to represent different truck speeds. The load ramped up at the first node to simulate the truck approaching that point and then decreased to simulate unloading. While the load ramped down at the first node it simultaneously ramped up at the next node. See Figure 14 for the graphical representation of the loading. In this way, the full force of each axle was continuously applied to the bridge.

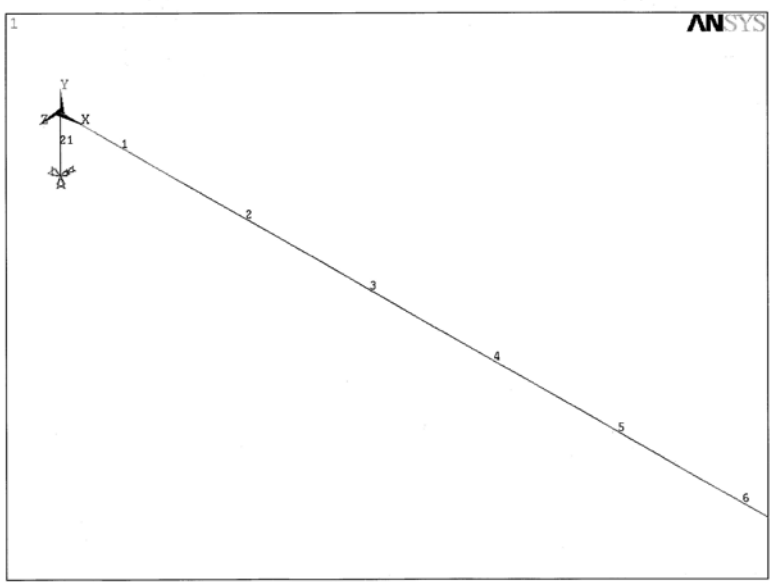

Figure 13. Model Abutment Detail

The amount of end constraint had the greatest effect on the calculated response to loading so the vertical beam stiffness was adjusted until the predicted deflections of the pre-tensioned bridge agreed with the measured values. With the properties of the bridge thus determined, the effects of the tensioned composite rods on the response of bridge to loads were considered. The effect of the rods was taken to be primarily due to the compressive load and

the corresponding moment about the neutral axis. It was assumed that the modulus of the composite rods would not contribute significantly to the effective modulus of the bridge (the fiberglass rods provided a negligible increase in either flexural or extensional rigidity). Because the rods were placed only on the outer beams, the post-tensioning effect is not even over the cross-section of the bridge. However, Klaiber et al. (1981, 1983) demonstrated the feasibility of strengthening a 4-beam simple span bridge on steel beams by post-tensioning only the exterior beams. The results of that study showed that when only the exterior beams were post-tensioned, about two-thirds of the post-tensioning remained in the exterior beams while the remainder was distributed among the interior members. Since the subject bridge is relatively small, the effects of the post-tensioning should contribute some added strength at the center, although less than at the outer beams. The LVDTs were placed below the center beams because this was where deflection would be greatest.

The composite rods were modeled as an applied compressive load and moment. The load was applied as a 285 kN force (8 rods x 36 kN design load) at the nodes representing the bracket locations. A moment of 46.5 kN·m, (285 kN x 0.163m) was applied to the same nodes. Both the moment and the force remained constant for the duration of the simulated truck loading.

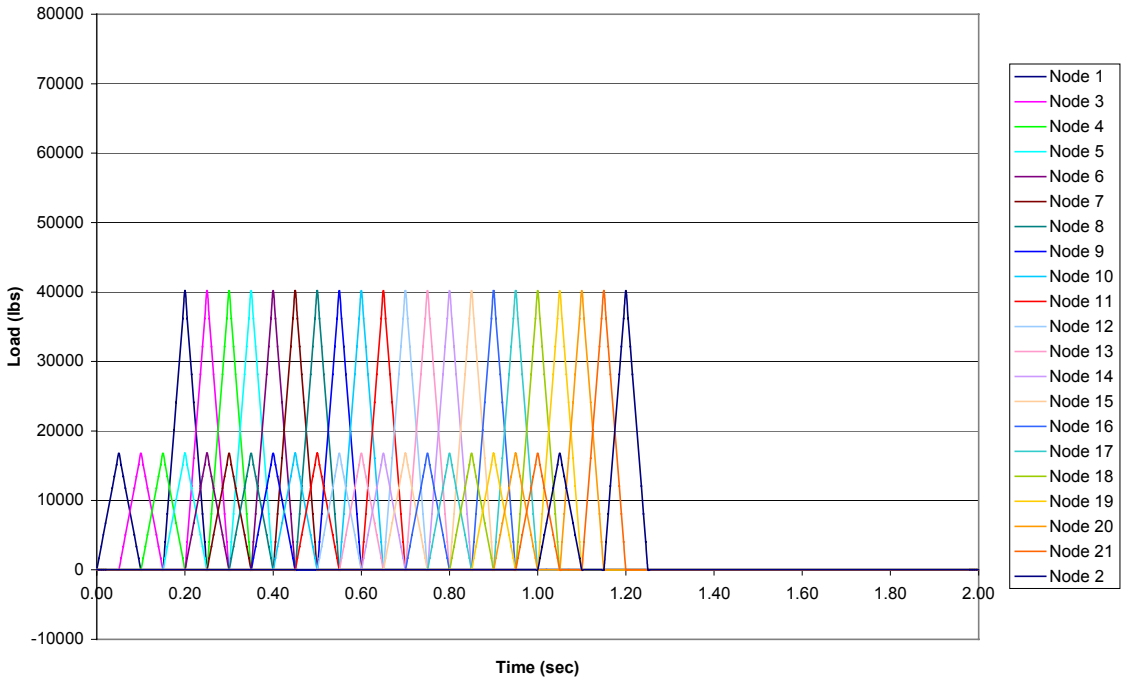

Figure 14 Ramped load function.

At a speed of 50 km/hr the ANSYS model predicted a decrease in maximum deflection of 2.4% for the reinforced bridge. Since the bridge is modeled as a 2-D beam, the compressive stress is applied evenly over the cross-section and the variation in stress across the beam is not properly accounted for. The actual bridge will have a higher concentration of stress near the brackets and less added compressive stress at the top and bottom of the beam and correspondingly less benefit. Although the model deflections match the tests within the limitations of the field measurements, further testing with greater tensile loads would verify the effectiveness of this method for stiffening bridges. The loads applied by the composite rods did not increase the stiffness enough to document a verifiable change in the deflection. The improvement suggested by the model is small enough that slight variations in the conditions between field tests (such as truck speed or position) could nullify the change. Using the numerical model to evaluate the effect of varying rod tension, a relationship between the decrease in deflection and rod tension can be developed. For example a 10% reduction in deflection would require each rod to carry 153 kN (34,500 lbs). Decreasing deflection by 10 to

20 percent is a large enough difference to minimize the effect due to test variables such as speed and transverse location of the trucks as they cross the bridge. However, incorporating loads five times, or greater, the original design load would require reanalyzing the design of all parts to determine if such loads are feasible. A greater total load could be applied by increasing the number of rods. Increasing the number of rods (without increasing the load on each rod) would spread the load more evenly across the width of the bridge by placing the additional rods on the center beams. Increasing the loads on individual rods might be best accomplished by using a better bracket assembly so that the rods could carry a larger load.

SUMMARY AND CONCLUSIONS

The deflection results suggest a small (4%) decrease in the maximum midspan deflection, after the installation and tensioning of the composite rods. However, this decrease is less than the variability that should be expected in the readings. Further the strain results suggest no improvement. Results from the Portsmouth bridge suggest the rods were unloaded during the time between the post-tensioning of the rods and the following tests. Therefore, no improvement was shown in the stiffness of this bridge.

Monthly load readings for the composite rods show the rods have not maintained their initial tension.

APPENDIX A

BIBLIOGRAPHY

Klaiber F.W., Dunker K.F., and Sanders W.W. 1981. "Feasibility Study of Strengthening Existing Single Span Steel Beam Concrete Deck Bridges". Final Report, Engineering Research Institute Project 1460, ISU-ERI-Ames-81251, Iowa State University.

Klaiber F.W., Dedic D.J., Dunker K.F., and Sanders W.W. 1983. "Strengthening of Existing Single Span Steel Beam and Concrete Deck Bridges". Final Report – Part I, Engineering Research Institute Project 1536, ISU-ERI-Ames-83185, Iowa State University.

Status of the Nation's Highways, Bridges, and Transit: Conditions and Performance. Federal Highway Administration, Washington, D.C., January 1999.

Weaver W. jr, Johnston P.R. 1987. *Structural Dynamics by Finite Elements*. Englewood Cliffs, New Jersey: Prentice-Hall.

APPENDIX B

RESULTS FROM
PORTSMOUTH BRIDGE
AFTER POST-TENSIONING

B.1 Results

The following are the results from the load test taken September 13, 2000. The time-history plots of the data are then shown for each test. The plots for each test are grouped according to transducer type – 1st strain gauges, 2nd load cells, 3rd LVDTs.

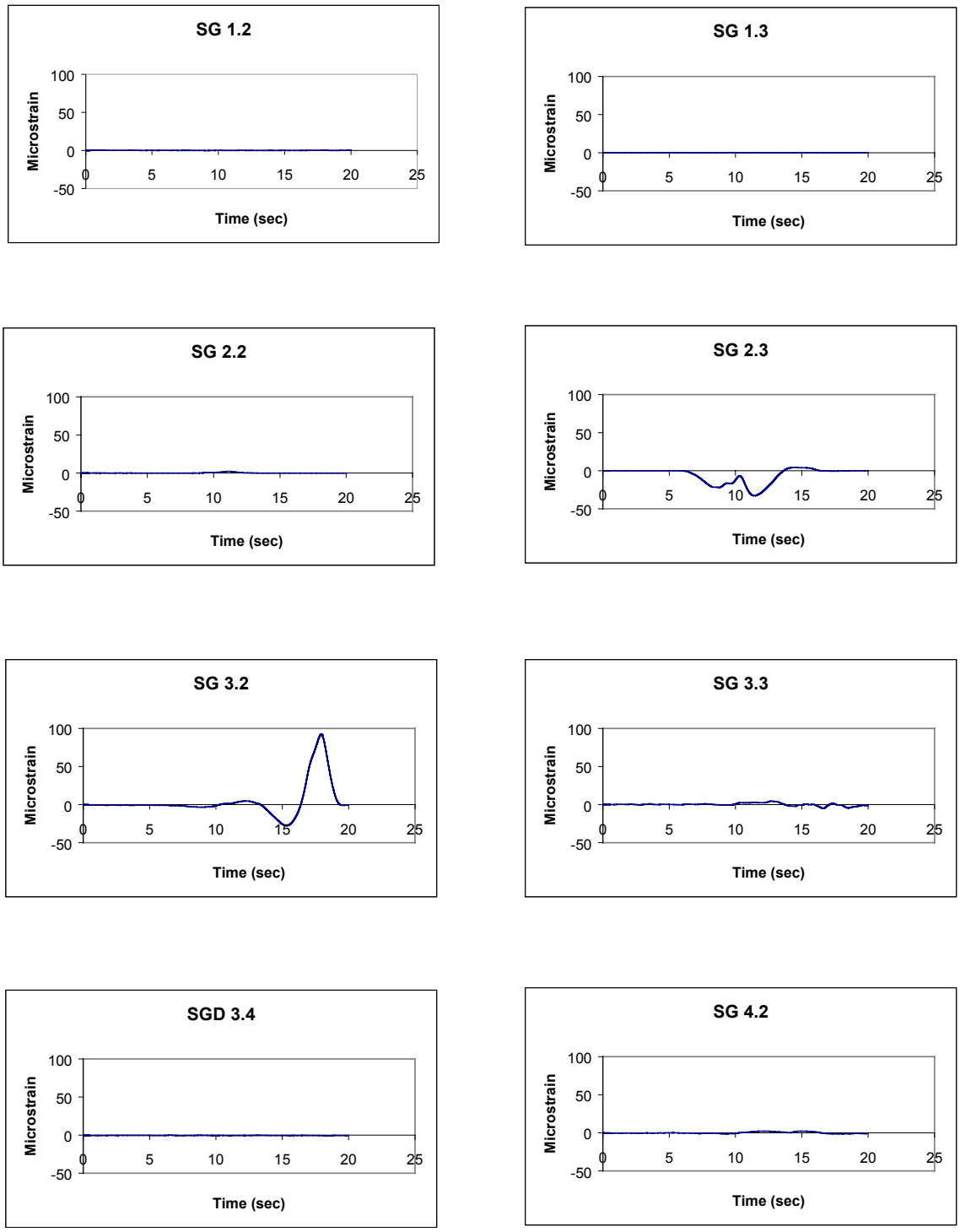

Figure B.1 Time-history of strain for test 0900-01.

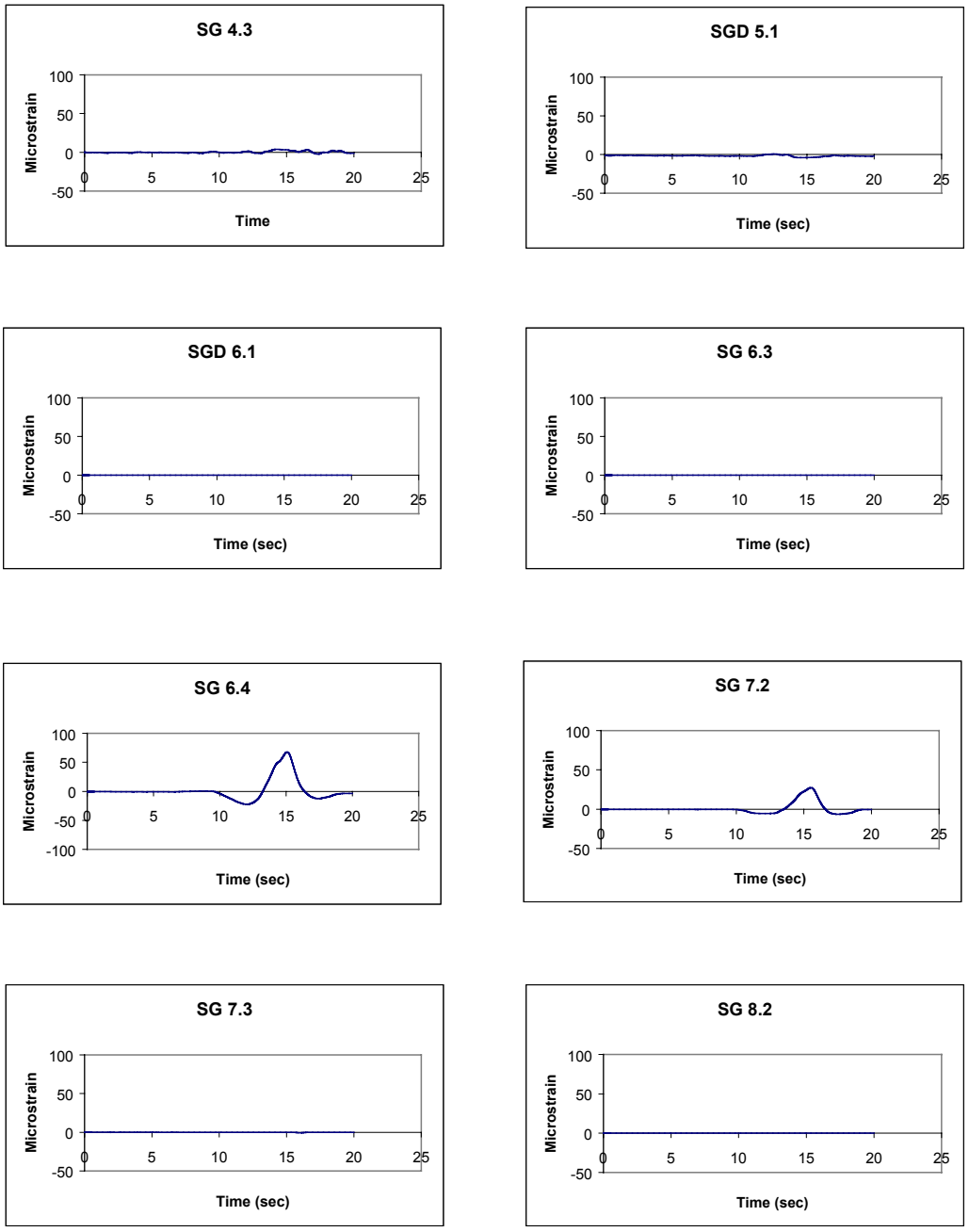

Figure B.2 Time-history of strain for test 0900-01.

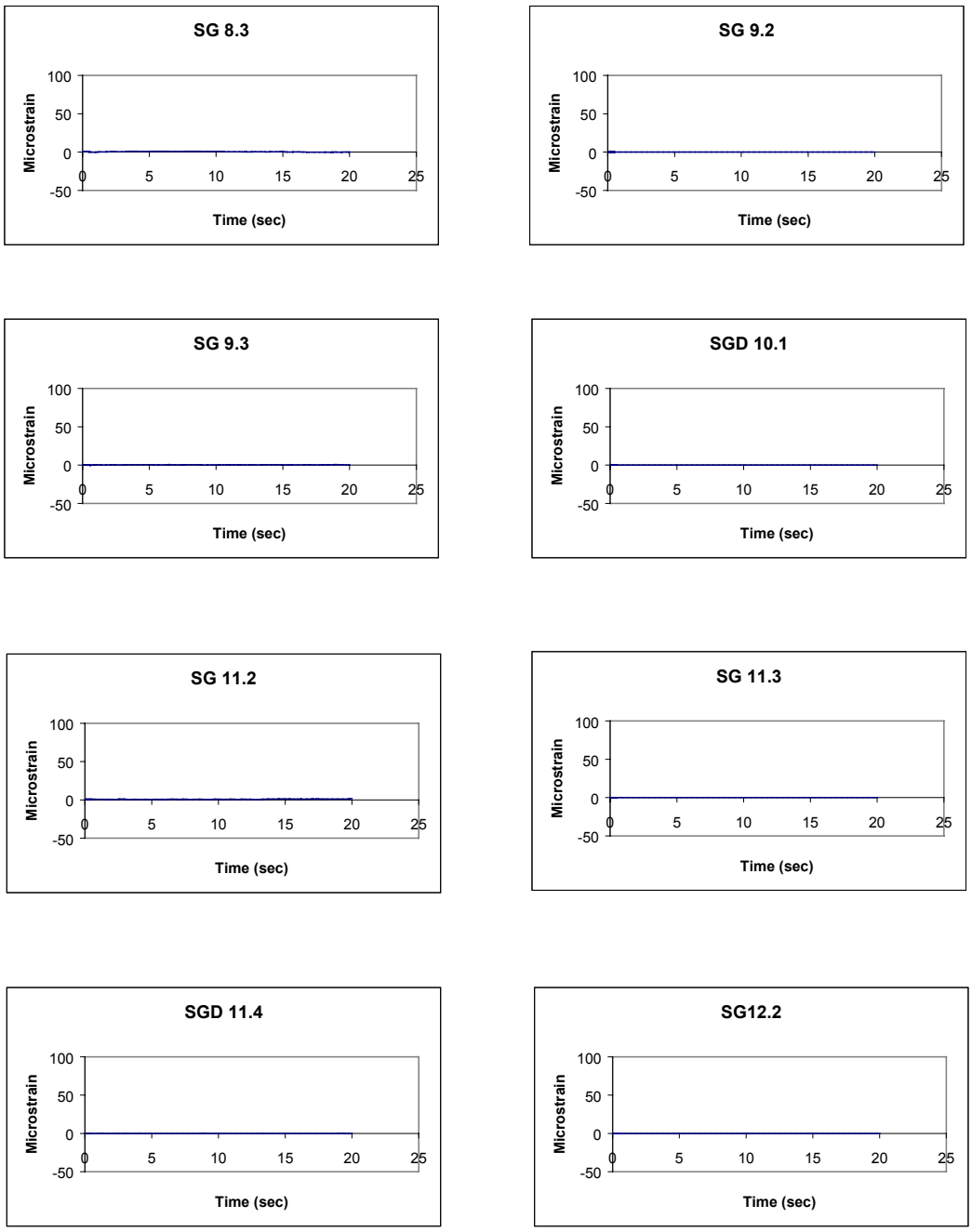

Figure B.3 Time-history of strain for test 0900-01.

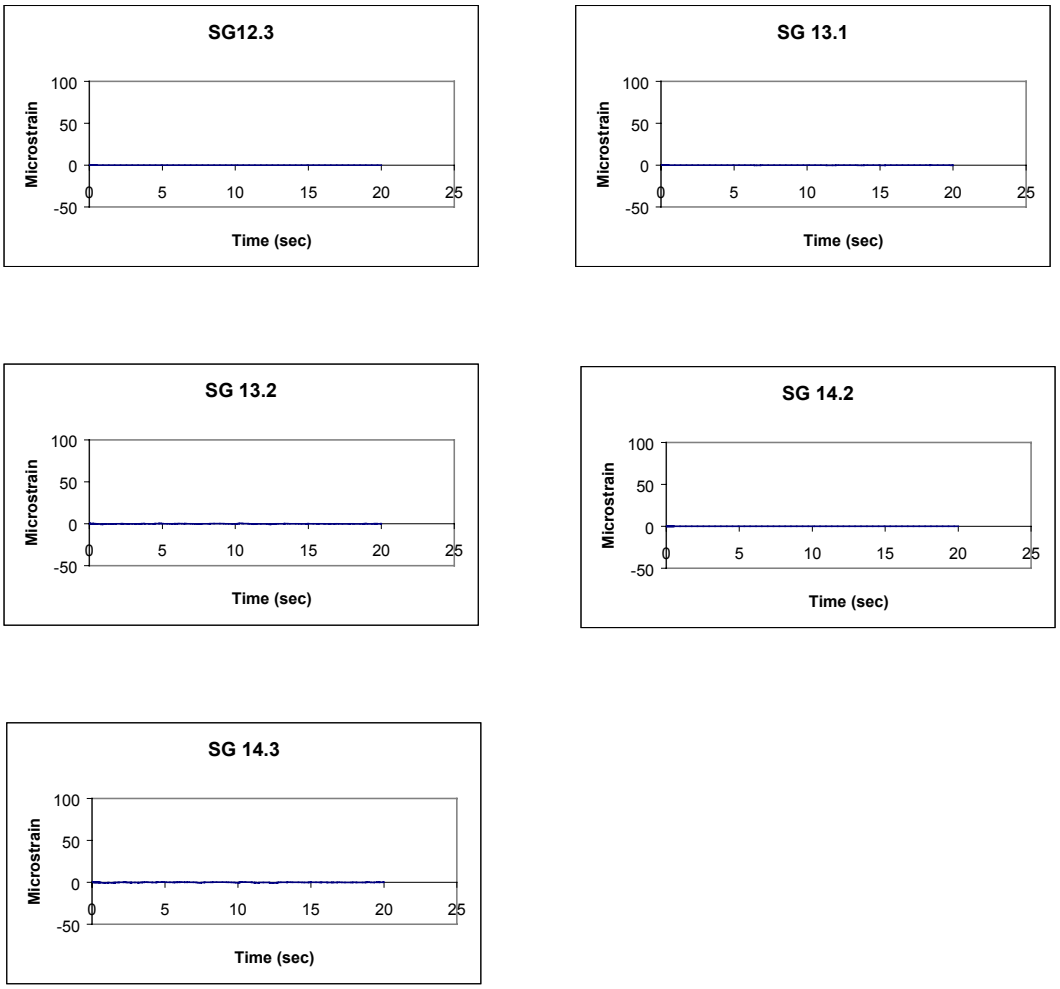

Figure B.4 Time-history of strain for test 0900-01.

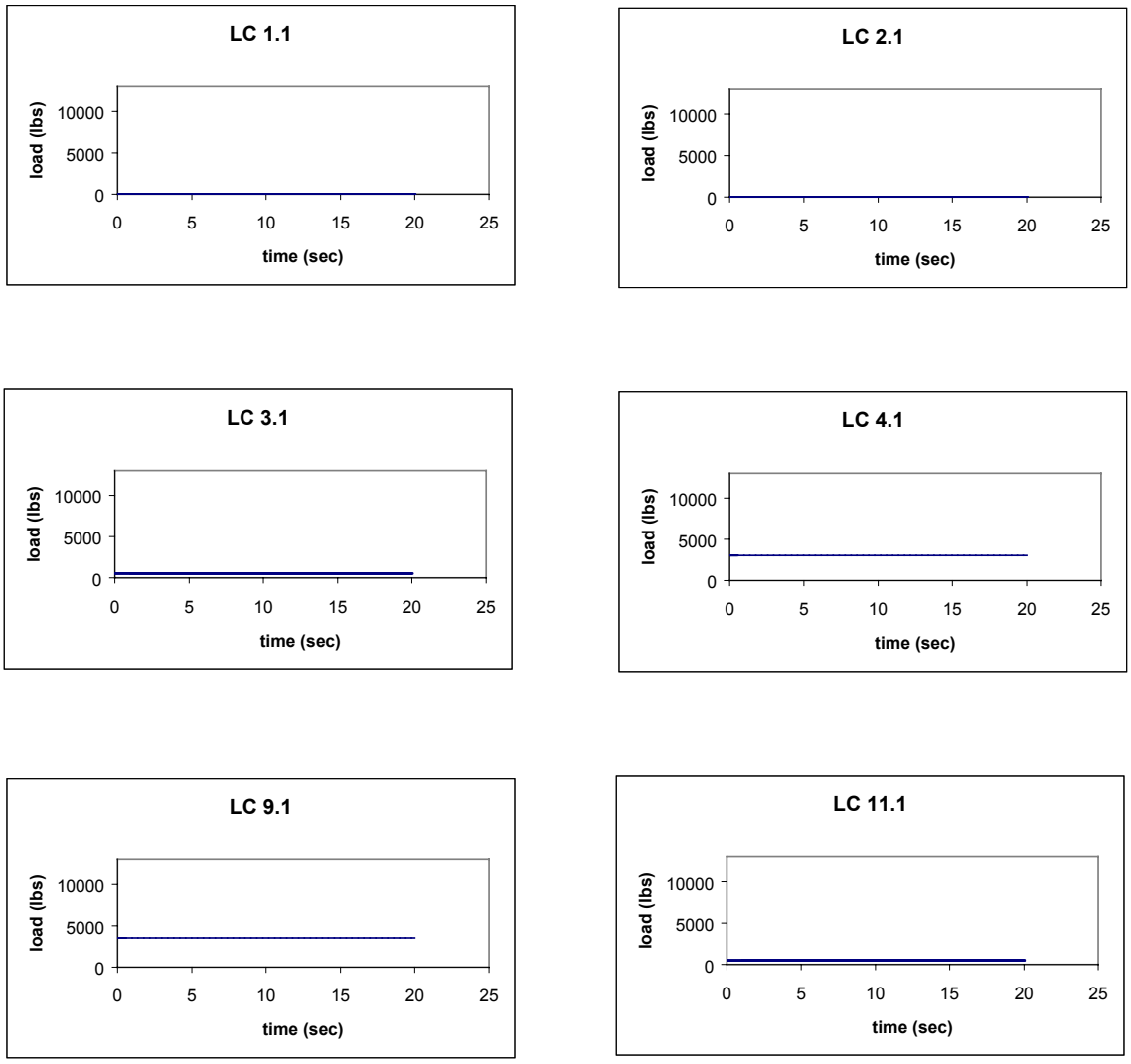

Figure B.5 Time-history of load for test 0900-01.

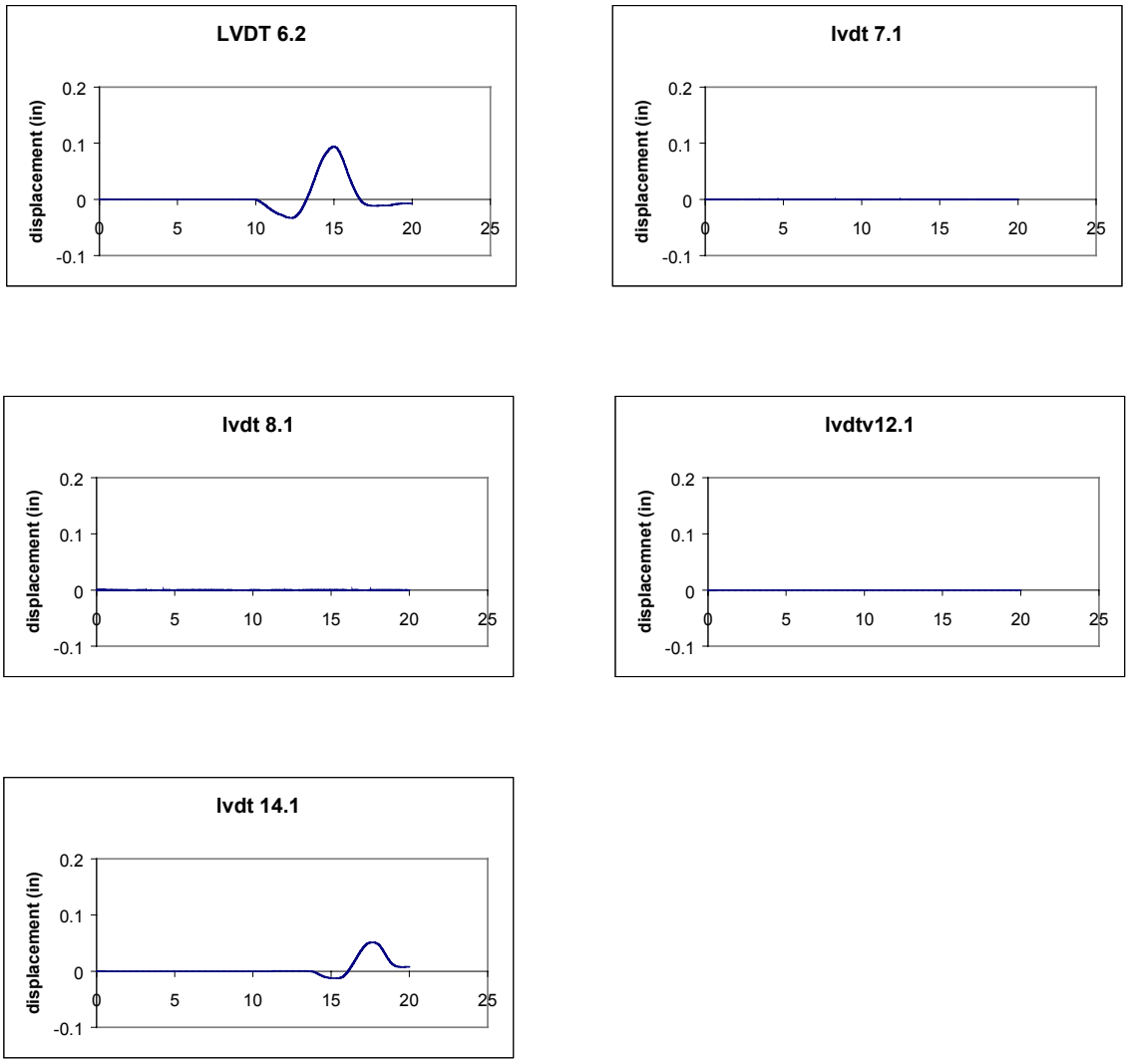

Figure B.6 Time-history of deflection for test 0900-01.

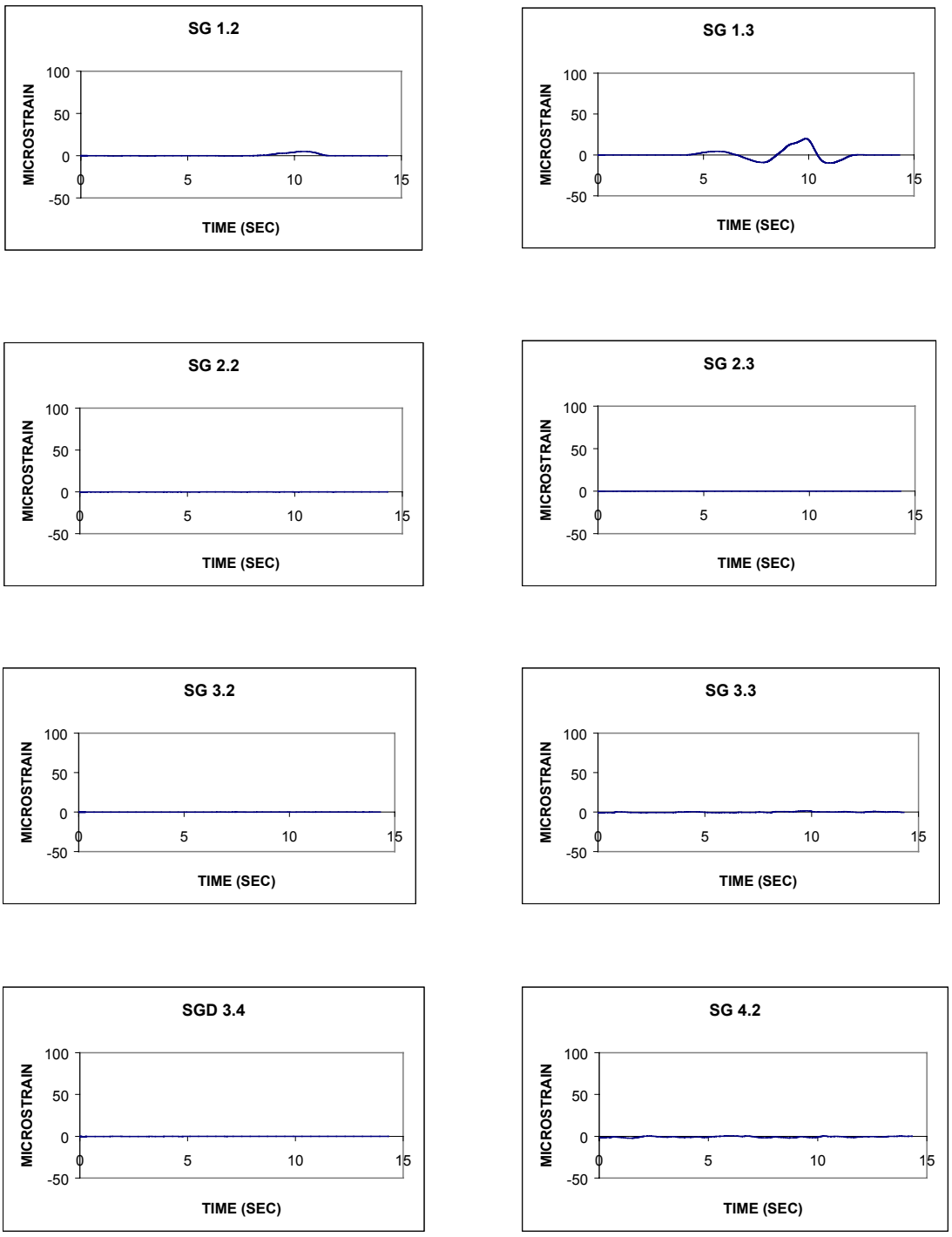

Figure B.7 Time-history of strain for test 0900-03.

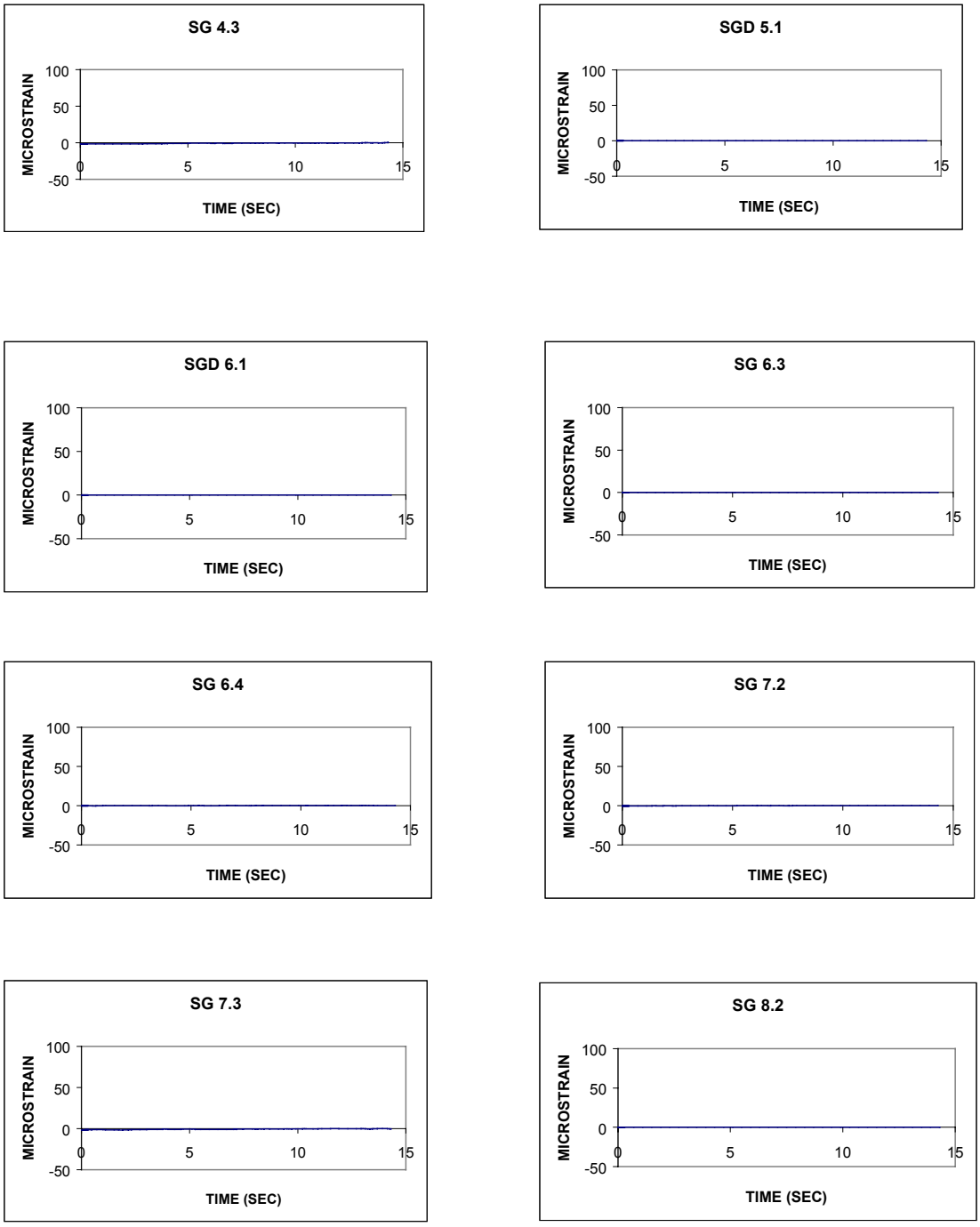

Figure B.8 Time-history of strain for test 0900-03.

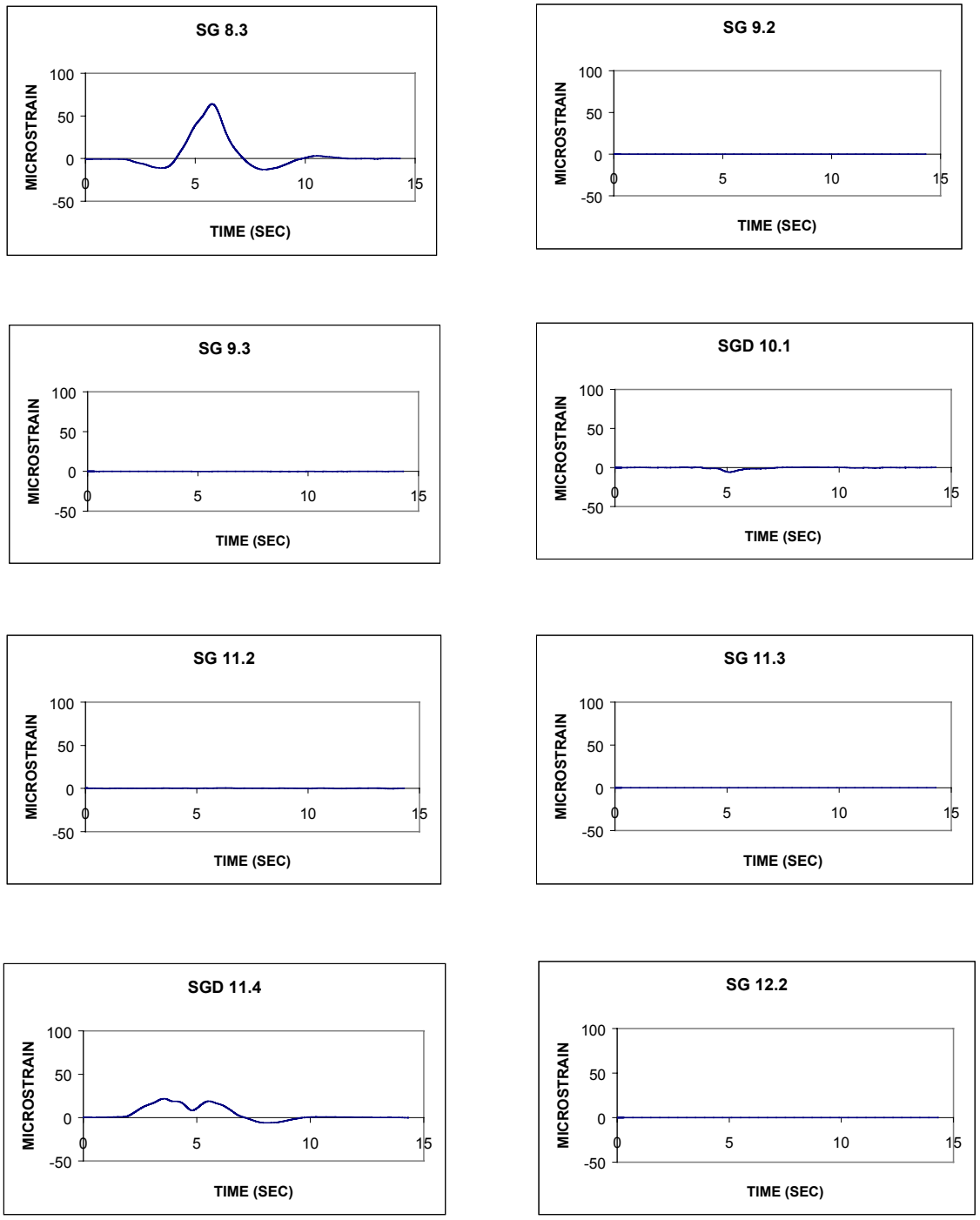

Figure B.9 Time-history of strain for test 0900-03.

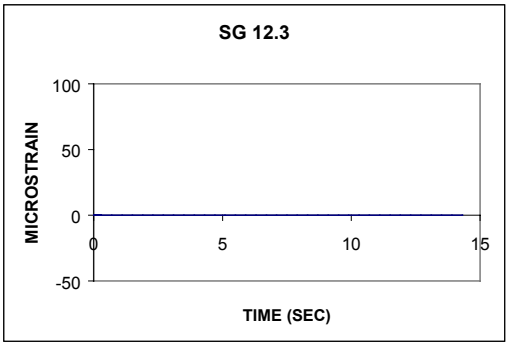

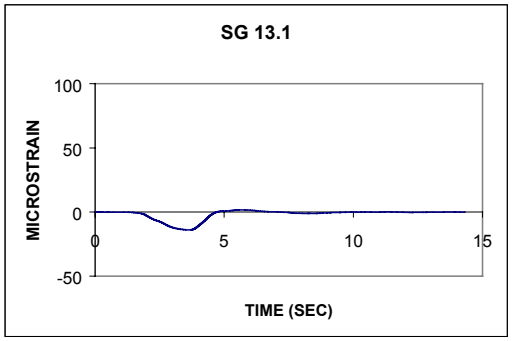

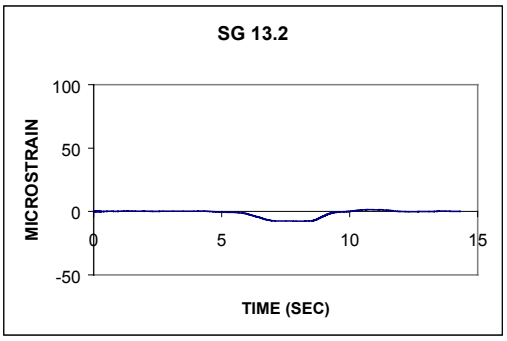

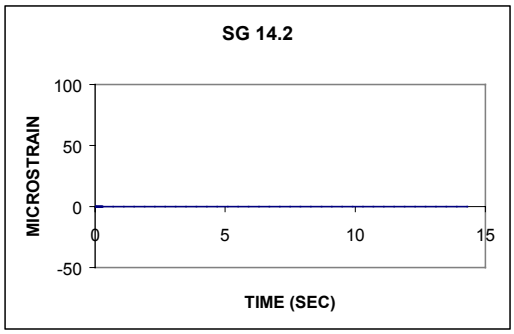

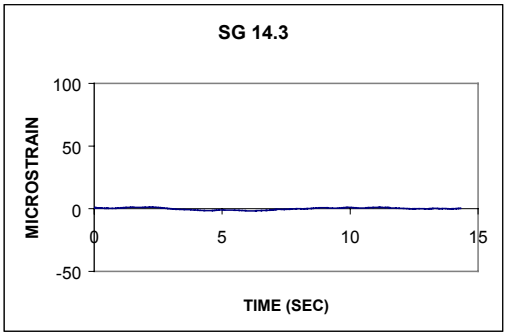

Figure B.10 Time-history of strain for test 0900-03.

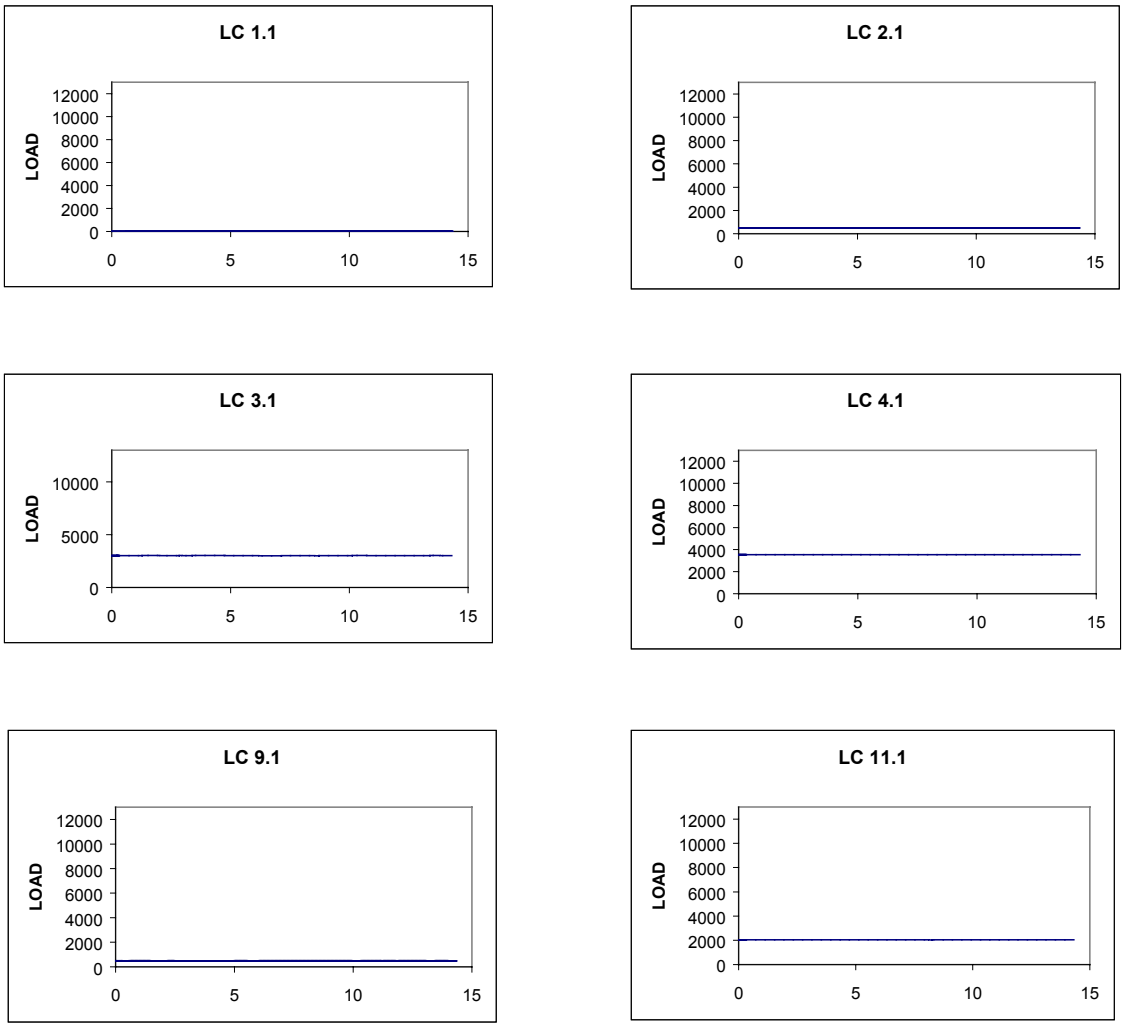

Figure B.11 Time-history of load for test 0900-03.

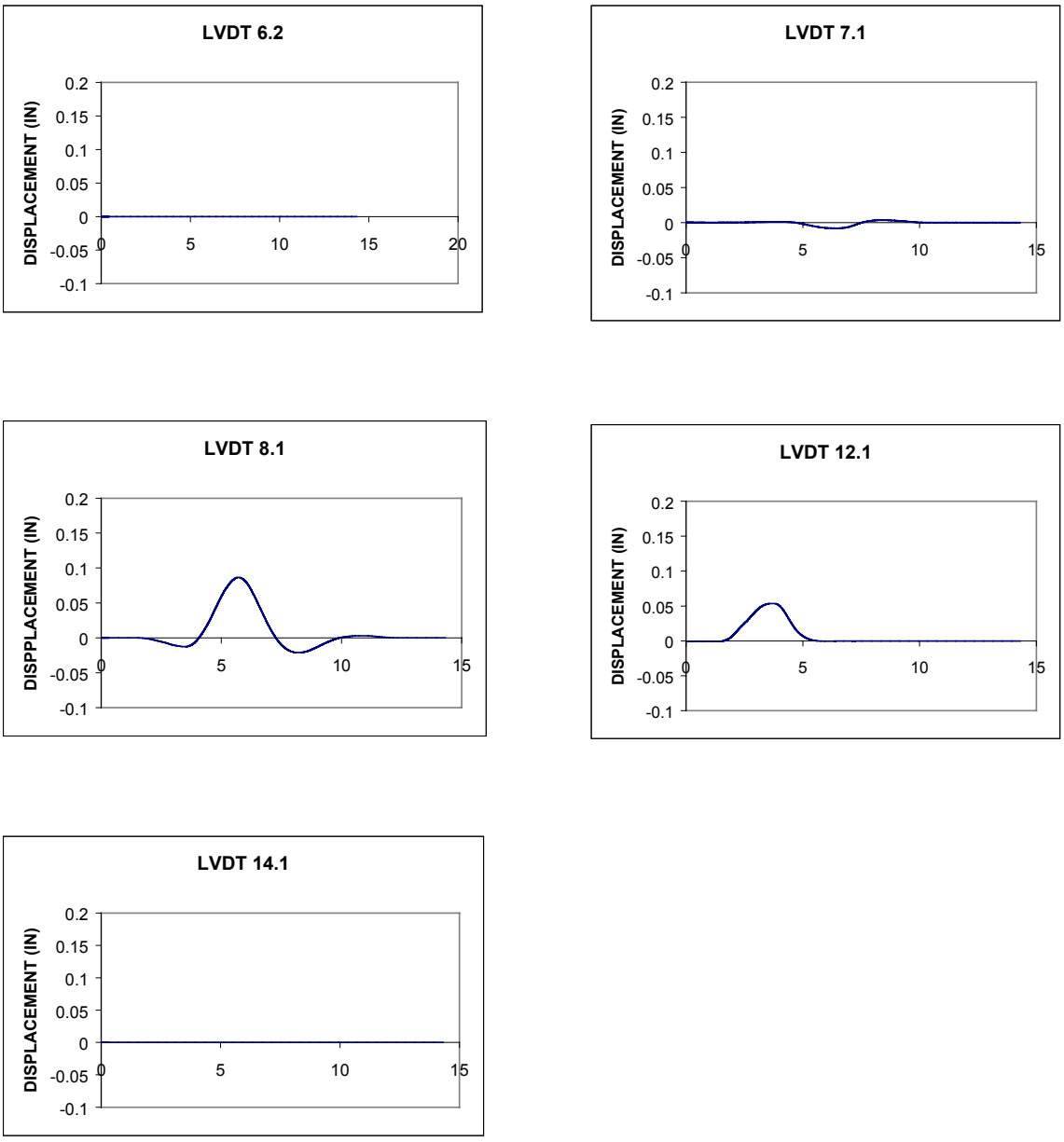

Figure B.12 Time-history of deflection for test 0900-03.

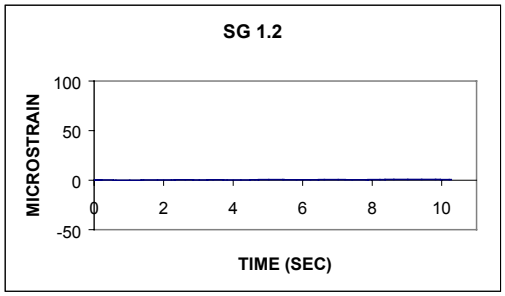

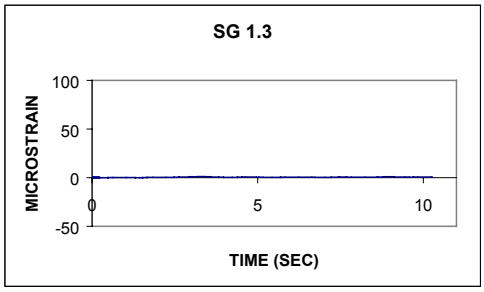

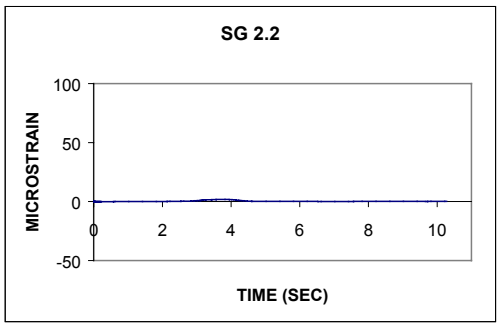

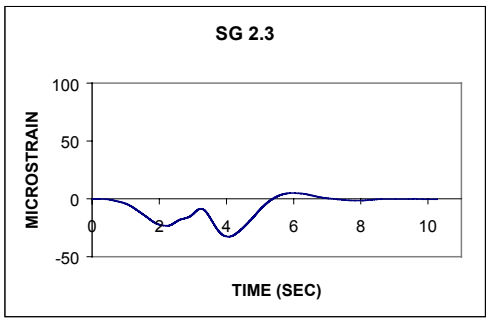

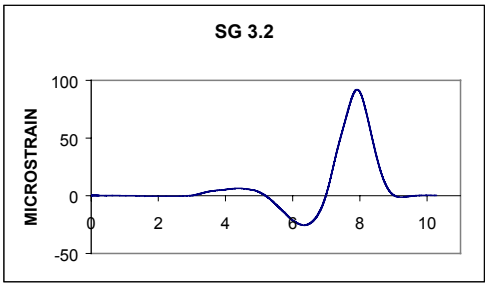

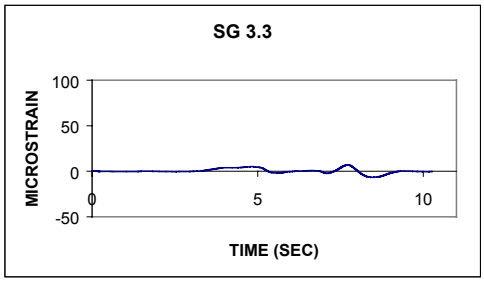

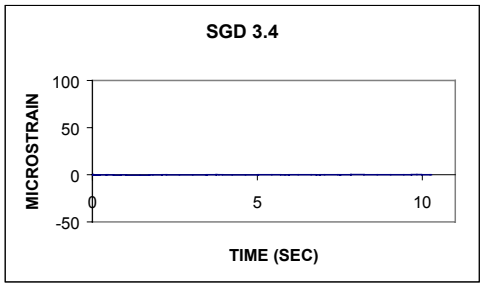

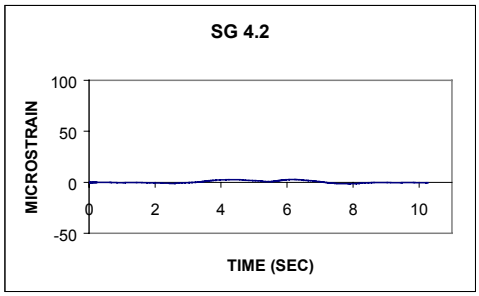

Figure B.13 Time-history of strain for test 0900-04.

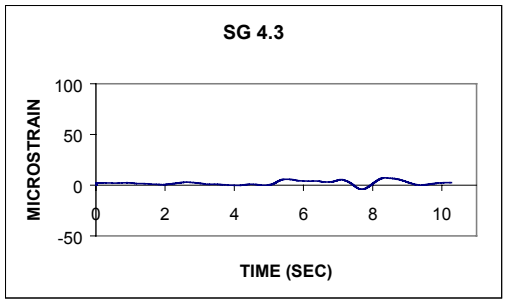

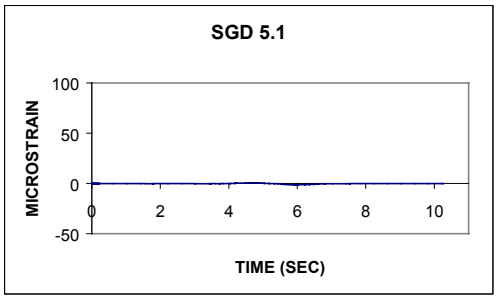

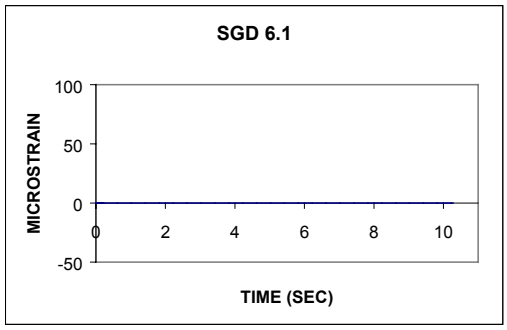

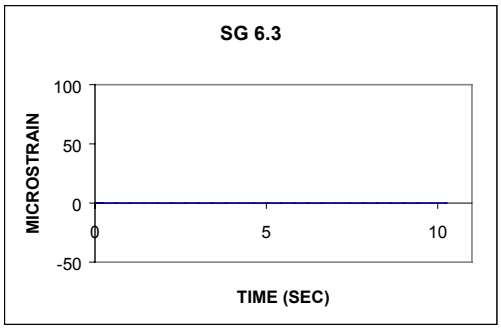

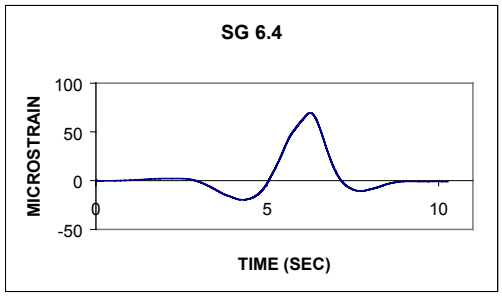

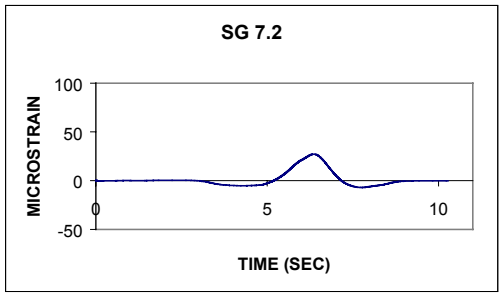

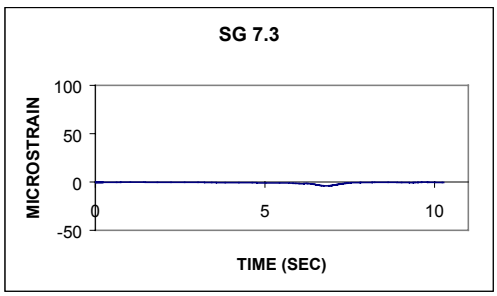

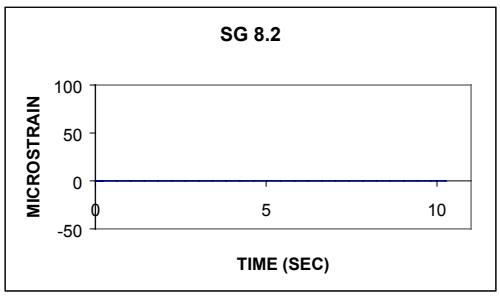

Figure B.14 Time-history of strain for test 0900-04.

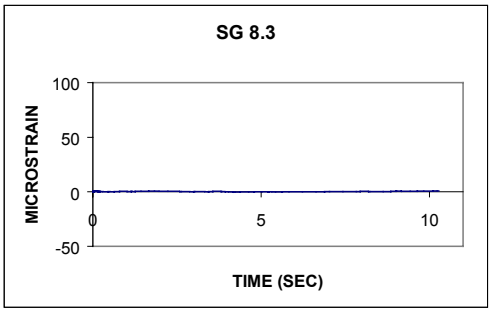

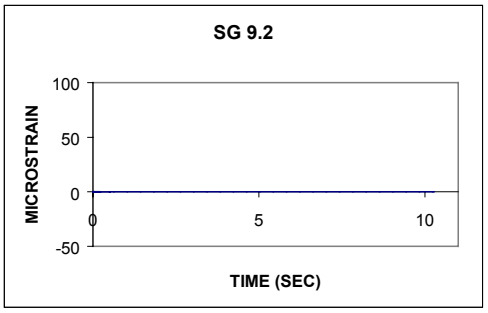

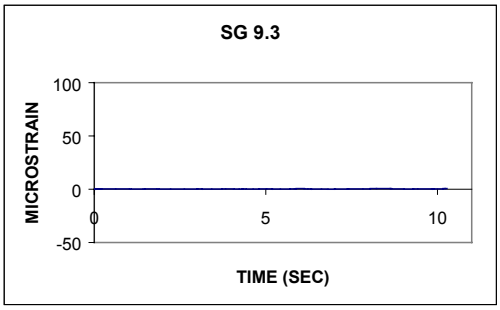

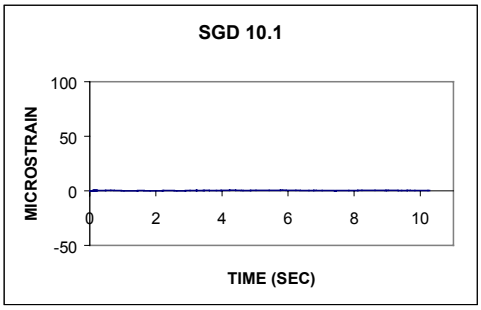

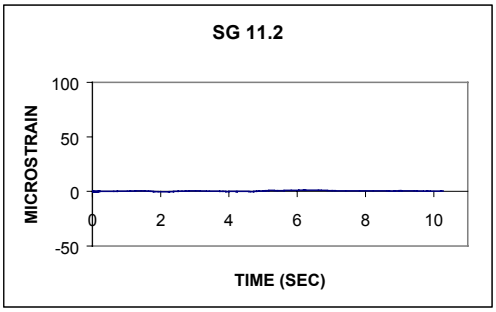

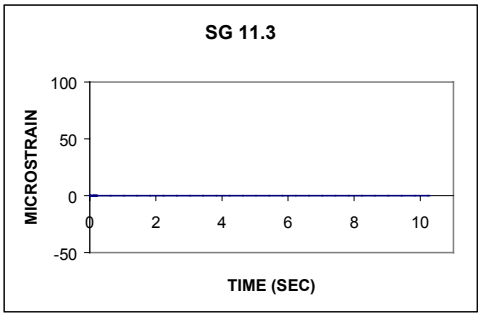

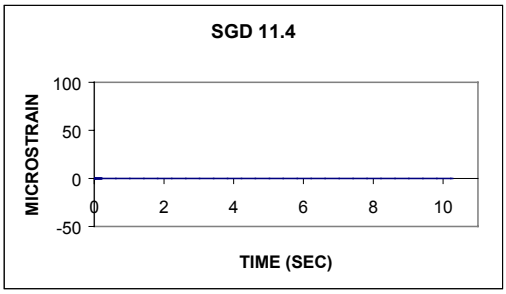

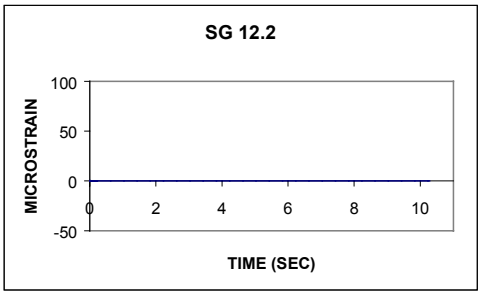

Figure B.15 Time-history of strain for test 0900-04.

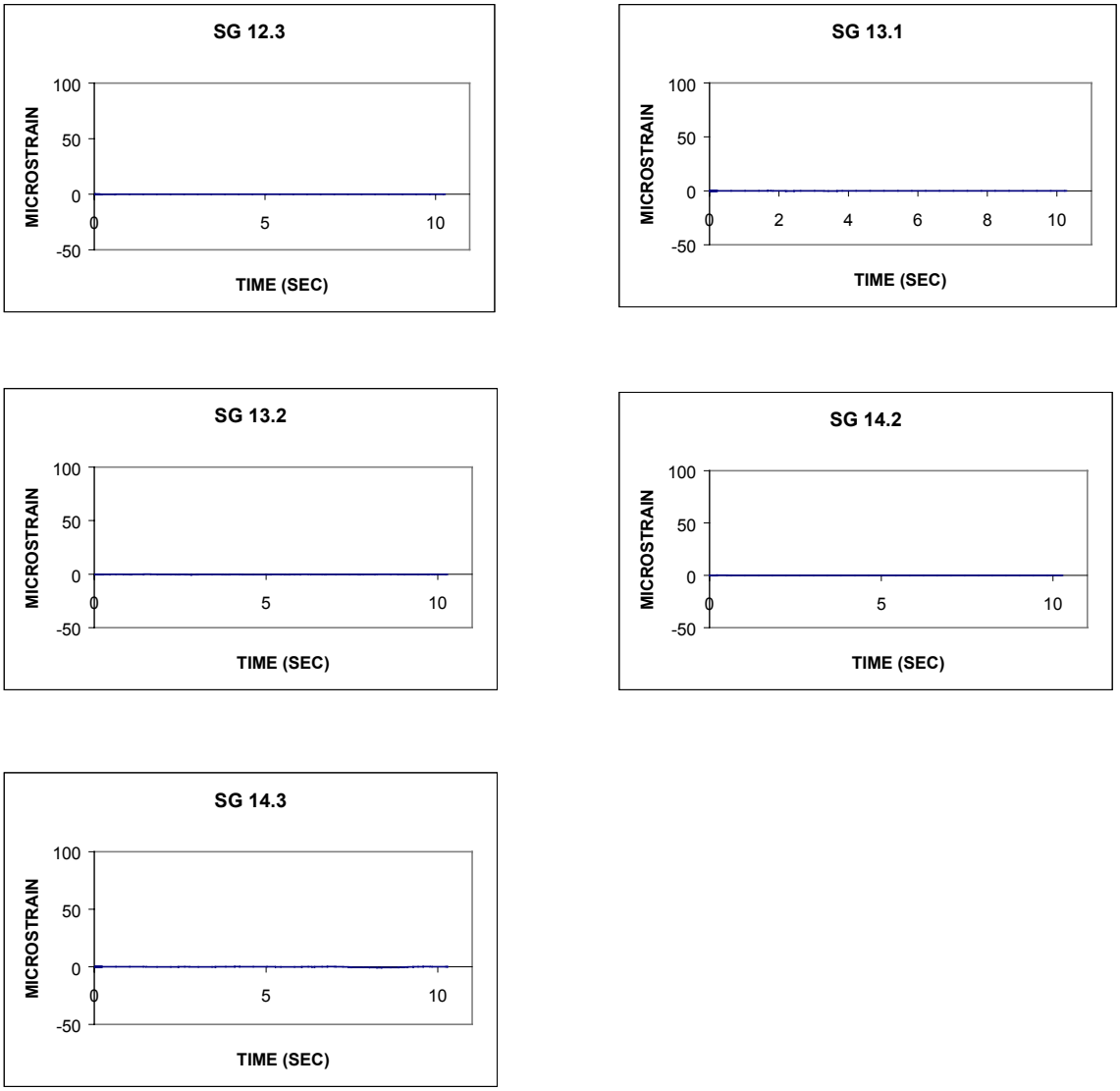

Figure B.16 Time-history of strain for test 0900-04.

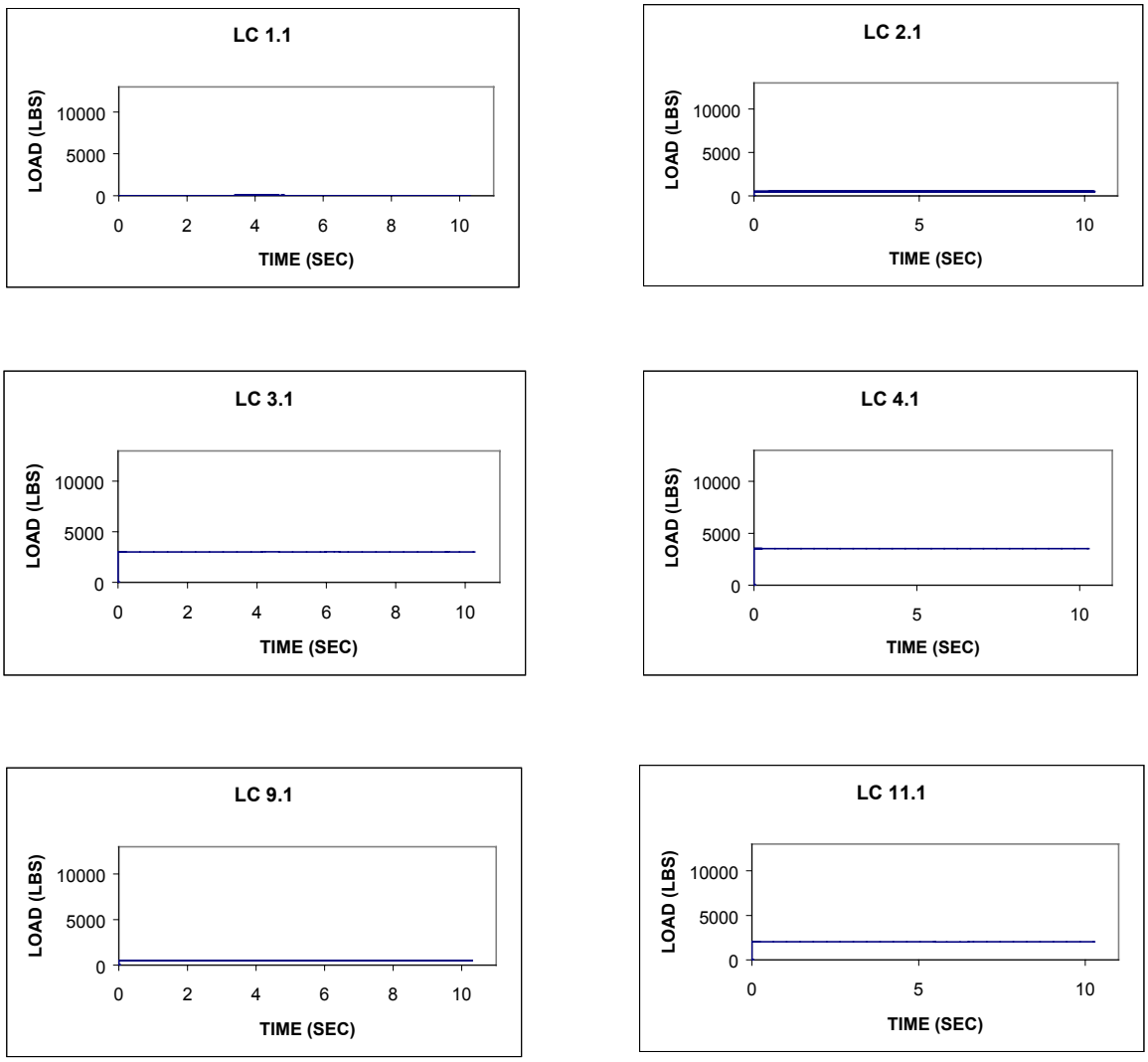

Figure B.17 Time-history of load for test 0900-04.

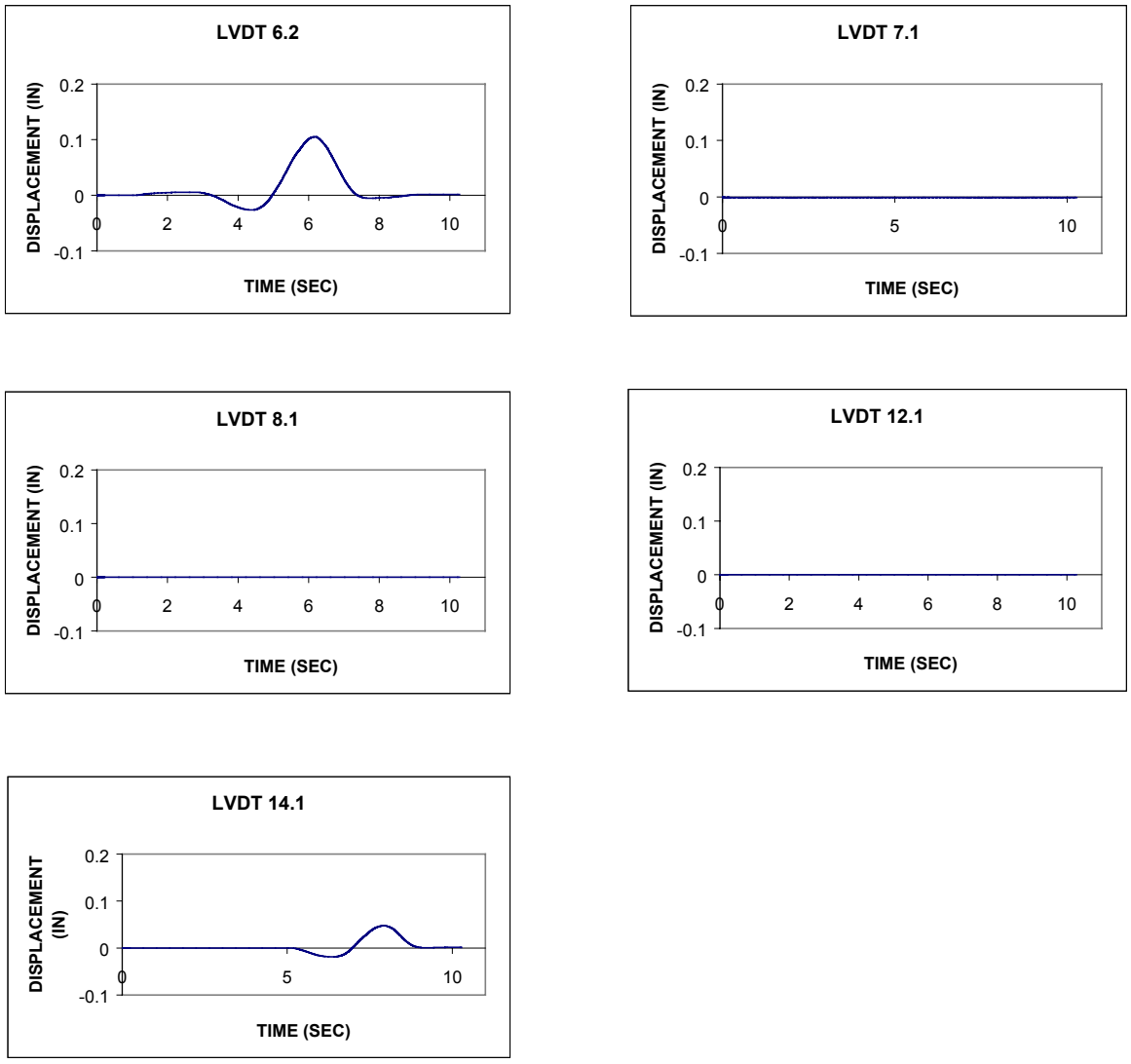

Figure B.18 Time-history of displacement for test 0900-04.

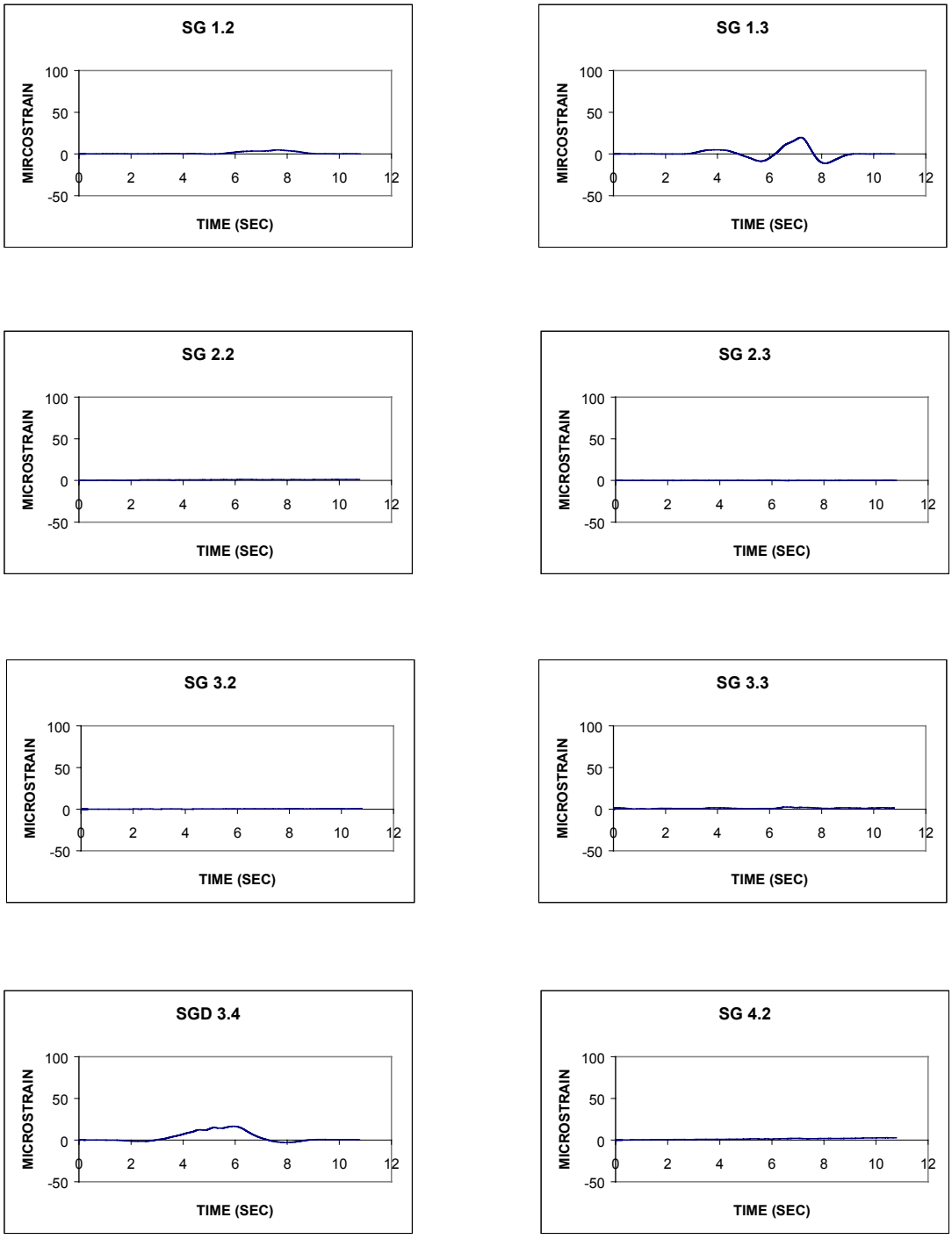

Figure B.19 Time-history of strain for test 0900-05.

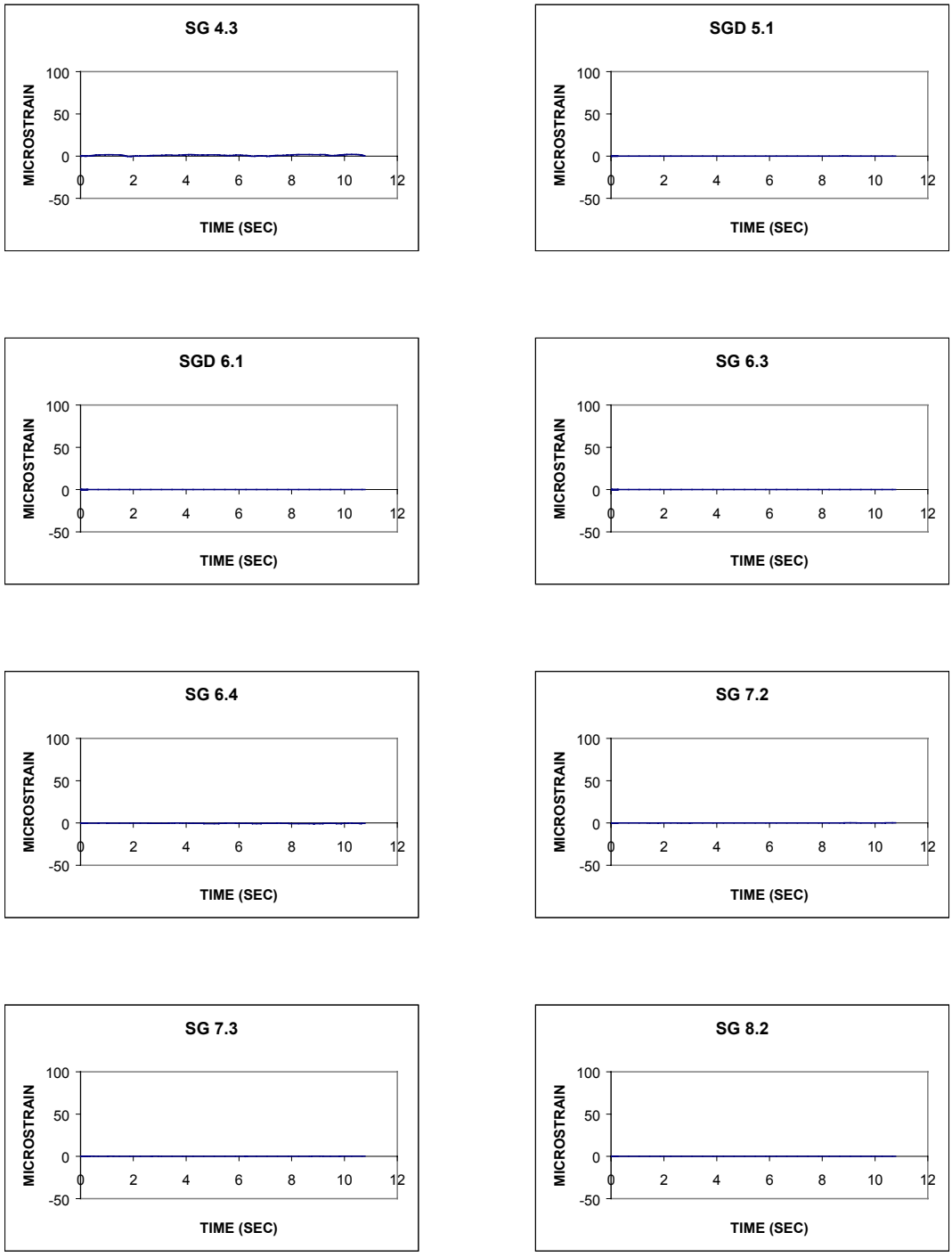

Figure B.20 Time-history of strain for test 0900-05.

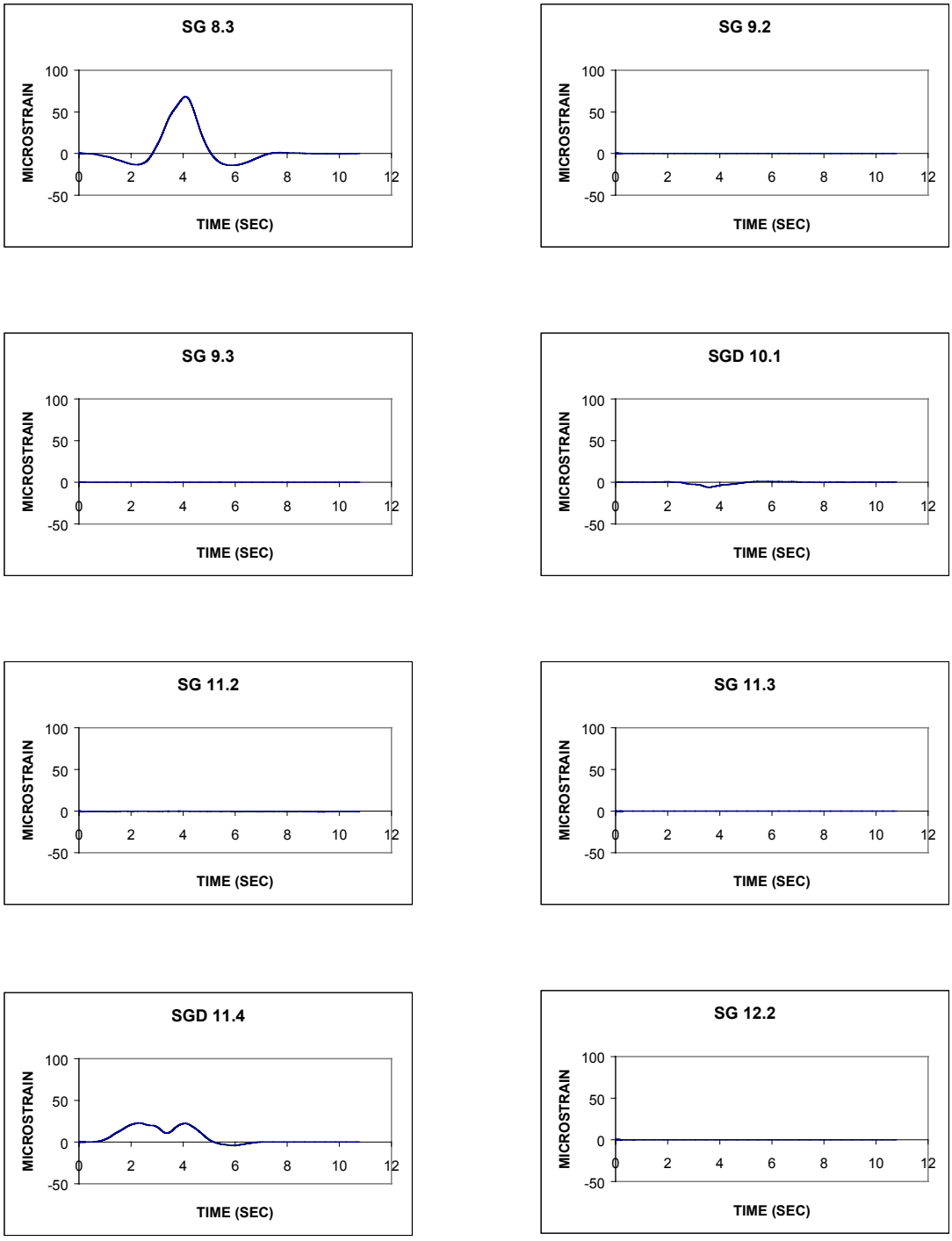

Figure B.21 Time-history of strain for test 0900-05.

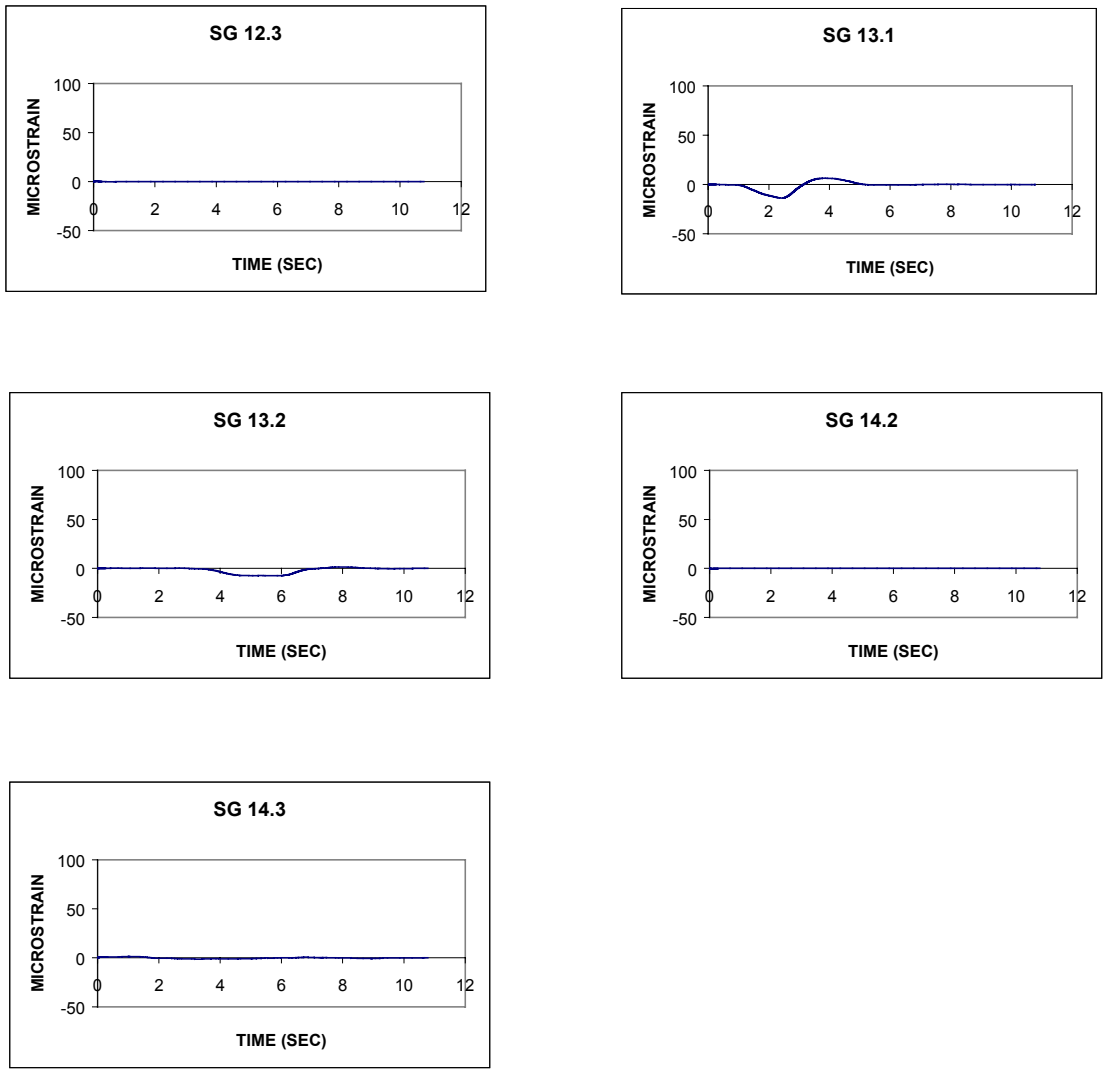

Figure B.22 Time-history of strain for test 0900-05.

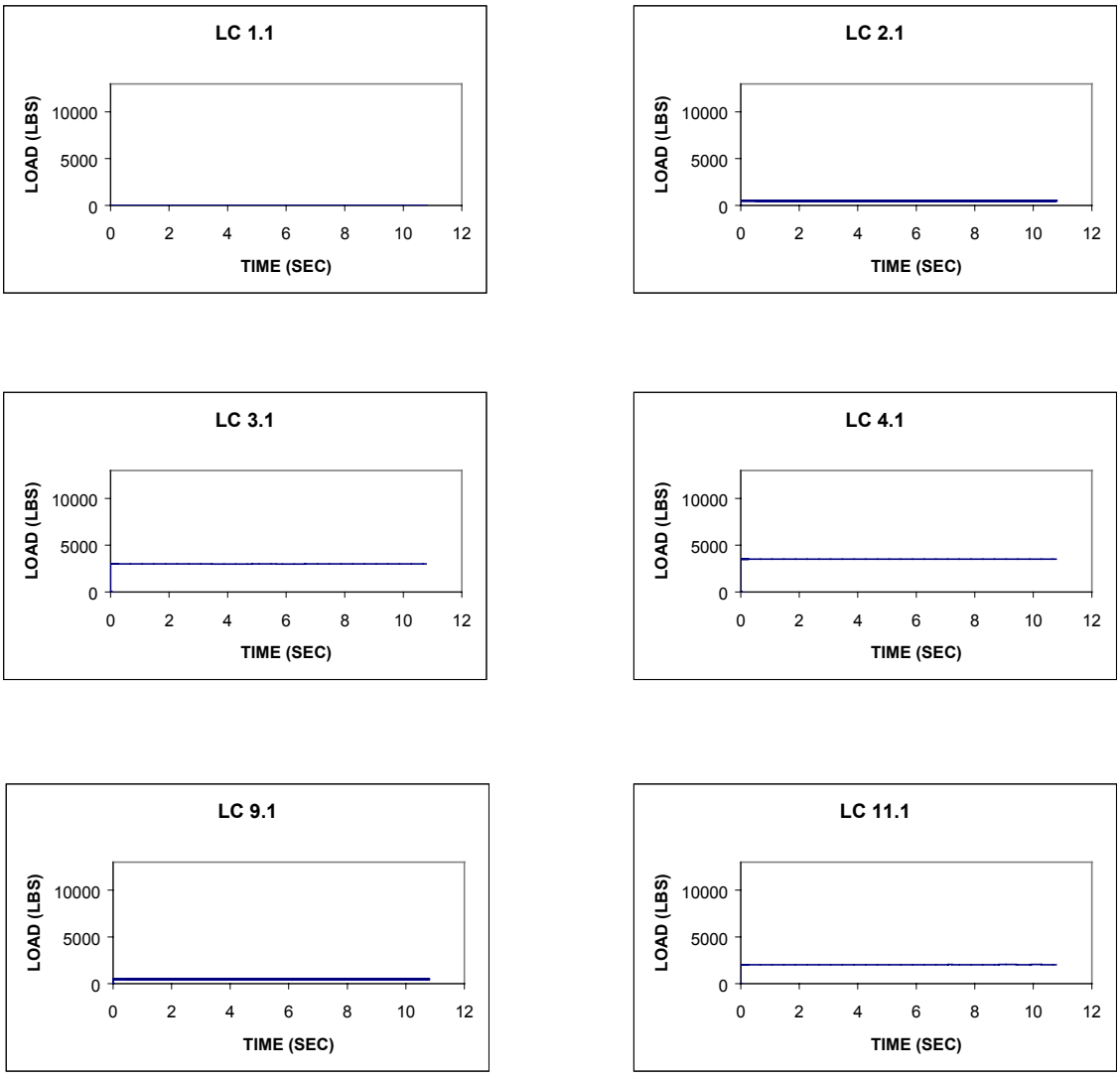

Figure B.23 Time-history of load for test 0900-05.

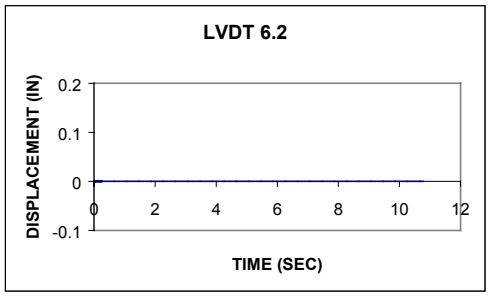

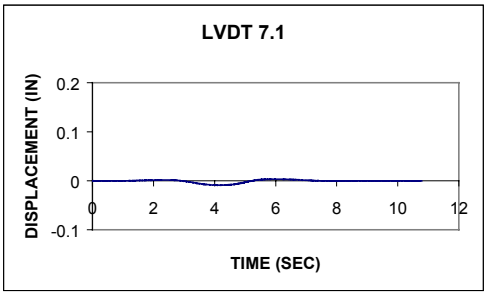

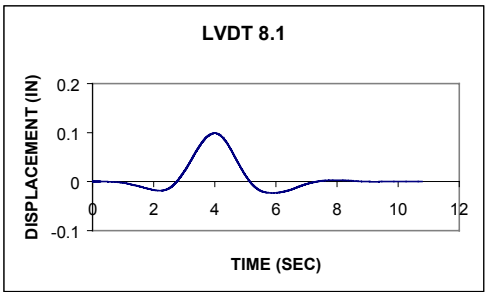

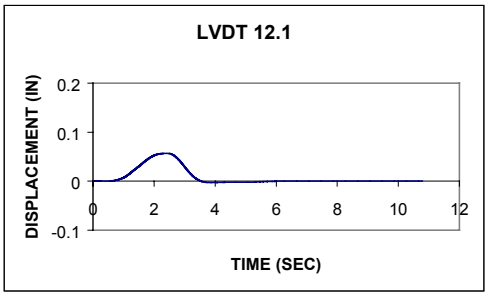

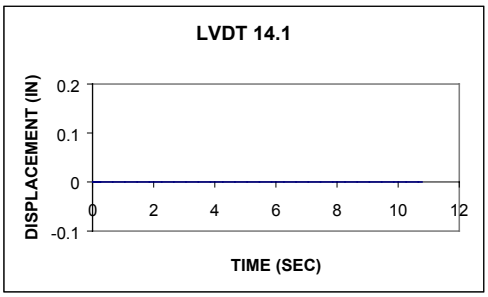

Figure B.24 Time-history of displacement for test 0900-05.

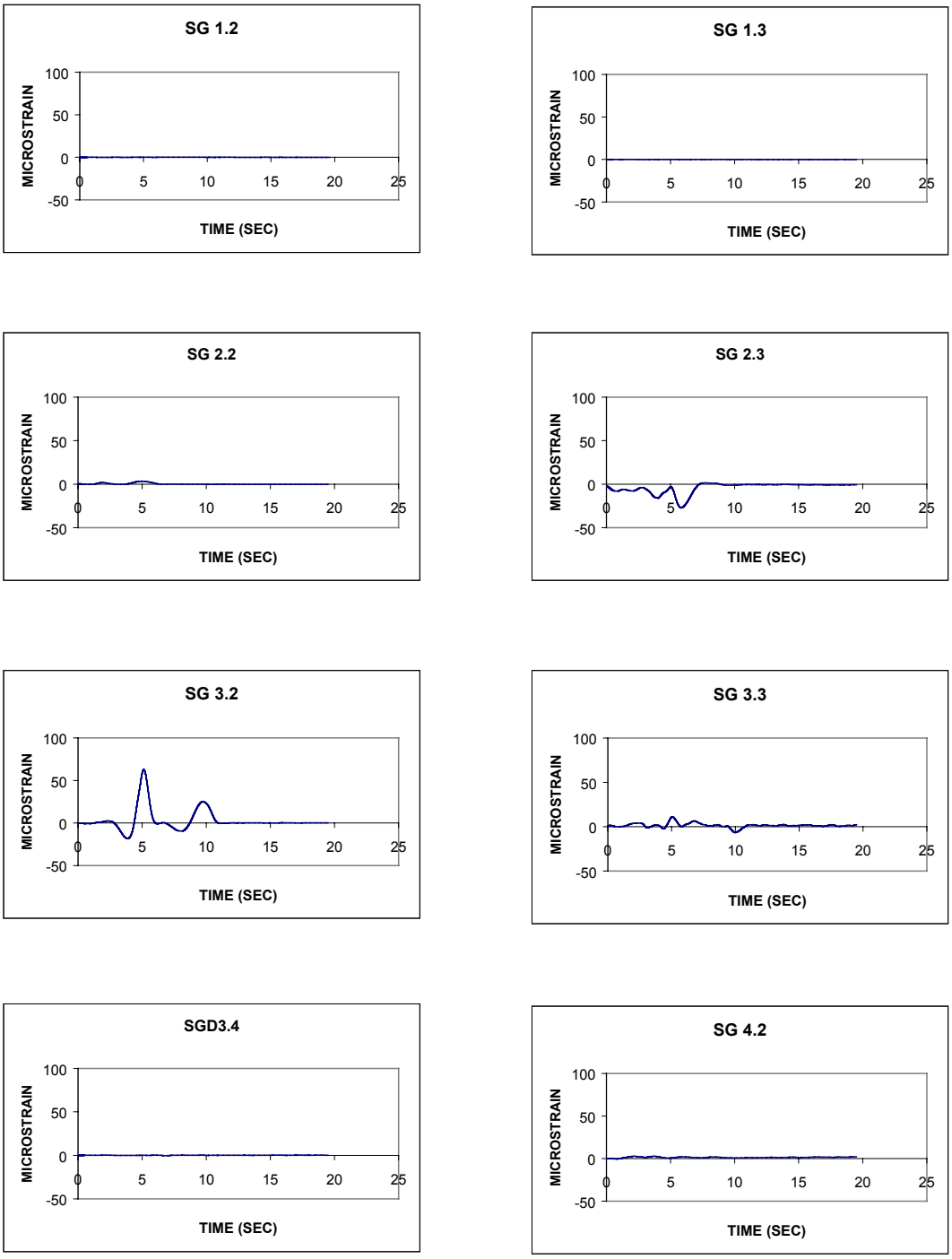

Figure B.25 Time-history of strain for test 0900-06.

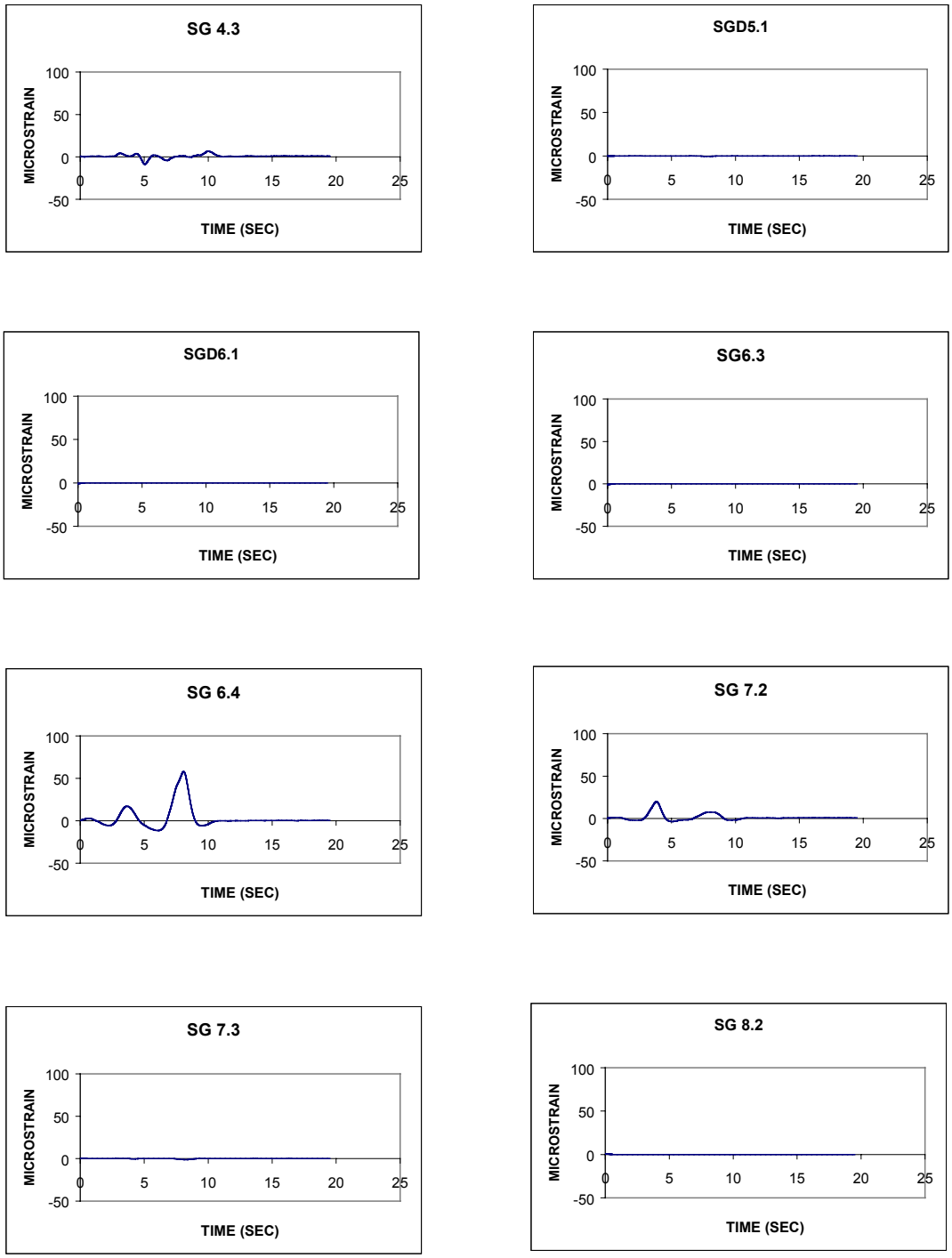

Figure B.26 Time-history of strain for test 0900-06.

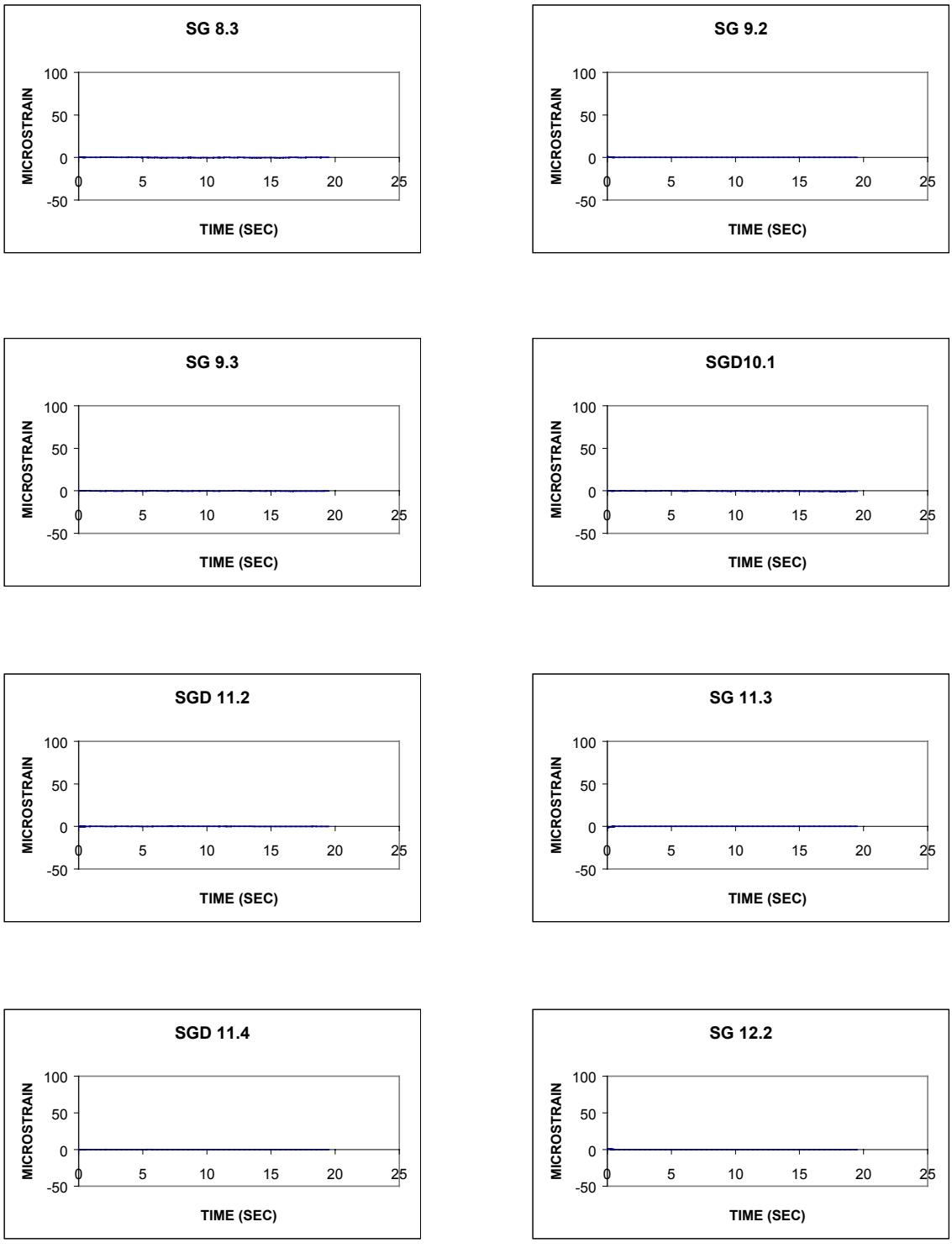

Figure B.27 Time-history of strain for test 0900-06.

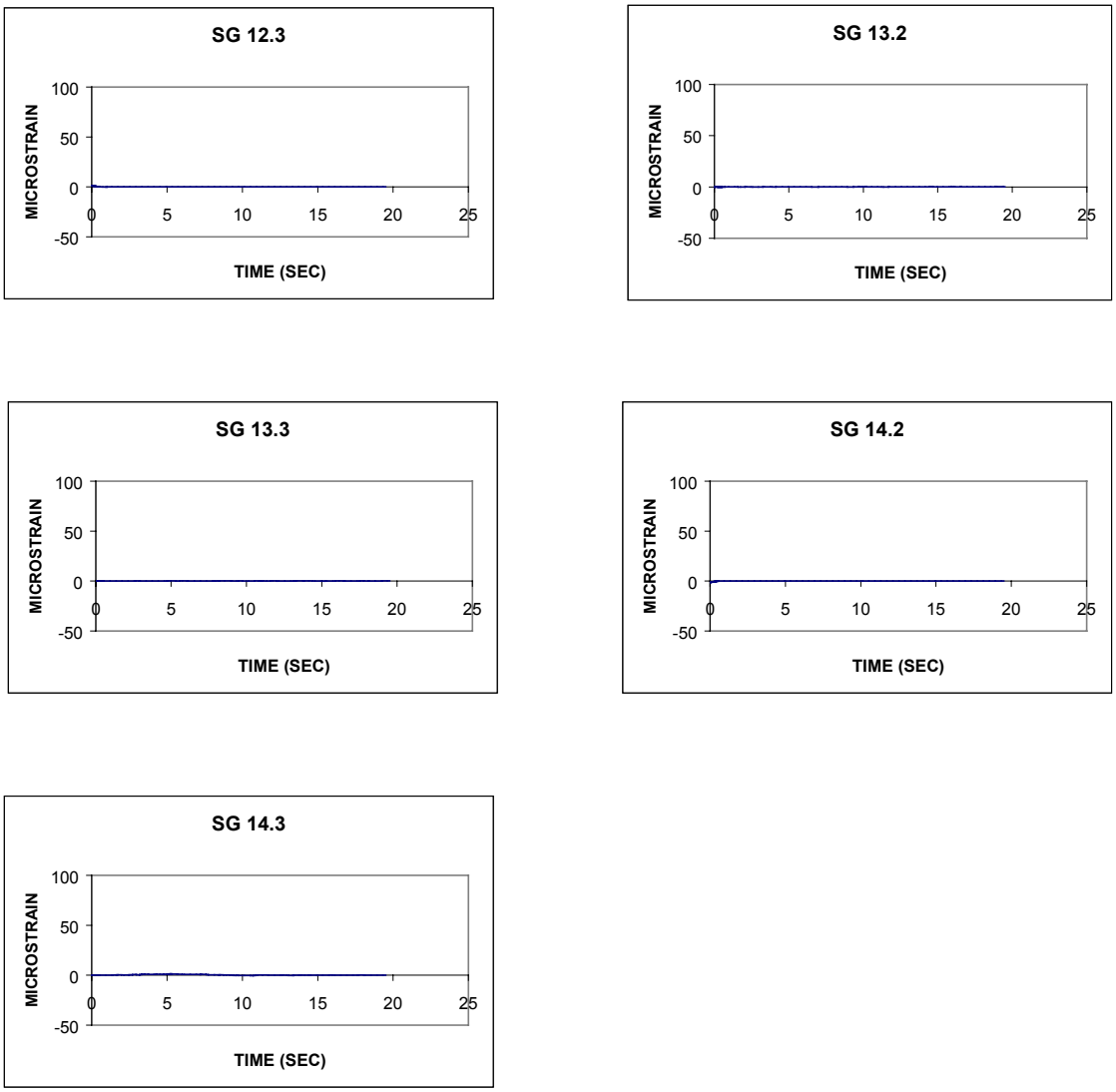

Figure B.28 Time-history of strain for test 0900-06.

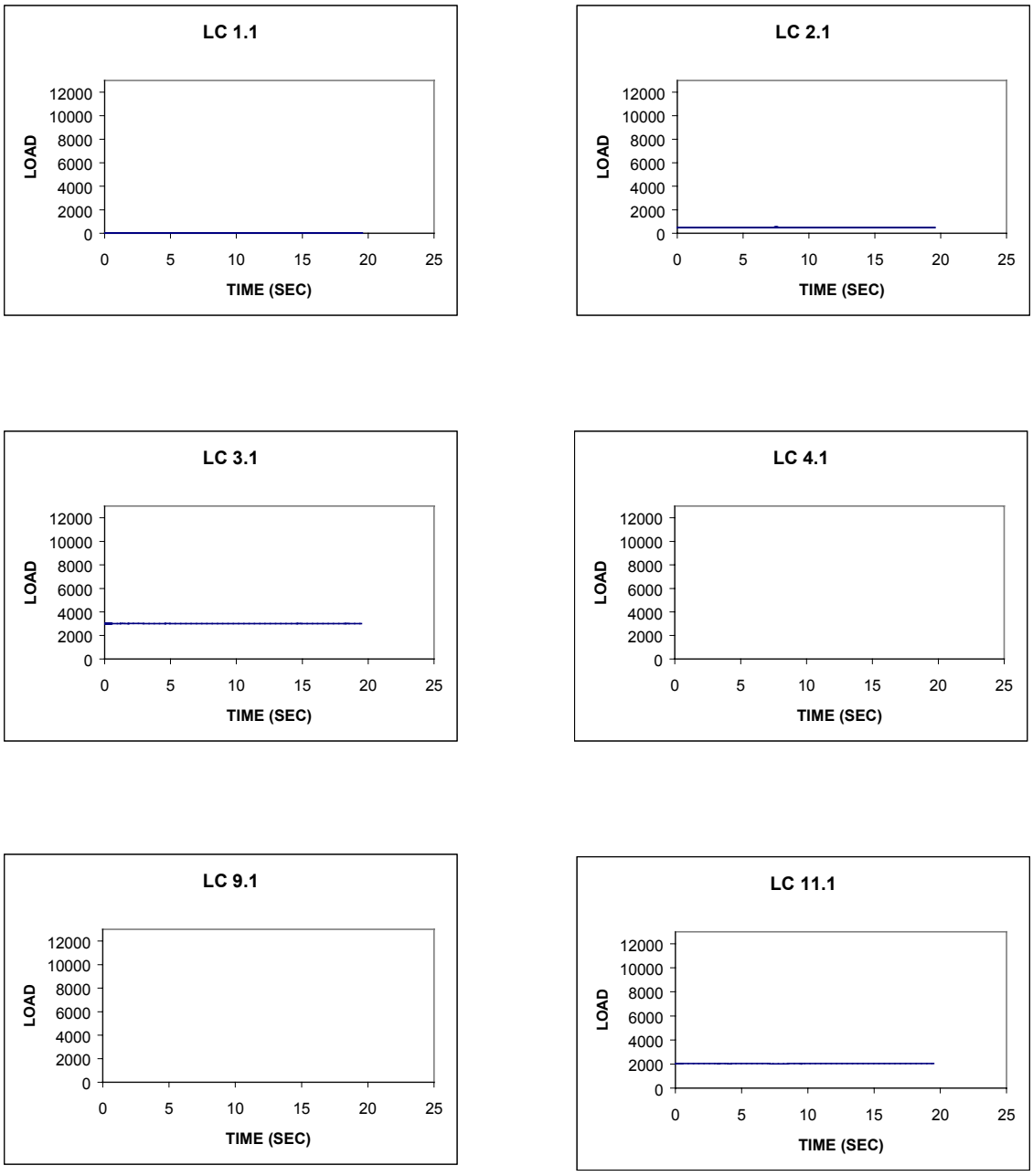

Figure B.29 Time-history of load for test 0900-06.

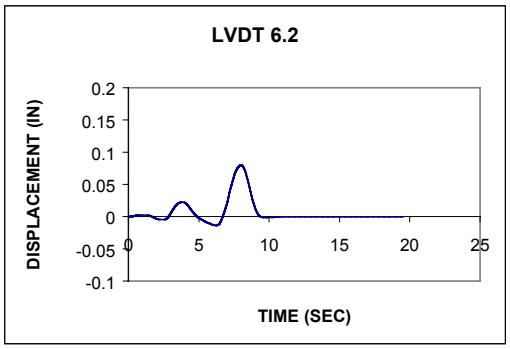

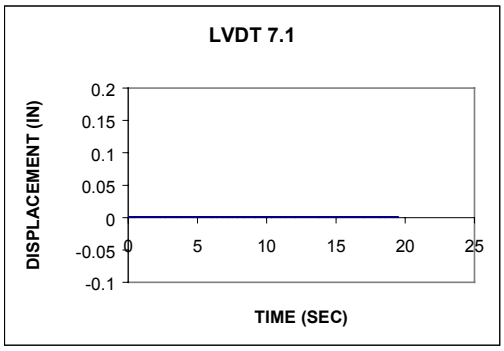

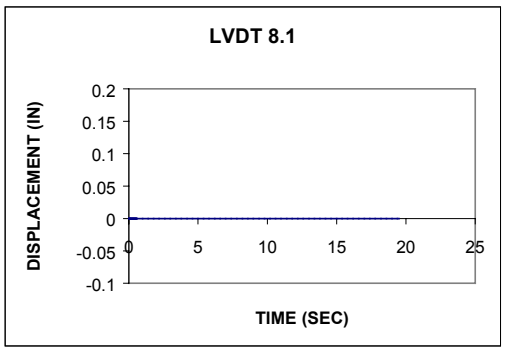

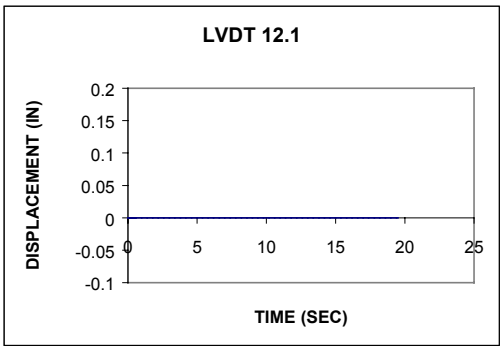

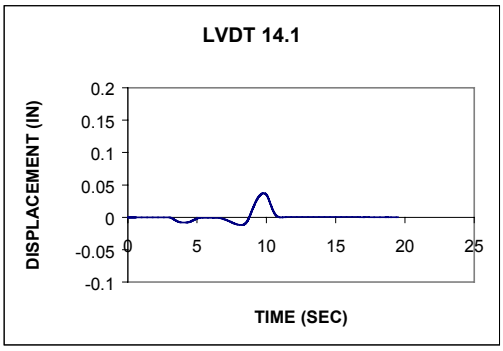

Figure B.30 Time-history of displacement for test 0900-06.

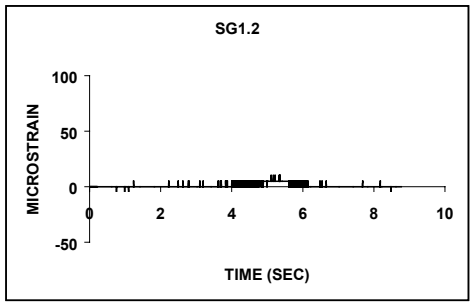

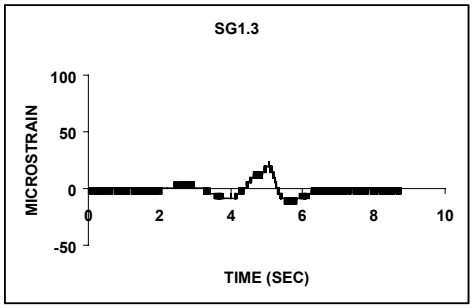

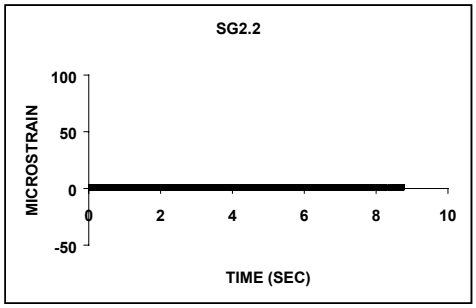

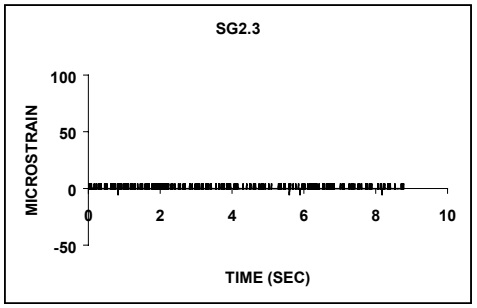

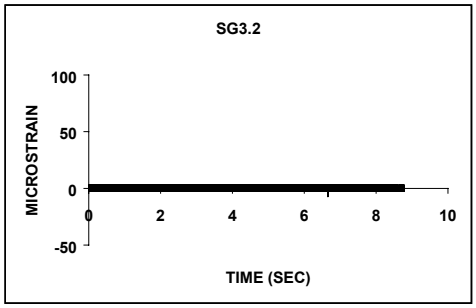

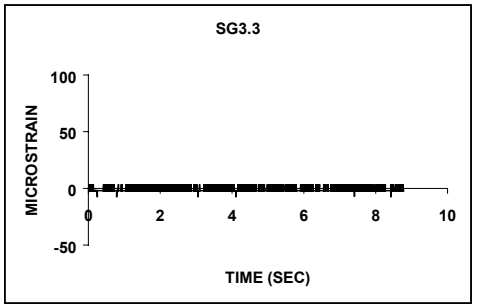

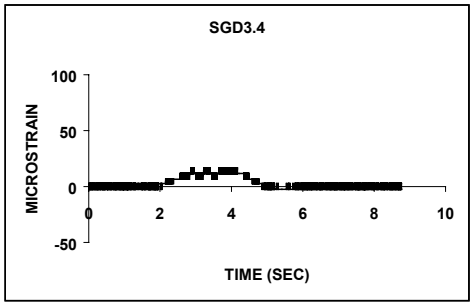

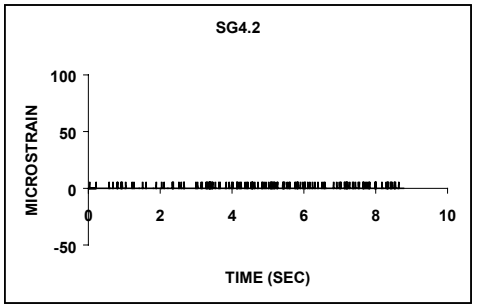

Figure B.31 Time-history of strain for test 0900-07.

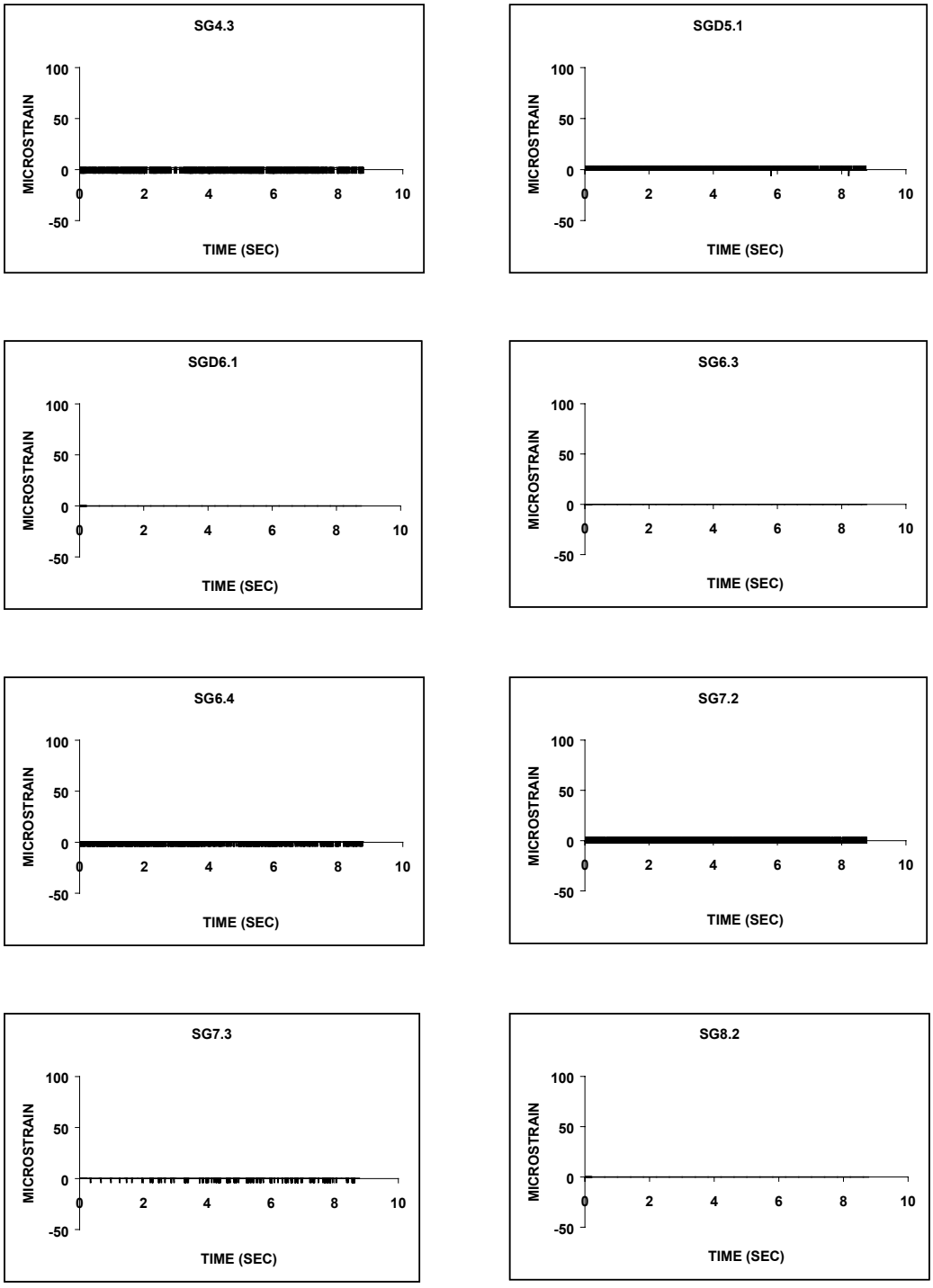

Figure B.32 Time-history of strain for test 0900-07.

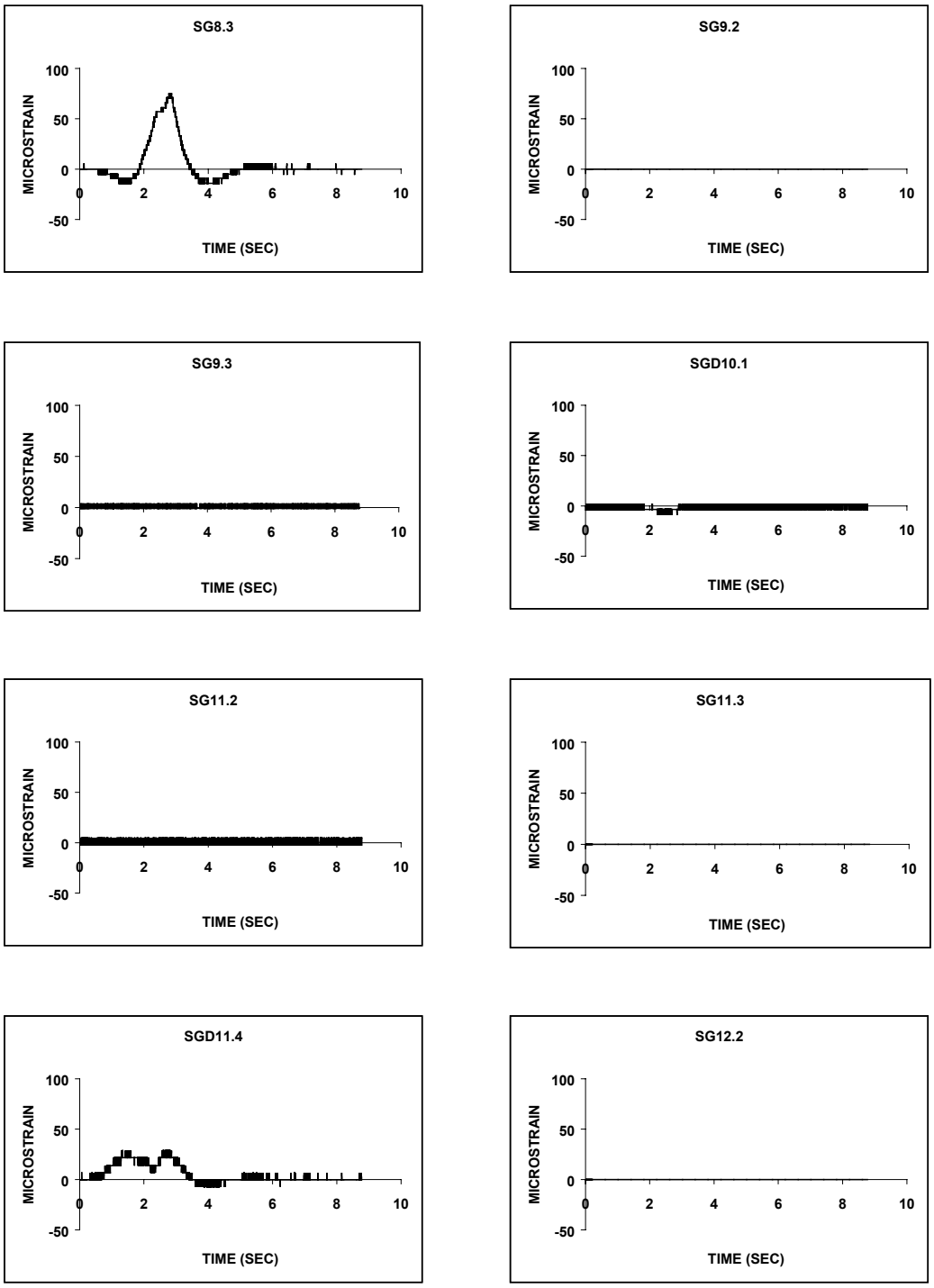

Figure B.33 Time-history of strain for test 0900-07.

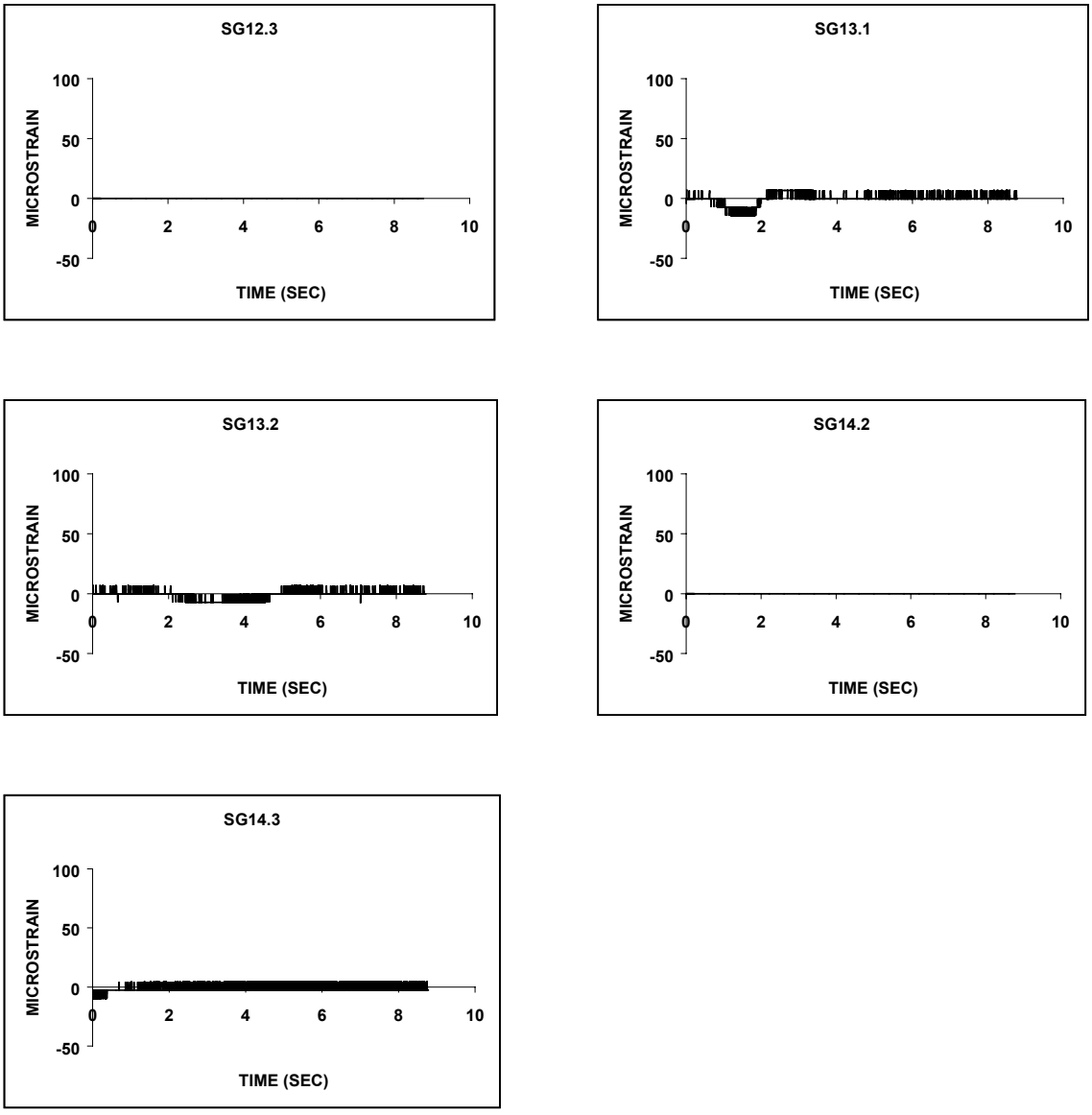

Figure B.34 Time-history of strain for test 0900-07.

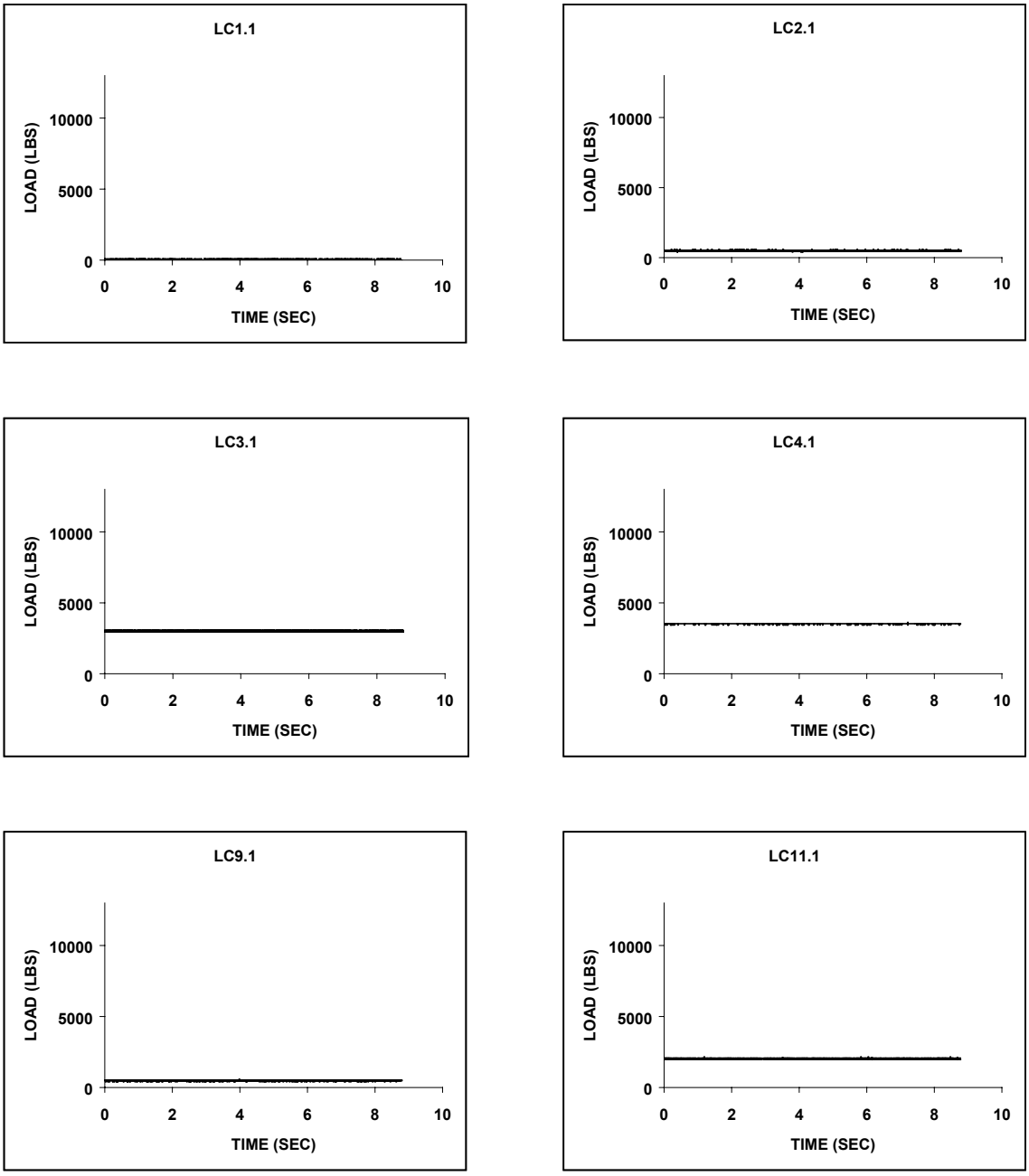

Figure B.35 Time-history of strain for load 0900-07.

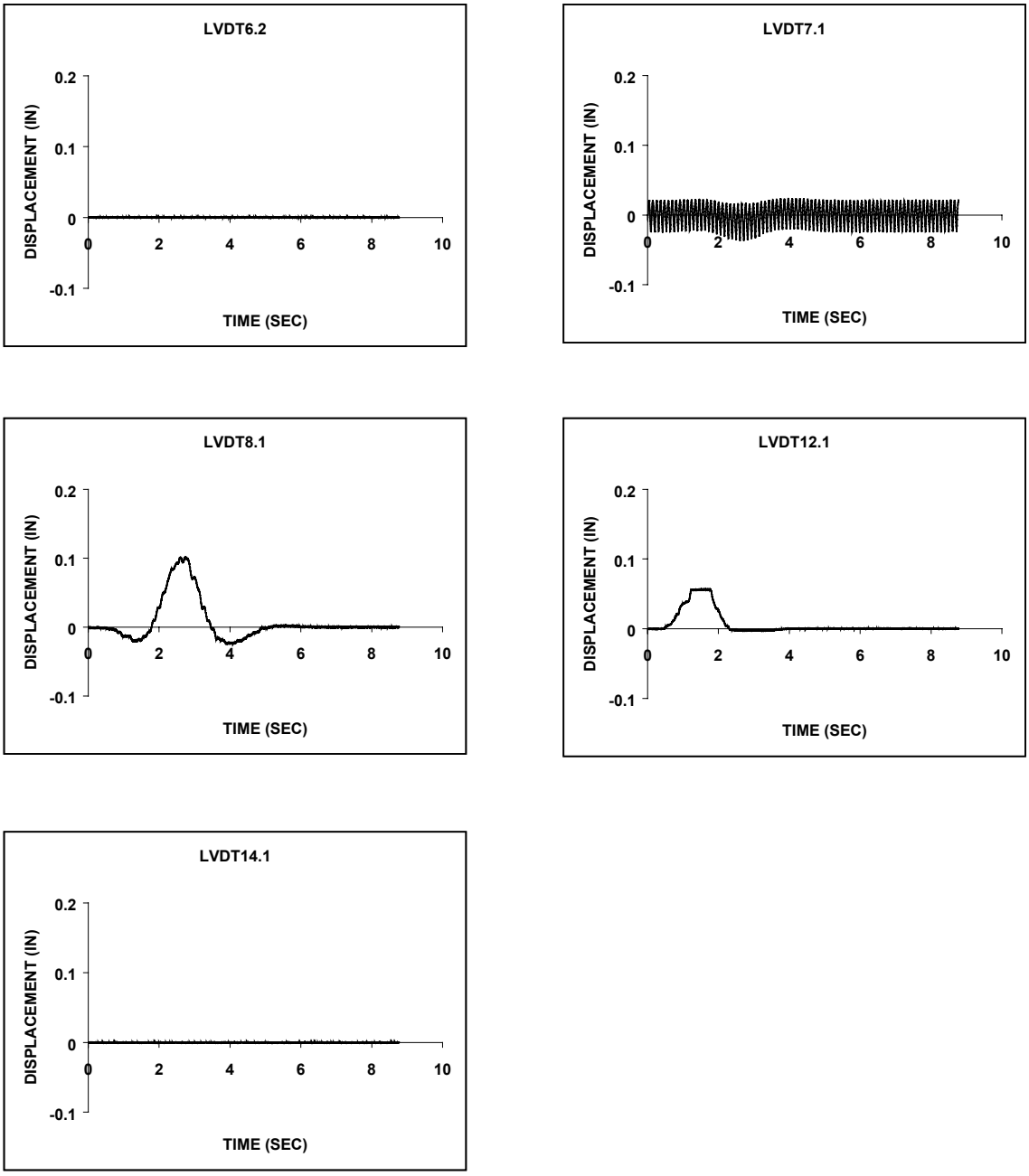

Figure B.36 Time-history of displacement for test 0900-07.

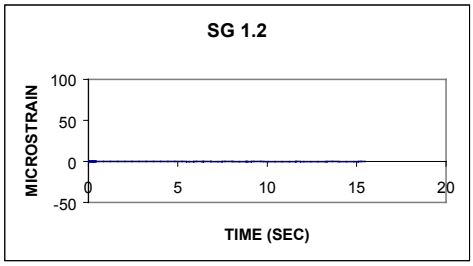

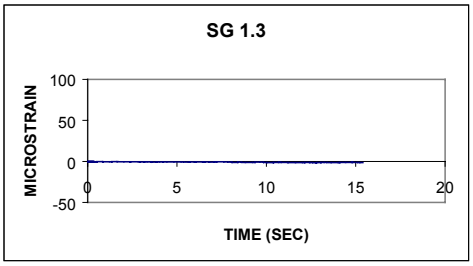

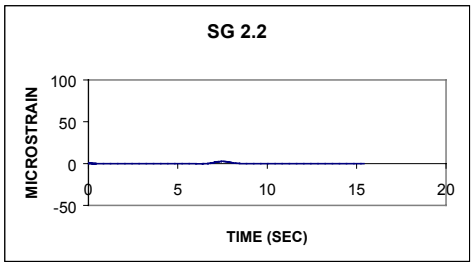

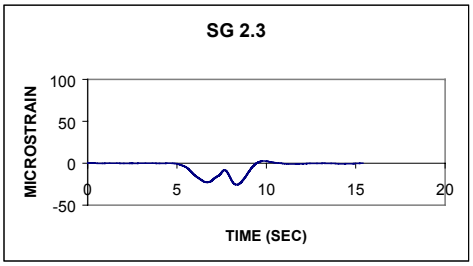

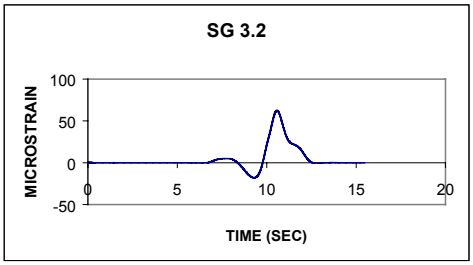

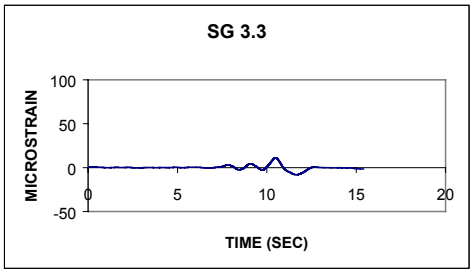

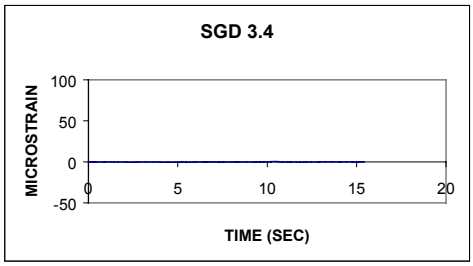

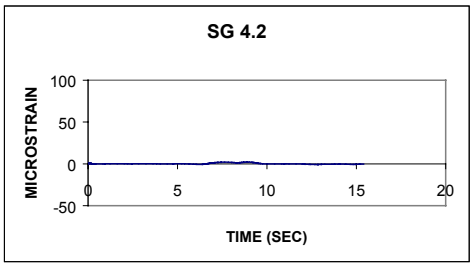

.

Figure B.37 Time-history of strain for test 0900-08

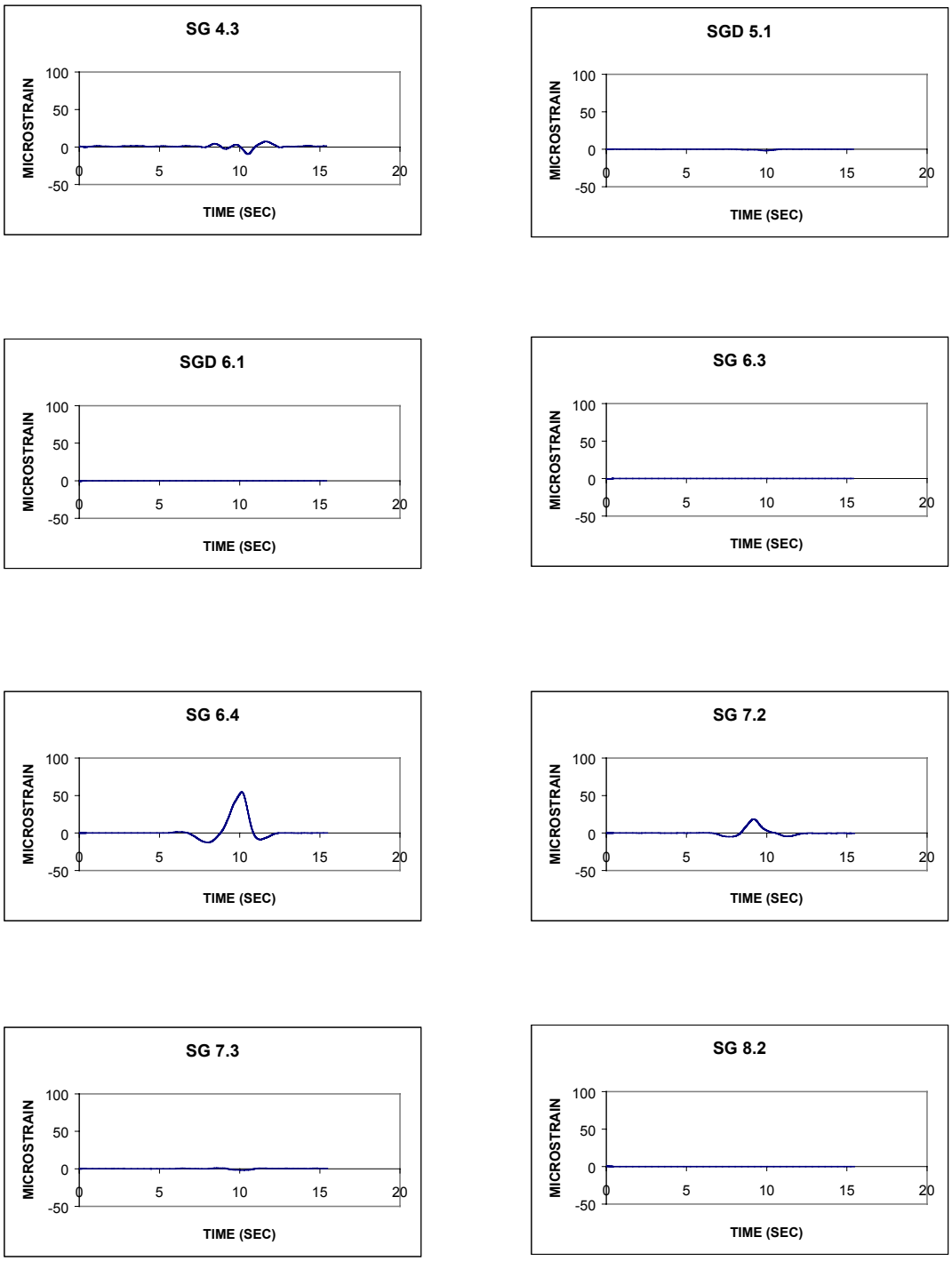

Figure B.38 Time-history of strain for test 0900-08.

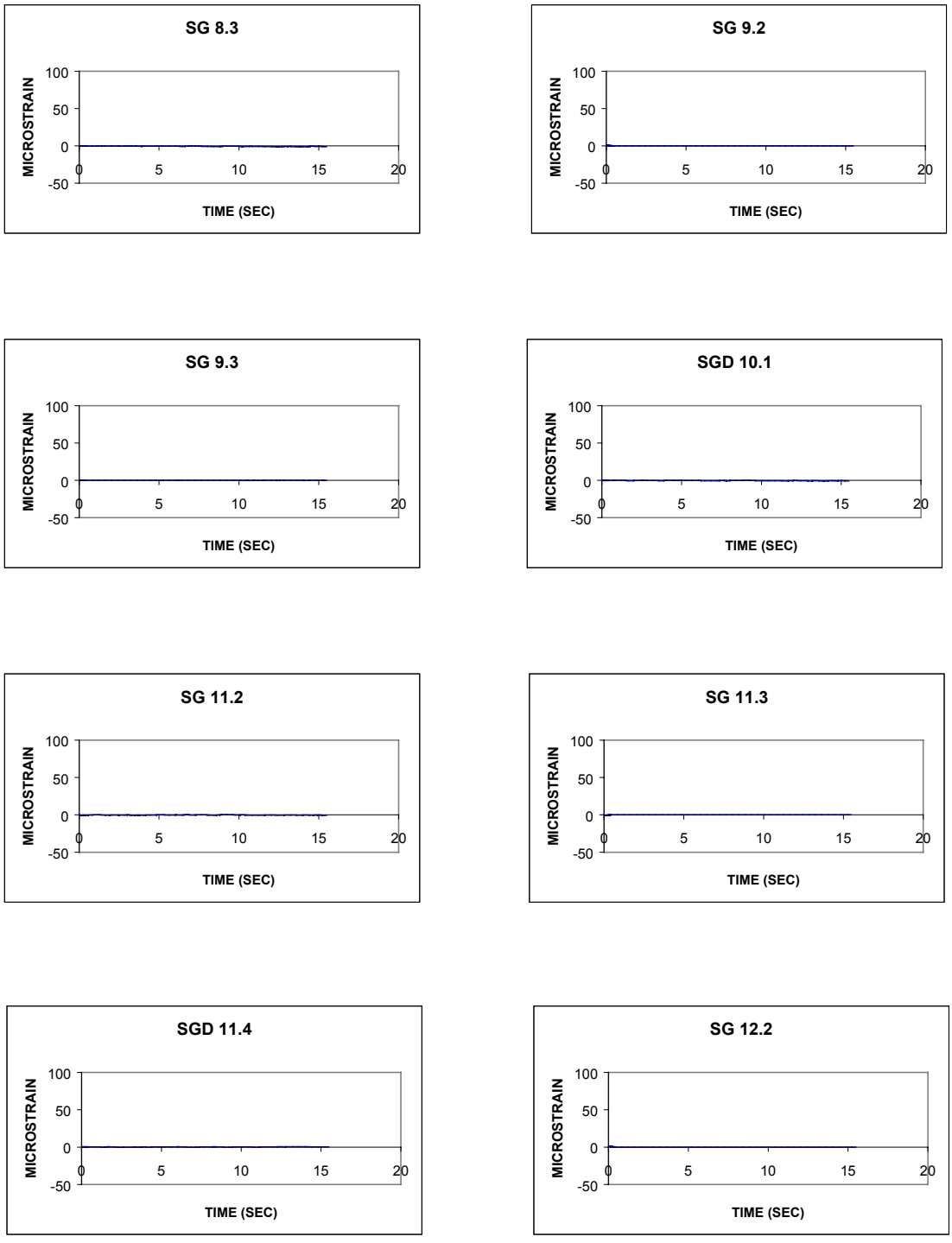

Figure B.39 Time-history of strain for test 0900-08.

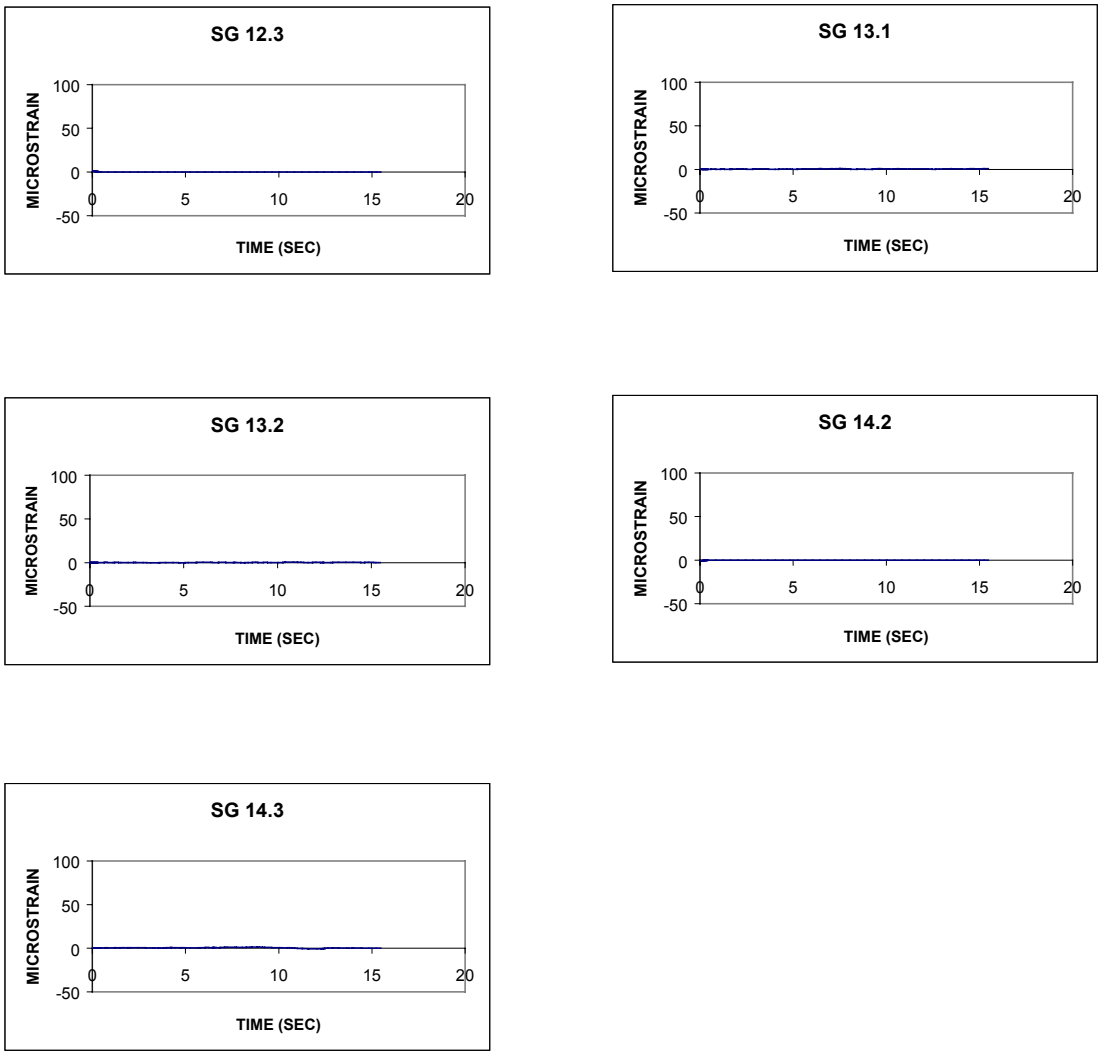

Figure B.40 Time-history of strain for test 0900-08.

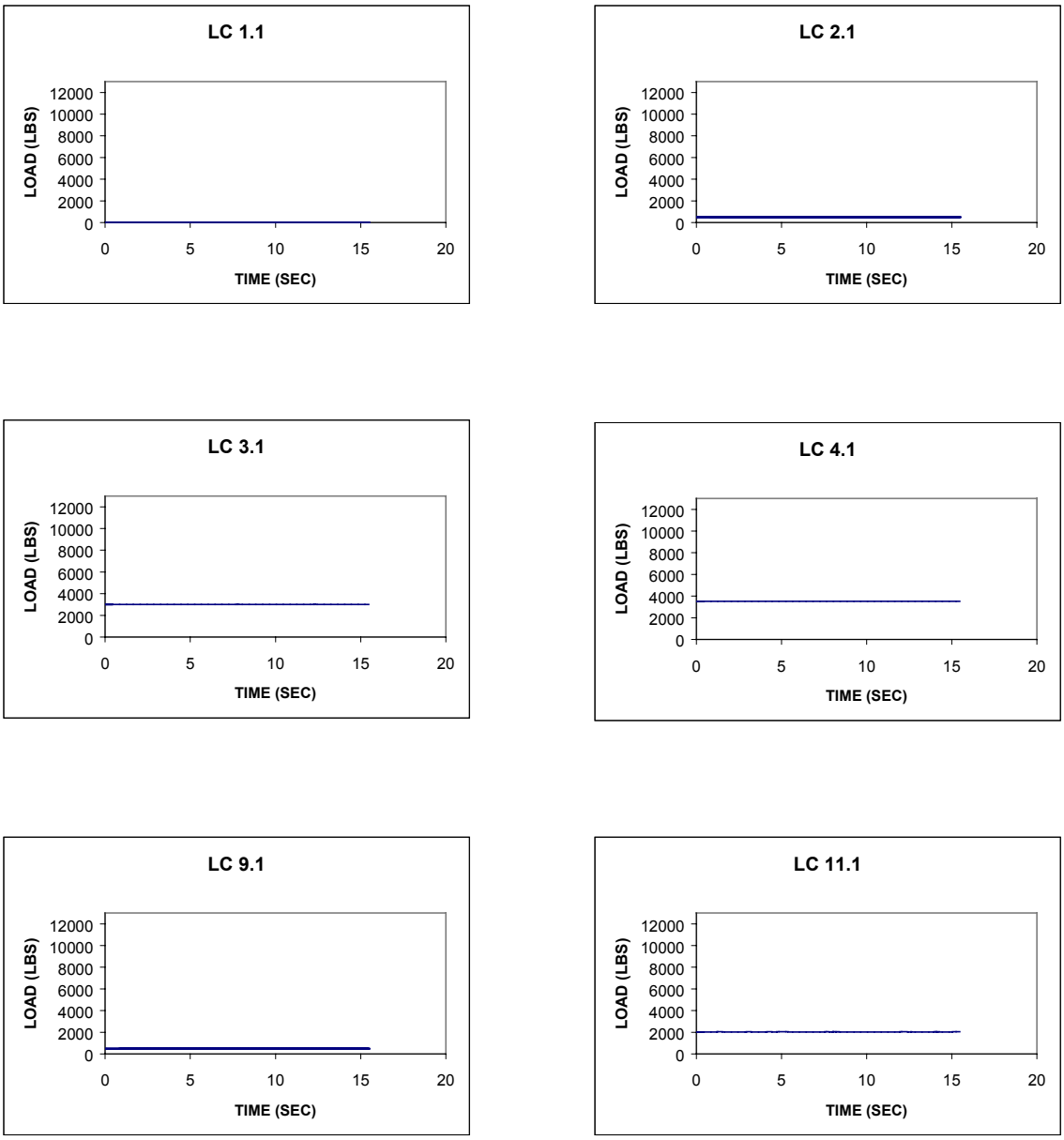

Figure B.41 Time-history of load for test 0900-08.

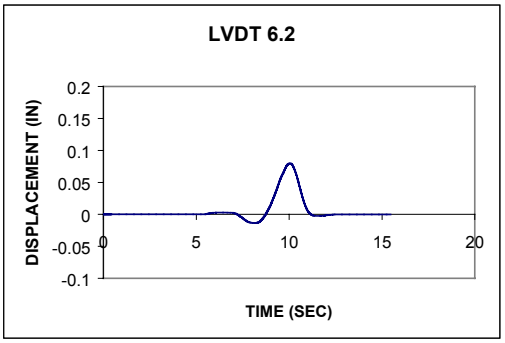

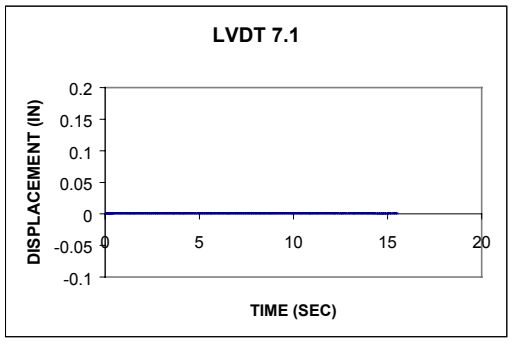

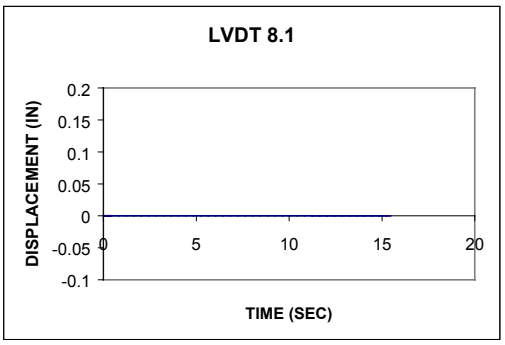

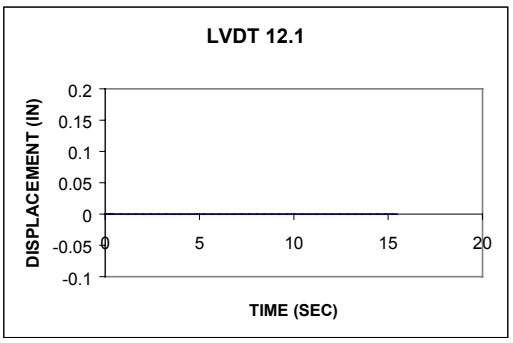

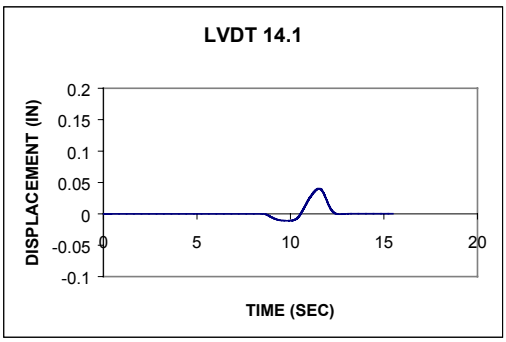

Figure B.42 Time-history of displacement for test 0900-08.

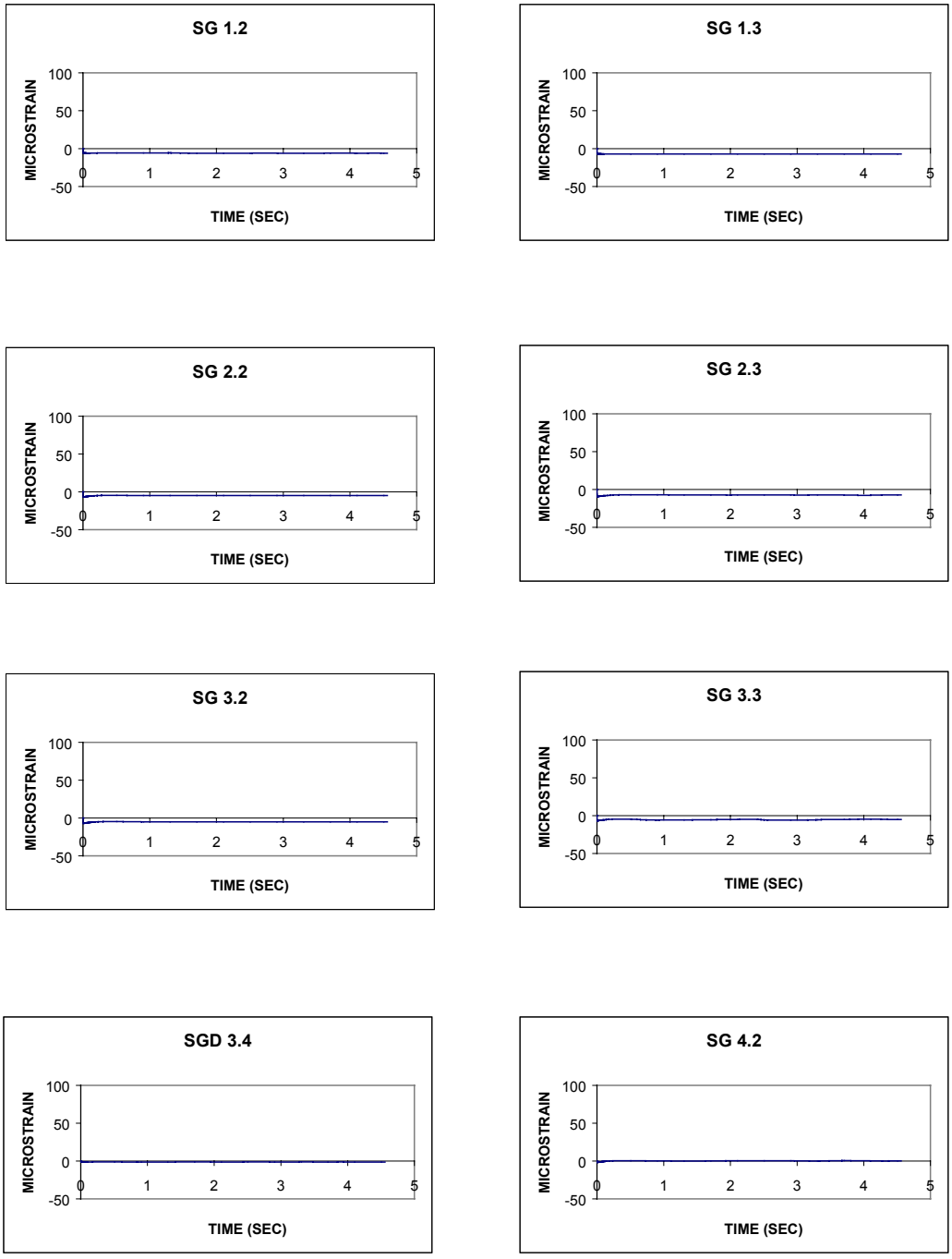

Figure B.43 Time-history of strain for test 0900-09.

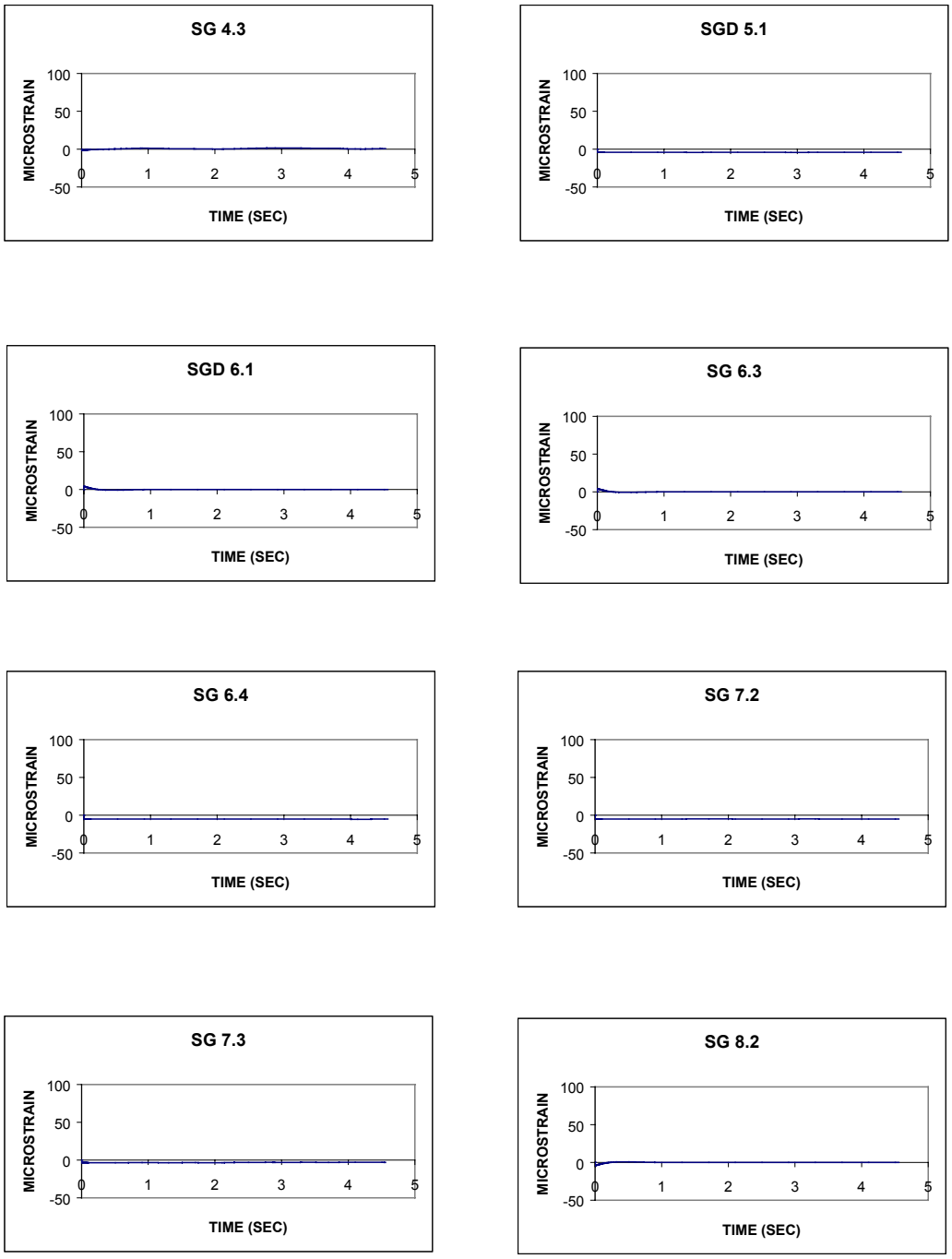

Figure B.44 Time-history of strain for test 0900-09.

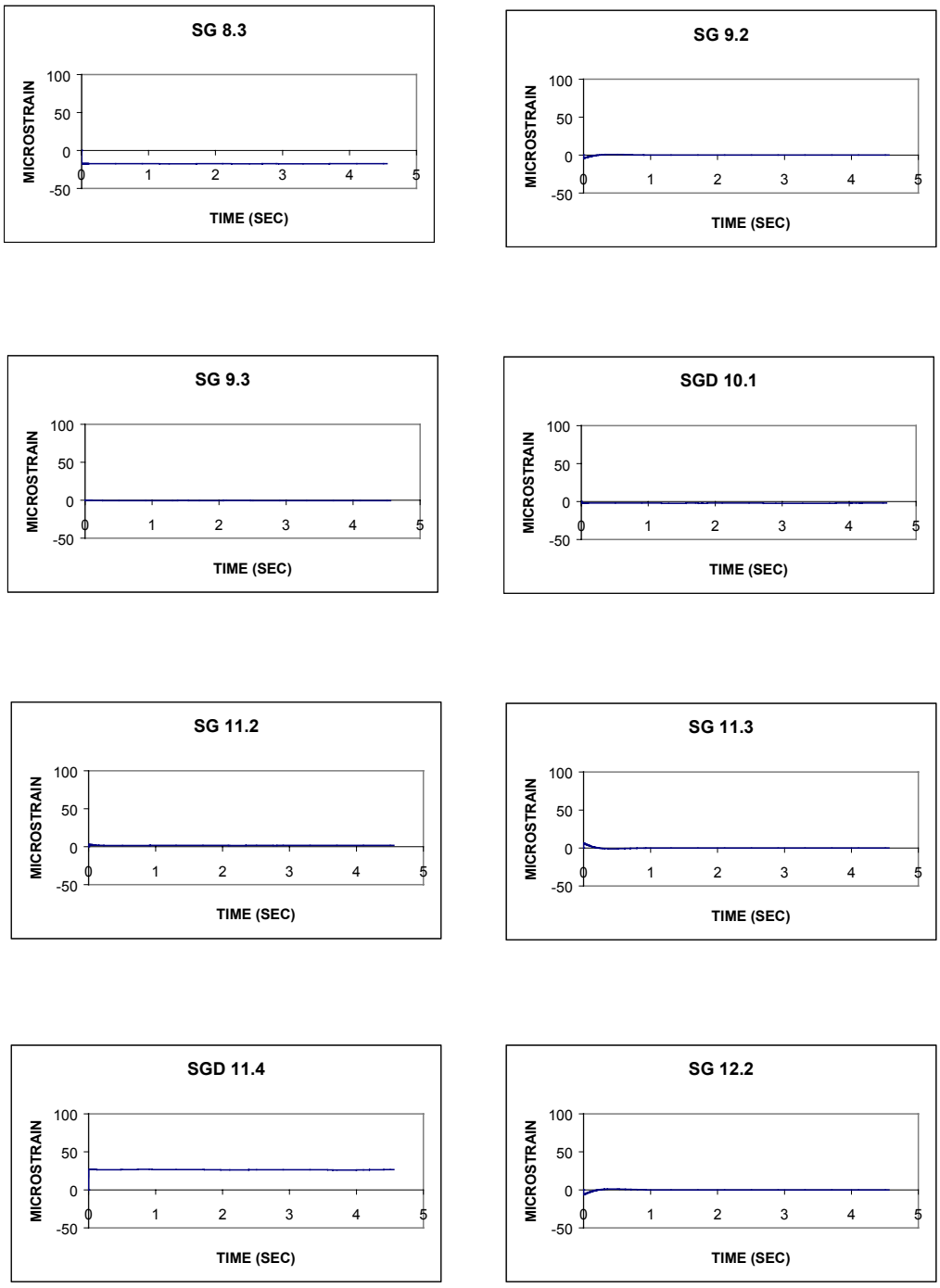

Figure B.45 Time-history of strain for test 0900-09.

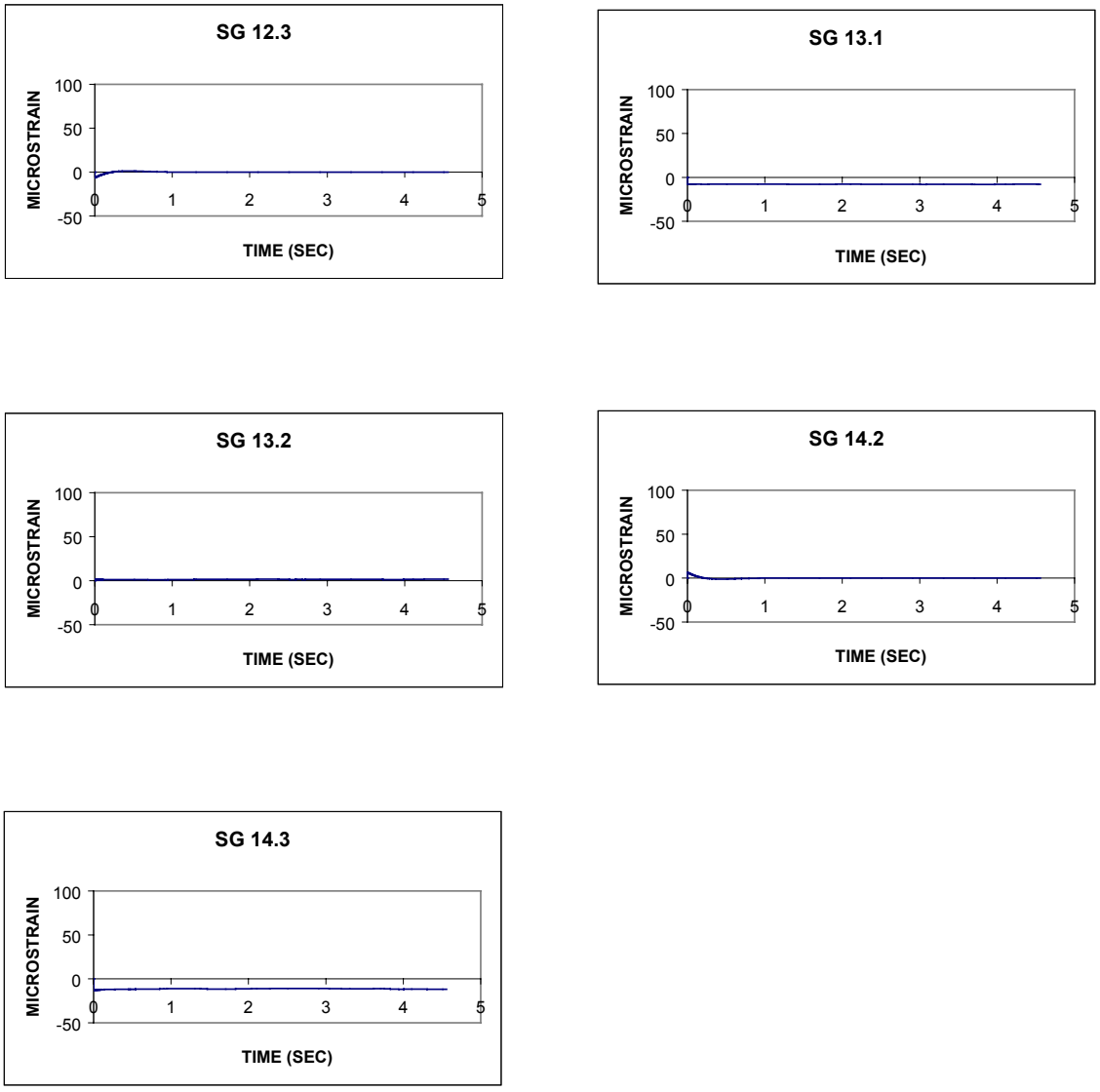

Figure B.46 Time-history of strain for test 0900-09.

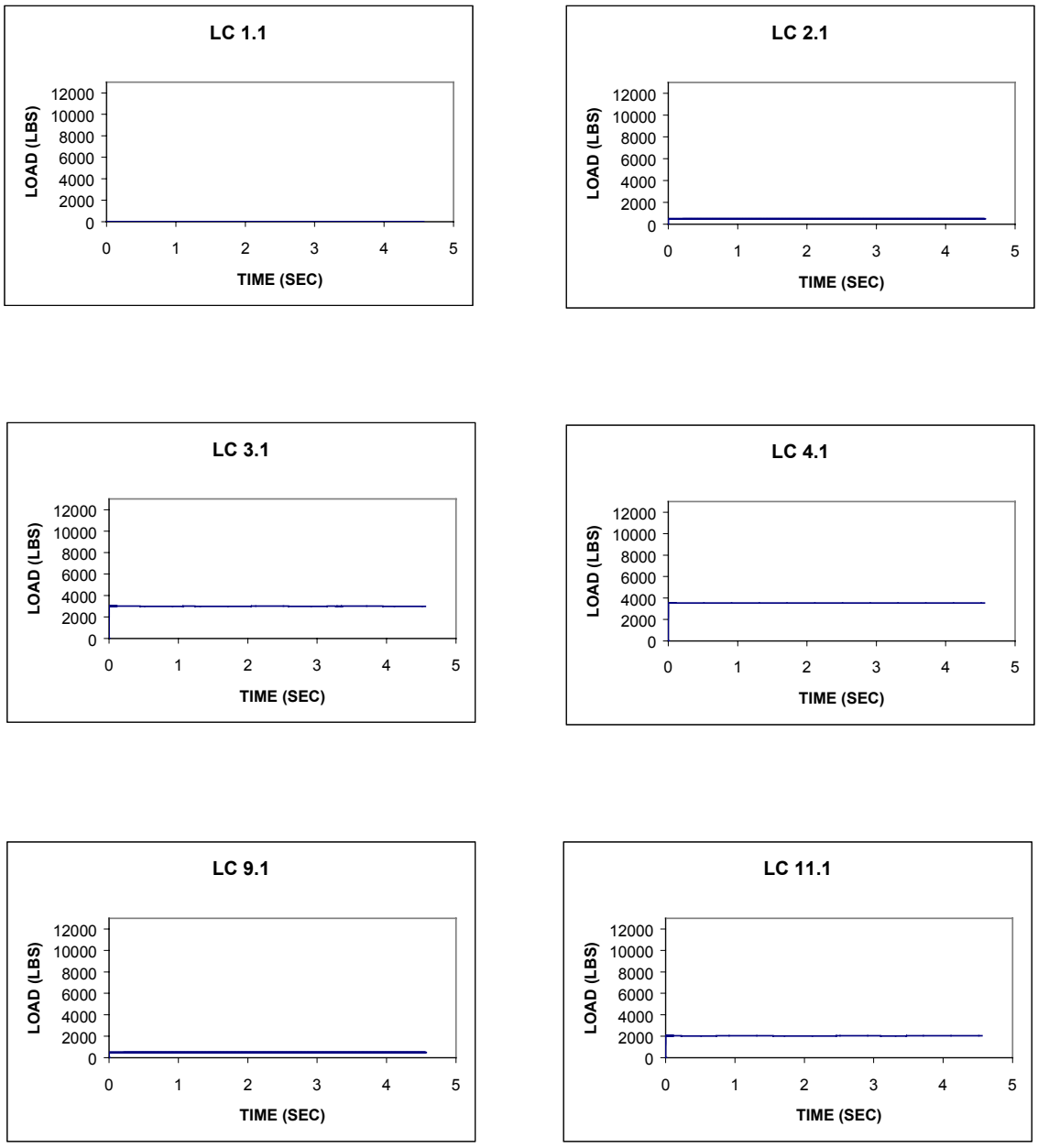

Figure B.47 Time-history of load for test 0900-09.

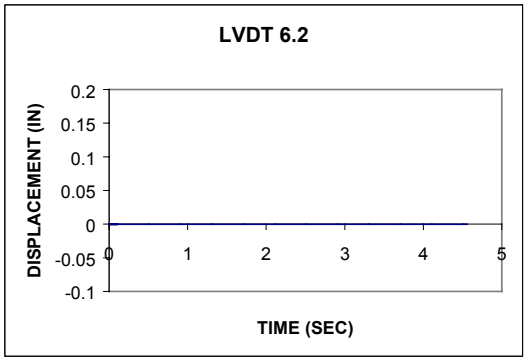

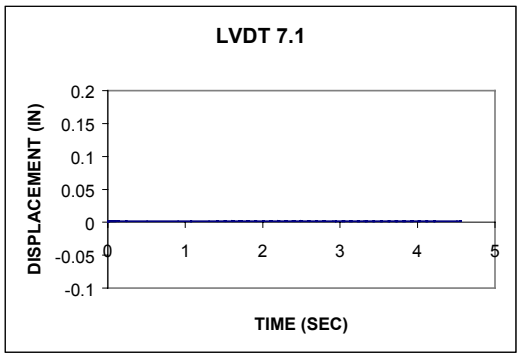

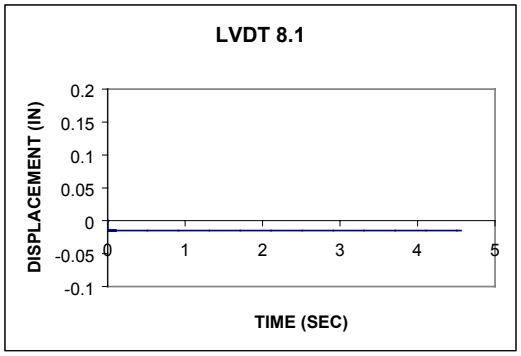

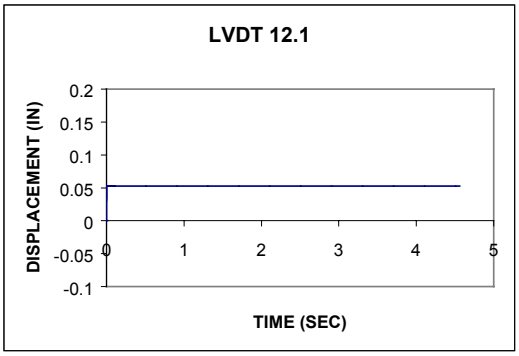

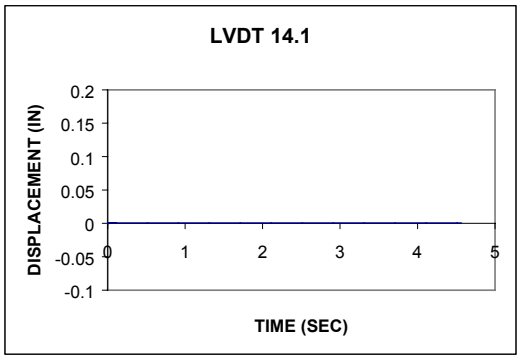

Figure B.48 Time-history of displacement for test 0900-09.

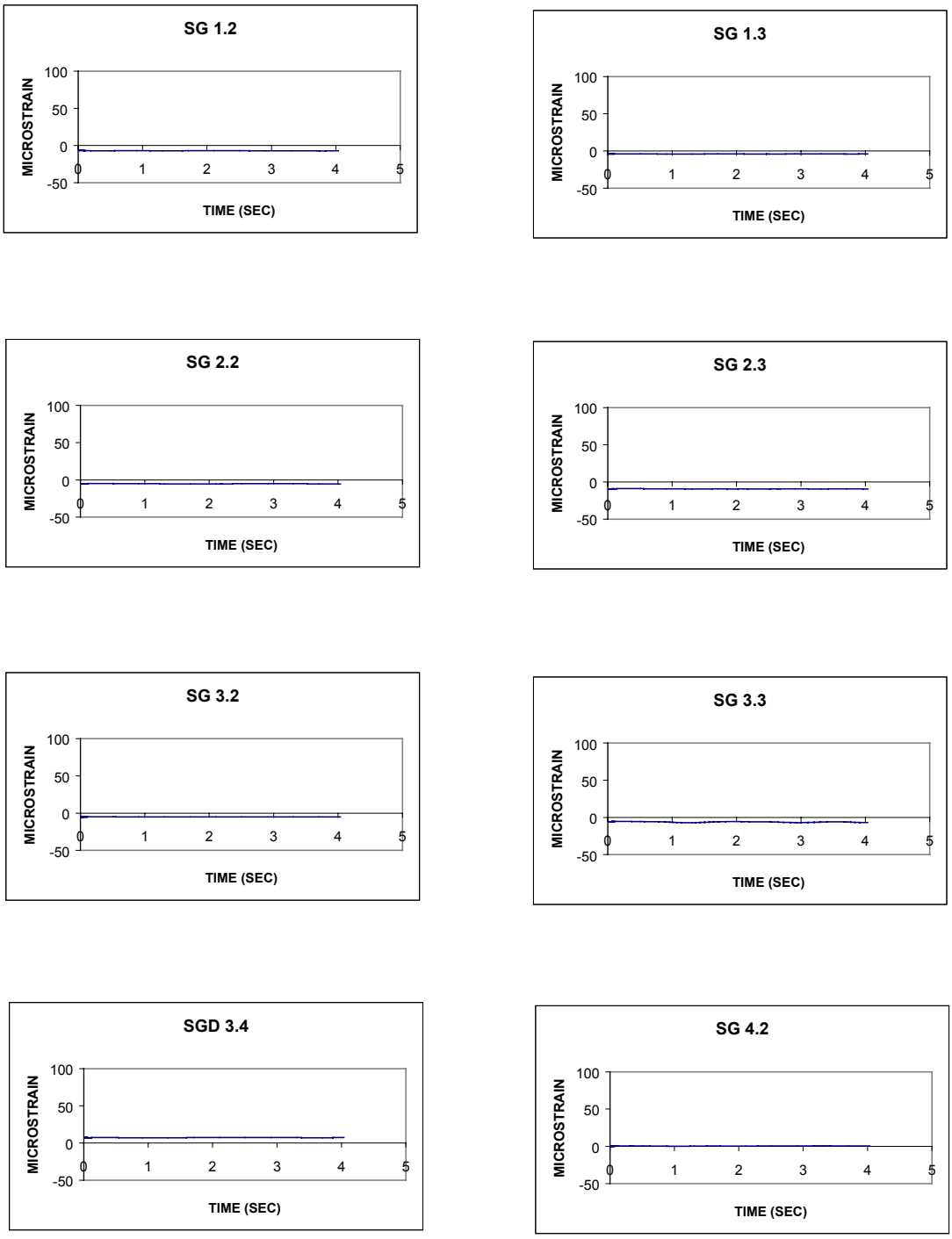

Figure B.49 Time-history of strain for test 0900-10.

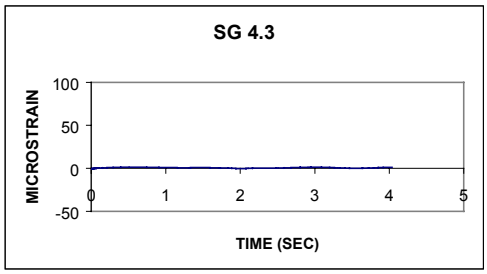

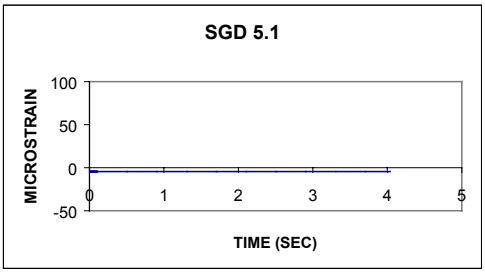

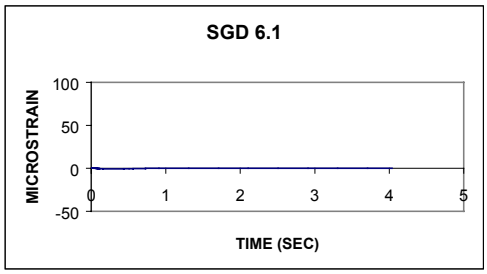

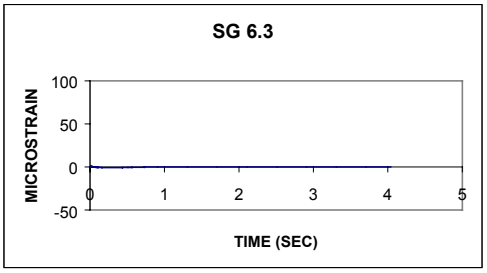

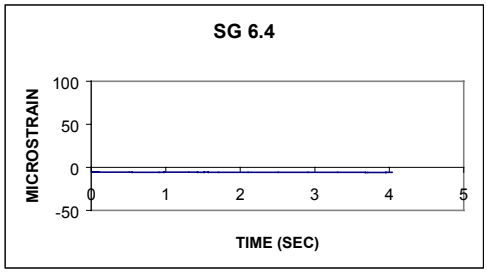

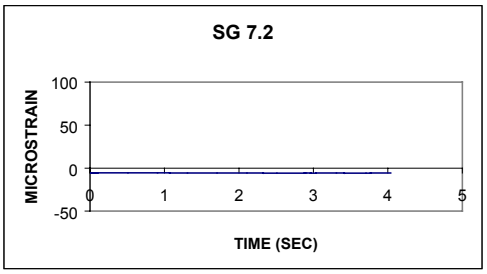

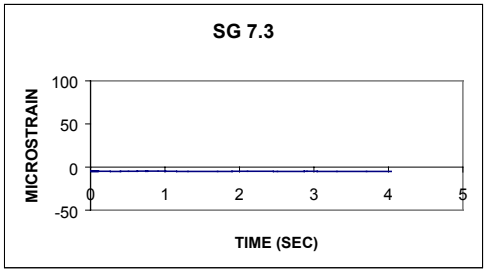

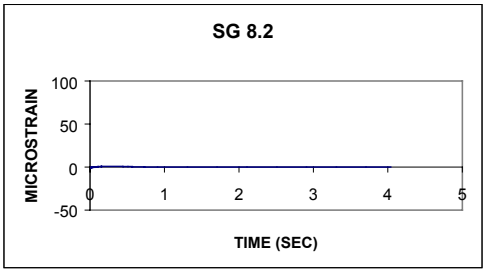

Figure B.50 Time-history of strain for test 0900-10.

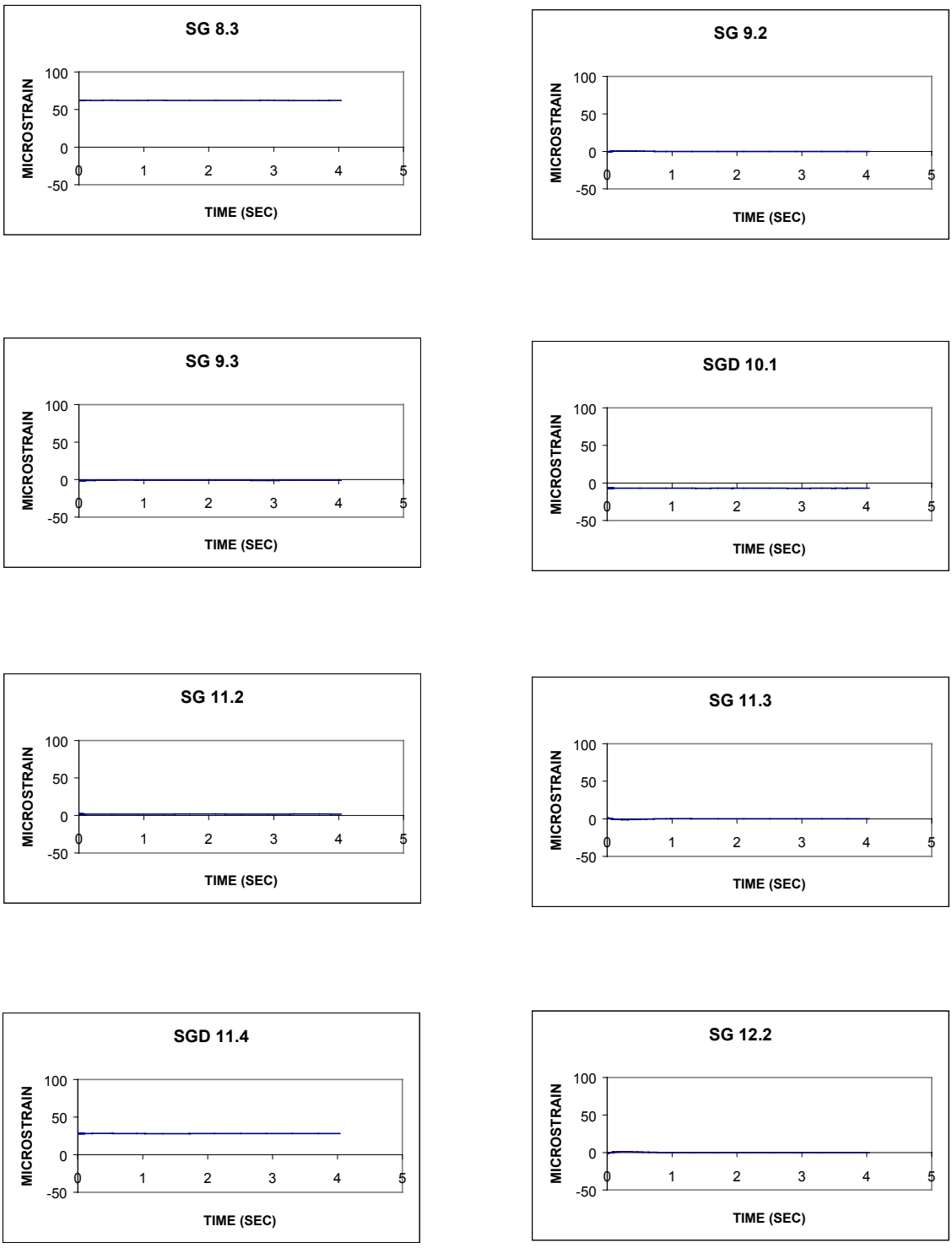

Figure B.51 Time-history of strain for test 0900-10.

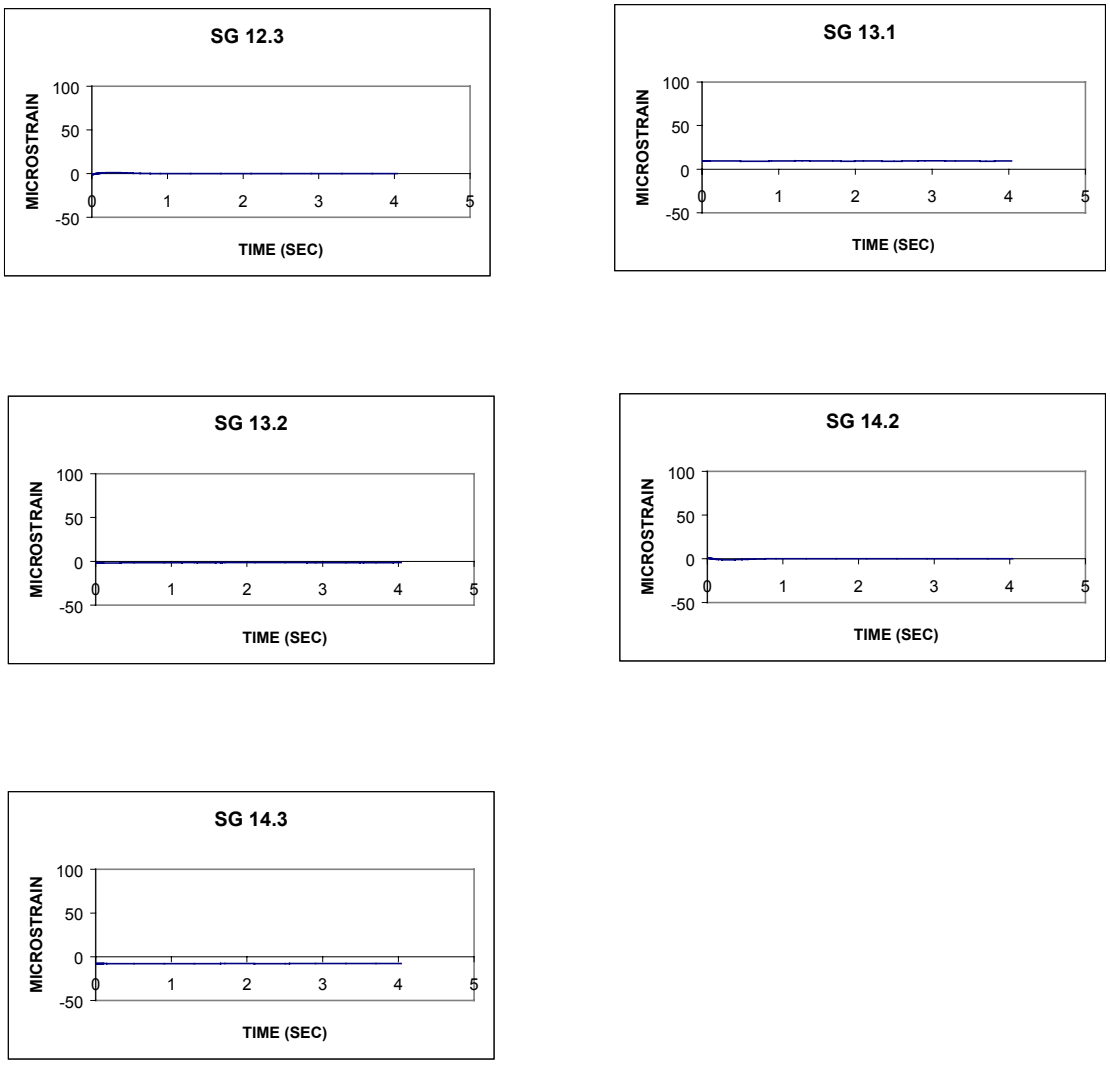

Figure B.52 Time-history of strain for test 0900-10.

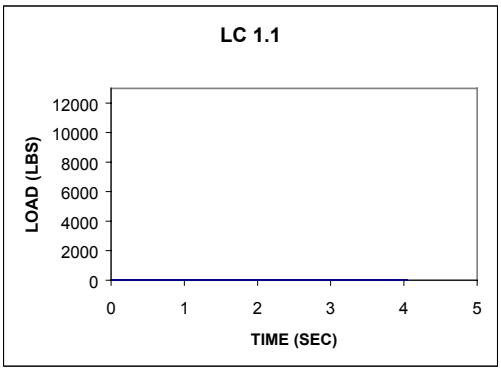

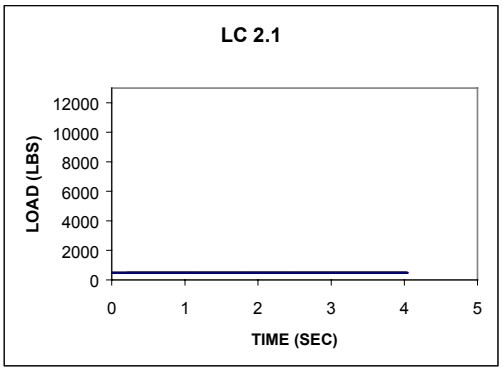

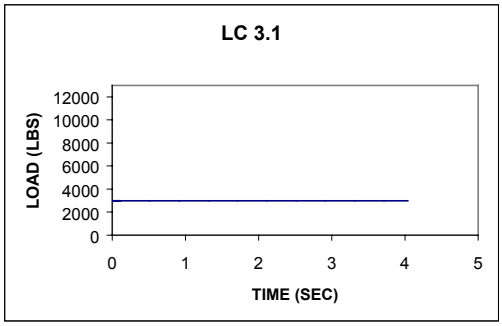

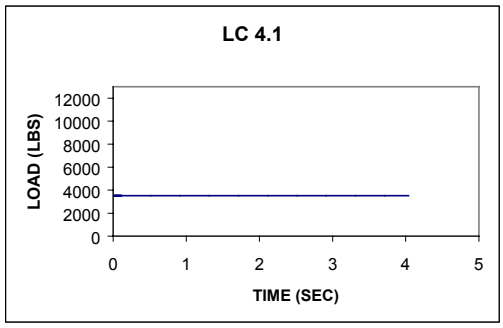

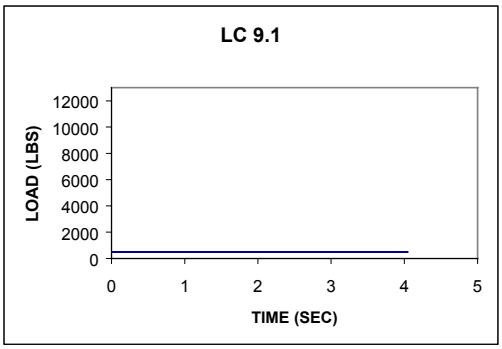

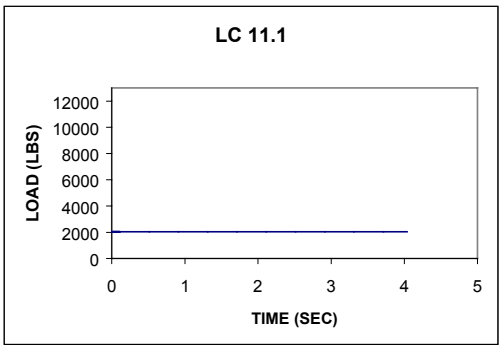

Figure B.53 Time-history of load for test 0900-10.

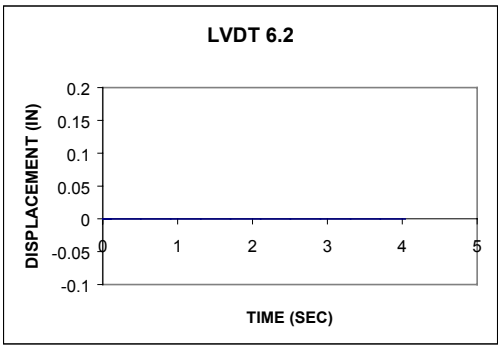

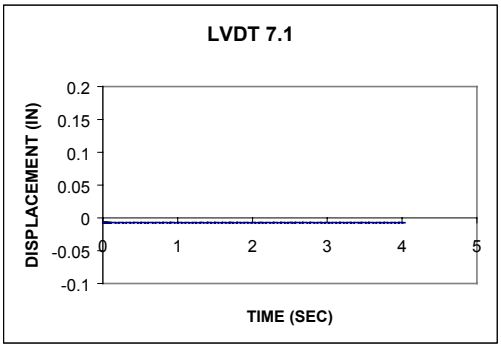

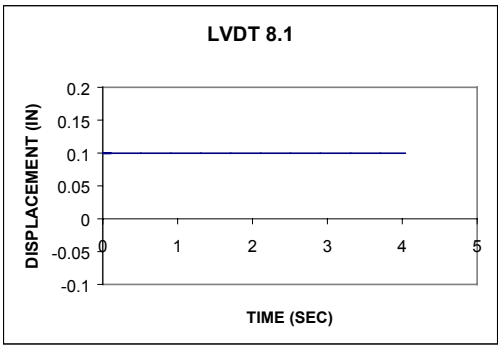

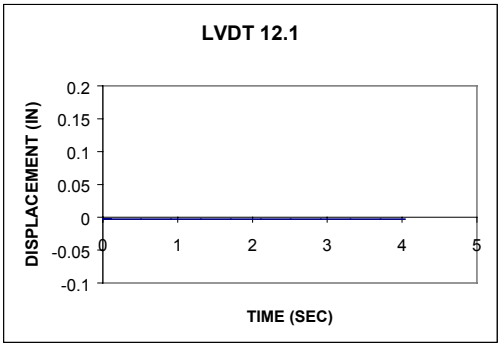

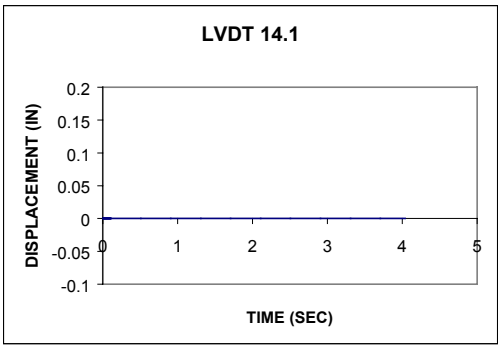

Figure B.54 Time-history of displacement for test 0900-10.